A SURVEY OF THE OUTER PLANETS JUPITER, SATURN, URANUS, NEPTUNE, PLUTO, AND THEIR SATELLITES*

R. L. NEWBURN, JR. and S. GULKIS
Jet Propulsion Laboratory, Pasadena, Calif., U.S.A.

(Received 3 July, 1972)

Abstract. A survey of current knowledge about Jupiter, Saturn, Uranus, Neptune, Pluto, and their satellites is presented. The best available numerical values are given for physical parameters, including orbital and body properties, atmospheric composition and structure, and photometric parameters. The more acceptable current theories of these bodies are outlined with thorough referencing offering access to the details. The survey attempts to cover the literature through May 1, 1972.

1. Introduction

Beyond the asteroid belt lie the giant planets, Jupiter, Saturn, Uranus, and Neptune, and their 29 satellites, plus Pluto, a small planet more like a satellite than any of its companions. The giant planets are huge, massive, low-density objects which rotate rapidly and have extensive, optically thick, reducing atmospheres. They contain more than 99% of the *planetary* mass in the solar system and 98% of the angular momentum in the solar system, *including* that of the Sun. One of the primary constraints upon any theory of the origin and development of the solar system is the necessity of logically explaining the extreme differences between these giants and the terrestrial planets, Mercury, Venus, Earth, and Mars. Jupiter's composition may be very simular to the primordial nebula, from which it is believed the entire solar system evolved, and thus the planet is a key object in cosmological studies (Newburn *et al.*, 1970).

It is the primary purpose of this review to present the state of observational knowledge of the outer planets as an aid to those planning to work in the field. Because of rapid observational progress in some areas and the highly speculative nature of others, comments on theory are limited chiefly to brief outlines and to literature references.

Table I presents many of the principal physical data for five outer planets. Some of these data are quite uncertain, particularly for the outermost three. Such uncertainties are indicated in the table and, where important, are generally discussed in some detail in the main text. Table II gives important information on planetary motions. Some quantities in both tables are known to much higher accuracy than that given, and additional figures can be found in the original references. The intent here is to include sufficient information for most calculations in physical planetology but not for studies in celestial mechanics. The masses quoted are from a comprehensive evaluation of all existing data by Klepczynski *et al.* (1971). The Jet Propulsion

* Prepared Under Contract No. NAS7-100 National Aeronautics and Space Administration.

Space Science Reviews **3** (1973) 179–271.

TABLE I

Physical data

Parameter	Jupiter	Saturn	Uranus	Neptune	Pluto
Gravitational mass GMp, $km^3\ s^{-2}$ (calculated from data in Klepczynski *et al.*, 1971 and $GM_\odot$ [a])	1.26711×10^8	3.7938×10^7	5.821×10^6	6.867×10^6	4.42×10^4
Reciprocal Mass	1047.37	3498.1	22800	19325	3000000 [a]
'Possible error in GMp' (see text and Kovalevsky, 1971)	$\pm 0.0024\%$	$\pm 0.04\%$	$\pm 0.9\%$	$\pm 0.5\%$	$\pm 25\%$
Mass (Earth = 1) [a] (calculated data in Melbourne *et al.*, 1968 and Klepczynski *et al.*, 1971)	317.89	95.18	14.6	17.2	0.11
Equatorial radius (Earth = 1) [b]	11.23	9.41	3.98 [c]	3.88	~ 0.5 [c] (see Section 5.1)
Equatorial radius, km	71600 (Hubbard and Van Flandern, 1972)	60000 (Dollfus, 1970b)	25400 [c] (Dollfus, 1970b)	24750 (Freeman and Lynga, 1970)	~ 3200 [c] (see Section 5.1)
Oblateness [d]	1/16.7 (Hubbard and Van Flandern, 1972)	1/9.3 (Dollfus, 1970b)	1/33 [c] (Dollfus, 1970b)	1/38.6 [c] (Freeman and Lynga, 1970)	unknown
Mean density, g cm^{-3}, calculated [e]	1.314	0.704	1.31 [c] (see Section 4.1)	1.66	~ 4.9 [c] (see Section 5.1)
Equatorial surface gravity, cm s^{-2}, calculated [f]	2288	905	830 [c]	1100	~ 430 [c]
Equatorial escape velocity, km s^{-1}, calculated [g]	59.5	35.6	21.4 [c]	23.6	~ 5.3 [c]
Color index [h], $B-V$, (Sun = 0.63) (Harris, 1961)	0.83	1.04	0.56	0.41	0.80
Bolometric bond albedo [h]	0.45 (Taylor, 1965)	0.61 (Walker, 1966)	0.35 [i] (Younkin, and Munch, 1967)	est. 0.35 [j]	est. 0.14 [k]
Effective temperature, K, predicted	105	71	57	45	42 [l]
Effective temperature, K, measured 1.5–350 μ	134 ± 4 (Aumann *et al.*, 1969)	97 ± 4 (Aumann *et al.*, 1969)	55 ± 3 (17.5–25 only) (Low, 1966a)	unknown	unknown
Mean surface brightness at zero phase [h], V mag/(arc s)^2 (calculated from data in Harris, 1961)	5.6	6.9	8.2	9.6	~ 18.2 [c]
Mean surface brightness at zero phase [h], Earth = 1	3.98×10^{-2}	1.20×10^{-2}	3.63×10^{-2}	1.00×10^{-3}	$\sim 3.6 \times 10^{-7}$ [c]

(Key index on next page.) →

Laboratory (JPL) Solar System Data Processing System (SSDPS) program offers potentially great improvements in all planetary masses and ephemerides and various astronomical constants, but at the moment, some results, particularly the outer planet masses, are still provisional and are therefore not used here (Lieske *et al.*, 1970). The 'possible' error column is based upon the judgment of Kovalevsky (1971) that the actual mass must almost certainly be within the range quoted.

2. Jupiter

2.1. Atmosphere

2.1.1. *Composition*

Absorption bands in the spectrum of Jupiter were seen by Vogel in the 1870's and considered evidence of an atmosphere. They were photographed in more detail by V. M. Slipher at Lowell Observatory shortly after the turn of the century. In the early 1930's, Wildt suggested and Dunham confirmed that these were due to the presence of methane and ammonia. However, model studies indicated that the bulk of Jupiter must be hydrogen and helium, as no other substances have sufficiently low density at the low temperatures measured to explain the observed mean density (see Section 2.2). In 1952, Baum and Code (1953) observed photoelectrically the occultation of σ Arietis by Jupiter. They measured an inverse scale height of 0.12 ± 0.04 km^{-1}, which corresponded to a mean molecular weight of 3.3 for their assumed stratospheric temperature of 86 K, thus confirming the dominance of hydrogen and/or helium in Jupiter's atmosphere. The recent occultation of β Scorpii by Jupiter indicated that the stratospheric scale height is in fact larger by a factor of about three (Hubbard *et al.*, 1972), while other studies have shown a somewhat higher stratospheric temperature ($\sim$115 K), but the extremely important fundamental conclusion that the atmosphere of Jupiter must be composed largely of one or both of the two lightest elements remains unchanged. In 1960, Kiess *et al.* (1960) reported spectroscopic detection of molecular hydrogen by means of its quadrupole rotation-vibration spectrum,

---

[a] $GM_{\odot} = 1.327125 \times 10^{11}$ km^3 s^{-2} (Melbourne *et al.*, 1968); $GM_{\oplus} = 3.986007 \times 10^5$ km^3 s^{-2} (Melbourne *et al.*, 1968, and Kelpczynski *et al.*, 1971). Pluto's mass is from Seidelmann *et al.* (1971).
[b] $R_{\oplus} = 6378.160$ km (Melbourne *et al.*, 1968).
[c] These values are particularly uncertain.
[d] Oblateness or optical flattening is defined as $(R_{\text{equatorial}} - R_{\text{polar}})/R_{\text{equatorial}}$.
[e] Calculated using $G = 6.673 \times 10^{-23}$ km^3 s^{-2} g^{-1} and assuming oblate spheroids.
[f] Including centrifugal term, $g_{\oplus} = 978$ cm s^{-2} at the equator.
[g] No rotational contribution included.
[h] Photometric terms are defined in Appendix B.
[i] See discussion in Section 4.1.4.
[j] Assumed to be the same as for Uranus.
[k] This is Harris' (1961) value for the visual albedo. It assumes a phase integral equal to Mars' and a radius of 0.45 times Earth's. The true value could be much different from that given.
[l] Pluto rotates slowly enough that the effective temperature for a nonrotating body, 50–1/2 K, may be more appropriate. The uncertainty in bolometric albedo noted in footnote k makes these values very uncertain also.

TABLE II

Mechanical data

Parameter	Jupiter	Saturn	Uranus	Neptune	Pluto
Mean distance, AU (Nautical Almanac Office, 1961)[a]	5.203	9.539	19.182	30.058	39.439
Orbital eccentricity (Nautical Almanac Office, 1961)[a]	0.0484	0.0557	0.0472	0.0086	0.2502
Orbital inclination (Nautical Almanac Office, 1961)[a]	1°18′	2°29′	0°46′	1°46′	17°10′
Sidereal Period (Nautical Almanac Office, 1961)[b]	11.862	29.458	84 013	164.793	247.686
Mean orbital velocity, km s^{-1} (Russell *et al.*, 1945)	13.06	9.65	6.80	5.43	4.74
Orbital angular momentum, kg km^2 s^{-1}, calculated	1.929×10^{37}	7.813×10^{36}	1.700×10^{36}	2.514×10^{36}	$\sim 1.8 \times 10^{34}$
Inclination of equator to orbit (Porter, 1960)	3.07°	26.74°	97.93°	28.80°	Unknown
Period of rotation	(see Section 2.1.5)	(see Section 3.1.4)	10.8 h (Moore and Menzel, 1930)[c]	15.8 h (Moore and Menzel, 1928)[c]	$6^d9^h17^m$ (Hardie, 1965)

[a] Mean elements for the epoch 1960 January 1.5 ET.

[b] Tropical years.

[c] These periods not accurately known (see Section 4.1.4).

thus completing the first stage in the study of Jupiter's atmosphere, i.e., the positive identification of the major component.

The next step, the determination of abundances, temperatures, and pressures for the denser part of the atmosphere, is still under way. It may not be completed without fairly extensive study by space probes. The most important problem at the present time is caused by the structure of the atmosphere itself. Classically, it was assumed that the gases in a planetary atmosphere could be considered a transparent layer, except for pure absorption at some discrete wavelengths, above a well defined reflecting surface or cloud layer. Abundances were determined from absorption line strengths, with allowance made for the path length through the atmosphere. Most atmospheric abundances are still quoted as if this assumption were valid, while recognizing that in many cases it is not. For example, in a dense atmosphere, Rayleigh scattering becomes important. If there are aerosols in the atmosphere, scattering by the particles increases the effective path through the atmosphere. If the aerosol density changes independently from the gas density as a function of altitude, the result is one form of a so-called inhomogeneous scattering atmosphere. While theory is adequate for predicting the behavior of radiation interacting with a simple one-dimensional atmosphere of known properties, the inverse problem, requiring definition of an atmosphere from observed radiation is far from a complete solution even for very simple cases.

On the basis of the reflecting layer model, absorption lines should increase in strength toward the limb of a planet, since the oblique path followed by radiation near the limb takes it through far more atmosphere (e.g., twice as much at 60° as at the center of the disk). Pioneering work in the 1930's indicated that Jupiter might not behave this way, and in 1953, Hess (1953) reported that the line strength of weak bands of CH_4 and NH_3 was nearly constant across the disk, decreasing slightly if anything. Many workers have since extended such studies to other bands, to higher resolution, and to polar as well as equatorial scans (e.g., Münch and Younkin, 1964; Teifel, 1966; Owen, 1969; Moroz and Cruikshank, 1969; Teifel, 1969; Avramchuk, 1970). The results show great complexity, but in no case do they agree with a pure reflecting layer model. The ingenious suggestion of Squires (1957), that the lack of change toward the limb is caused by the geometrical effect of towering cumulus-like cloud columns seen obliquely near the limbs while one looks deep between them near the disk center, seems to be defeated by the fact that CH_4 and NH_3 behave similarly in spite of their differing scale heights. The latest work, discussed in some detail in Section 2.1.4, indicates that a pure reflecting layer model is an adequate first-order description *for the center of the disk*, near zero phase, while a full inhomogeneous, two-cloud model is required to explain the center-to-limb variations of spectral absorption lines (Margolis, 1971; Hunt, 1972b). It is most important that *relative* abundances apparently can be determined with fair accuracy by studying infrared absorption bands near the disk center.* A complication is the strong possibility that the

* See Appendix A for abundance definitions and relations.

abundances are different for the belts and zones. Absolute abundance determinations will remain suspect for this and other reasons. The dynamic nature of the Jovian atmosphere almost guarantees that the apparent abundances will fluctuate with time. A 'calibration' of the simple 'reflecting layer abundances' by means of a full inhomogeneous model treatment will also be needed, and this requires improved observations.

The problem of molecular hydrogen abundance offers additional complications. Molecular hydrogen is a homopolar molecule and therefore has no normal dipole spectrum. A dipole moment can be induced by sufficient pressure, but only the fundamental (1–0) induced band at 2.4μ has been seen on Jupiter, and that has been observed only at low resolution (~ 200 cm^{-1}) from Stratoscope II. Danielson (1966) assumed a reflecting layer model, and derived an abundance of 45 km atm* from the Stratoscope II data. The first-overtone (2–0) pressure-induced band at 1.2μ was hopelessly blended with CH_4 at the resolution available. The higher overtones have not been observed on Jupiter.

Molecular hydrogen does have a quadrupole moment. In 1960, Kiess *et al.* (1960) reported identification of four lines of the second-overtone (3–0) band of the quadrupole rotation-vibration spectrum, and shortly afterwards, Spinrad and Trafton (1963) added a line from the 4–0 band. These lines are intrinsically very weak, of course, and appear only because the H_2 abundance on Jupiter is very large. A problem is introduced by the fact that these lines undergo observable collisional narrowing before ordinary pressure broadening sets in, making the lines quite narrow and making it difficult observationally to determine their shape. The theoretical shape of such a line narrowed by weak collisions is given by the Galatry profile, calculation of which has been discussed recently by James (1969). The Galatry theory is consistent with existing measurements of molecular hydrogen, but it has not been completely confirmed because of inadequate spectral resolution even in the laboratory. Specific application of the Galatry profile to Jovian hydrogen lines has been made by Margolis and Hunt (1972). Their abundance determination of 55–75 km amagat is the result of a reanalysis of earlier observations. In fact, earlier values (Owen, 1969; Fink and Belton, 1969; Beckman, 1967) are not greatly different, since much of the error lies in the observations of these weak lines. Trafton (1972a) has made new, higher precision observations of the quadrupole lines which should improve the present uncertain hydrogen abundance of ~ 65 km amagat when they have been reduced.

Methane has a rich dipole spectrum extending well into the visible. Unfortunately, the methane spectrum is sufficiently complex that these higher-overtone bands in the visible have not been theoretically analyzed. No rotational quantum number assignments exist for any overtones higher than (the R branch only of) the $3\nu_3$ band at 1.1μ, and that analysis is quite new. Even some vibrational assignments are uncertain. Until recently, abundance determinations rested completely upon empirical comparison with laboratory data taken at different temperatures, pressures, and resolution than those observed in Jupiter's atmosphere. Without quantum state assignments, no

* See Appendix A for abundance definitions and relations.

theoretical temperature correction was possible. The widely quoted empirical value for methane on Jupiter, 150 m atm, the result of Kuiper's (1952) pioneering efforts, is based on these high-temperature laboratory data. The analysis of the $3\nu_3$ methane band was reported by Margolis and Fox (1968) in 1968. Several new methane abundance determinations are based on the use of this analysis on both old and new data. Margolis and Fox derived an abundance that is a function of the spectral saturation, a quantity not completely determined because of insufficient spectral resolution in the available observational data. For a Lorentz half-width of 0.08 cm^{-1} measured by Bergstralh (1971), Margolis (1972) and Hunt (1971) find an abundance of 45 ± 5 m amagat, assuming a reflecting layer model, and that value is accepted here as the best available at the moment.

Ammonia also has a rich dipole spectrum. Vibrational quantum numbers have been assigned to 42 bands in the most recent analysis by McBride and Nicholls (1972a). These authors (1972b) have also carried out a rotational analysis of the $5\nu_1$ band of ammonia at 6450 Å. The analysis is very new and the band is quite complex, so it is not yet clear whether an accurate Jovian abundance and temperature analysis can be carried out at available laboratory and observatory resolutions.

Very careful empirical studies of the $5\nu_1$ and $3\nu_1$ bands of ammonia (the latter at 10800 Å) have been presented by Mason (1970), who derived abundances of 15 ± 8 and 13 ± 3 m atm, respectively, from the two bands. These values assume a reflecting model and, of course, are uncorrected for changes in the population of the energy states caused by temperature differences between laboratory and planet measurements. Earlier results have tended toward somewhat lower values (5–10 m atm) but were done without Mason's complete curve-of-growth analysis. An abundance of 13 m atm is suggested for use until a quantum analysis of the bands is accomplished.

It has been 'traditional' to assume that helium is present on Jupiter. The crude molecular weight derived for Jupiter's atmosphere by Baum and Code (1953) seemed to support this idea. In fact, as McElroy (1969) has pointed out, those observations will actually accommodate almost any composition from pure molecular hydrogen to pure helium. Unfortunately, helium has no useful spectral lines observable from Earth. Its resonance line is at 584 Å in the far-ultraviolet. Lines accessible from the Earth's surface are between levels lying ~ 20 eV above the ground state, hence virtually unpopulated in conditions anywhere near thermodynamic equilibrium. There has been some thought that there might be excitation of such He lines by electron bombardment from the radiation belts, but the lines have not been observed. The common approach has been to attempt to determine the helium abundance from its pressure-broadening effect upon methane. Unfortunately both observations and theory are still in an insecure state. Owen (1969) has suggested that an *upper limit* of 34 km atm of helium can certainly be supported by the observations. It is currently fashionable to use the solar He to H ratio for Jupiter, a value of about 8 km atm for He, assuming 65 km atm for H_2. This certainly causes no observational conflicts, but it must be stressed that any value between zero and about 35 km atm is equally good.

Of great interest is the recent detection of two isotope bands on Jupiter. Beer *et al.*

(1972) have reported the positive detection of the ν_1 parallel band of CH_3D. The observed mean abundance over the disk was 2.6 cm atm, which implies a one air-mass abundance of about 1.3 cm atm, assuming no limb darkening (Beer and Taylor, 1972). The mixing ratio is about 1.5×10^{-7} relative to the total atmosphere, assuming Divine's (1971) model atmosphere for Jupiter. Beer and Taylor (1972) have also considered the more difficult problem of the fractionation of deuterium among the various atmospheric molecules and derived a deuterium-to-hydrogen ratio of 5×10^{-5}. Fox *et al.* (1972) have made a tentative identification of $C^{13}H_4$ on Jupiter and derived a $C^{12}:C^{13}$ ratio of 110 ± 40.

Recent spectroscopic searches have placed upper limits on many molecular species in Jupiter's atmosphere. The limits set depend upon the wavelength of the molecular band used as well as the intrinsic strength of the band. Near 5μ, for example, the brightness temperature of Jupiter is higher than the effective temperature, and pene-

TABLE III

Upper limits on undetected gases in the Jovian atmosphere

Gas	Wavelength, μ	Upper limit of abundance, cm atm	Reference
C_2H_2	13.7	0.5	Gillett *et al.* (1969)
(acetylene)	1.538	4	Cruikshank and Binder (1969)
	1.0372	300	Owen (1969)
C_2H_4	10.5	0.5	Gillett *et al.* (1969)
(ethylene)	5.3	5	Gillett *et al.* (1969)
	0.8715	200	Owen (1969)
C_2H_6	12.2	3	Gillett *et al.* (1969)
(ethane)	0.9045	250	Owen (1967)
CH_3NH_2	12.8	0.05	Gillett *et al.* (1969)
(methylamine)	1.52	2	Cruikshank and Binder (1969)
	1.0325	300	Owen (1969)
HCN	14	1	Gillett *et al.* (1969)
(hydrogen)	4.75	70	Gillett *et al.* (1969)
cyanide)	1.53	5	Cruikshank and Binder (1969)
	1.0385	200	Owen (1969)
C_2N_2	4.7	2	Gillett *et al.* (1969)
(cyanogen)			
H_2S	8.0	300	Gillett *et al.* (1969)
(hydrogen	1.58	25	Cruikshank and Binder (1969)
sulfide)			
	0.22	0.08	Anderson *et al.* (1969)
SiH_4 (silane)	10.5	1	Gillett *et al.* (1969)
	0.9738	2000	Owen (1969)
PH_3	9.5	3	Gillett *et al.* (1969)
(phosphine)			
HD	0.7377, 0.7464	50000	Owen (1969)
(deuterium			
hydride)			

tration to deeper layers through a transparent region in the Jovian atmosphere is thought to be the explanation. Therefore, more than one value is given in Table III in some cases to provide information corresponding to determinations made in different spectral regions.

There have been balloon, rocket, and satellite observations of Jupiter during the past decade, leading to some knowledge of the ultraviolet geometric albedo (see Section 2.1.5d), but the available spectral resolution to date has been insufficient for any positive identification of new absorption bands. For example, Jenkins (1969) has reported on work at 1-Å resolution which indicated sharp absorption features at 2312, 2410, 2519, and 2600 Å and which needs confirmation. Further into the ultraviolet at 1216 Å, the Ly-α line of atomic hydrogen has been seen in emission, as has an unidentified feature near 1325 Å (Moos *et al.*, 1969). The Ly-α feature is probably largely the result of resonance scattering of solar radiation. The latest value for the Ly-α disk brightness is 4.2 kilo-Rayleighs* (Moos and Rottman, 1972). Other species must also be present in the Jovian ionosphere, of course (see Section 2.1.4).

Several workers have made large-scale computer calculations of the probable molecular composition of the Jovian atmosphere, assuming it is in thermodynamic chemical equilibrium. The most comprehensive of these is that of Lewis (1969a), which begins with solar abundances. The calculations show that for temperatures greater than the freezing point of water, virtually all oxygen is contained in H_2O molecules, all carbon in CH_4, all nitrogen in NH_3, and all sulfur in H_2S. There are also a series of complex condensed phases present (see below). Jupiter clearly exhibits a complex of colors which are definite indications of species other than those discussed above and of lack of homogeneity in the atmosphere. This problem will be discussed further (in Section 2.1.5).

2.1.2. *Temperature*

Pioneering measurements of the temperature of Jupiter were made in the mid-1920's, at Lowell Observatory by Menzel, Coblentz, and Lampland and at Mt. Wilson Observatory by Pettit and Nicholson, using vacuum thermocouples. Fundamentally better detectors for the middle- and far-infrared did not become available until the early 1960's, and at about this same time improved sensitivity of radio telescopes made astronomical studies of Jupiter at millimeter wavelengths worthwhile. Recent measurements of Jupiter's brightness temperature T_b include those as shown in Table IV (which, except where noted, are averages over the entire disk).

At longer wavelengths, synchrotron emission which originates in the Jovian radiation belts (see Section 2.2.3) makes a significant contribution to Jupiter's total radio emission, thus making it difficult to measure the planet's thermal spectrum. Attempts to separate the thermal from the nonthermal emission have been made by making certain assumptions about the polarization or by using radio interferometer techniques. Dickel (1967) assumes that Jupiter's thermal radiation is unpolarized, and that the

* One Rayleigh equals an apparent emission rate of 10^6 photons cm^{-2} s^{-1}.

TABLE IV

Jovian brightness temperatures to 1 cm

Wavelength	T_b, K	Reference
5 μ	230[a]	Gillett *et al.* (1969)
5 μ	310[b]	Westphal (1969)
7.5–8.3 μ	140[a]	Gillett *et al.* (1969)
8.2–9.2 μ	135 in belts 130 in zones	Westphal (1971)
8.8 μ	139	Sinton (1964)
9.2–12 μ	127[a]	Gillett *et al.* (1969)
8–14 μ	128.5 ± 2.0[c]	Murray *et al.* (1964)
8–14 μ	129[c]	Wildey *et al.* (1965)
17.5–25 μ	150 ± 5 (equator) 130 (poles)	Low (1966b) (more recently found to be variable, 120–150 K, over disk and perhaps with time; Gillett *et al.*, 1969)
1.5–350 μ	134 ± 4	Aumann *et al.* (1969)
1 mm	155 ± 15	Low and Davidson (1965)
2.3 mm	140 ± 20	Efanov *et al.* (1970)
3.3 mm	153 ± 15	Epstein *et al.* (1970)
3.4 mm	140 ± 5	Epstein (1968)
3.87 mm	150^{+45}_{-35}	Kislyakov and Lebskii (1968)
8.15 mm	144 ± 23	Efanov *et al.* (1970)
8.4 mm	157.0 ± 8	Wrixon *et al.* (1971)
8.6 mm	140^{+18}_{-14}	Kalaghan and Wulfsberg (1967)
8.6 mm	149 ± 15	Braun and Yen (1968)
9.0 mm	149 ± 9	Wrixon *et al.* (1971)
9.6 mm	157 ± 8	Hobbs and Knapp (1971)
9.8 mm	130 ± 7	Wrixon *et al.* (1971)

[a] 65% of the disk was observed on three nights, 17% on the other two.
[b] A hot spot in the north equatorial belt. Five other similar isolated sources were observed in the north equatorial belt on 5 April 1971 (Westphal, 1972).
[c] At the subsolar point.

nonthermal radiation is 22% polarized at 6-cm wavelength as it is at longer wavelengths, thus allowing him to separate the thermal from the nonthermal. Berge (1966) and Branson (1968) used interferometer techniques to make the separation at 10.4 and 21 cm, respectively. Recently, Berge (1971) re-analyzed Branson's data and arrived at a value of the disk brightness at 21 cm, which is considerably greater than Branson's estimate. The collected *thermal component* data at wavelengths greater than 1 cm are as shown in Table V.

Table V shows that Jupiter's intrinsic disk brightness temperature increases markedly at wavelengths greater than 6 cm. The higher temperatures are presumably indicative of greater penetration into Jupiter's atmosphere.

TABLE V

Jovian disk temperatures, 1–21 cm

Wavelength, cm	T_b, K	Reference
1.05	132.0 ± 8	Wrixon *et al.* (1971)
1.18	139.5 ± 5	Wrixon *et al.* (1971)
1.18	120 ± 11	Law and Staelin (1968)
1.28	120 ± 11	Law and Staelin (1968)
1.28	139 ± 10	Klein and Gulkis (1971)
1.28	136.0 ± 6	Wrixon *et al.* (1971)
1.33	139.0 ± 6	Wrixon *et al.* (1971)
1.35	107 ± 12	Law and Staelin (1968)
1.46	144.5 ± 9	Wrixon *et al.* (1971)
1.48	112 ± 12	Law and Staelin (1968)
1.5	144 ± 10	Klein and Gulkis (1971)
1.58	136 ± 28	Law and Staelin (1968)
1.90	145 ± 15	Kellermann and Pauliny-Toth (1966)
2.1	157 ± 14	Baars *et al.* (1965)
3.1	145 ± 26	Mayer *et al.* (1958)
3.2	177 ± 22	Giordmaine *et al.* (1959)
3.3	193 ± 60	Bibinova *et al.* (1963)
6	224	Dickel (1967)
10.4	260	Berge (1966)
21	250 ± 40	Branson (1968)
21	450	Berge (1971)

A large number of rotational temperatures have been given for Jupiter. Obviously, these would have the most meaning for an isothermal layer, and the molecular band must have known quantum numbers. The former condition is unlikely to be satisfied except in the stratosphere, but the Curtis-Godson approximation allows accurate comparison of homogeneous and inhomogeneous paths, even for collision-narrowed lines which have a Galatry profile (Margolis and Hunt, 1972). As previously noted, the $3\nu_3$ band of CH_4 at 1.1 μ has been carefully analyzed. For a halfwidth of 0.08 cm^{-1}, Margolis and Fox (1969b) derive a methane rotational temperature of 184 ± 13 K. Fink and Belton (1969) found a rotational temperature of 145 ± 20 K using two lines of the 3–0 H_2 quadrupole band near 8200 Å, perhaps, as Belton suggests, because the H_2 lines are so extremely narrow that they saturate at a high level in the atmosphere (Owen, 1969). It must be noted that their S(1) equivalent width differs considerably from other determinations, however, and no rotational temperature based upon only two lines is really 'secure' under the best of circumstances.

Danielson (1966) found that temperatures of 200–225 K are necessary to match the apparent overall width of the pressure-induced H_2 fundamental at 2.4 μ. The temperature in the ammonia inversion band at 1.25 cm appears to be about 132 K, rather than the lower values quoted from earlier measurements (Klein and Gulkis, 1971; and Wrixon *et al.*, 1971). An additional temperature has often been quoted in the past for the 'cloud tops' based on the assumptions that ammonia is in saturation equilibrium there and that the pure reflection model base is the ammonia cloud tops.

This is almost certainly not the case. Modern models are discussed in Section 2.1.4.

As a final paragraph on temperature, the very peculiar discovery of Murray, Wildey, and Westphal (1964) must be recorded. On October 26, 1962, they found the temperature of the shadow of satellite III, Ganymede, in the 8–14 μ region to be much warmer than its surroundings. On December 15, 1962, the shadow of the second satellite, Europa, caused a similar warming. However, on December 14, 1964, the shadow of satellite I (Io) caused no effect, and on February 4, 1965, no effect was caused by Europa (Wildey, 1965). Westphal* says that careful checks were made later, and there is no possibility that the two shadows were observed on top of the NEB (north equatorial belt) with its hot spots. He believes in the validity of the observations. Possible explanations are limited by the short time a satellite shadow remains on a given spot of the visible disk, and no completely adequate one has yet been offered. It will be interesting to see if a spacecraft radiometer observes any warming of the Jovian disk immediately beyond the terminator.

2.1.3. *Energy Balance***

An apparent discrepancy between solar energy absorbed by Jupiter and energy emitted by the planet was emphasized by Opik (1962). Taylor's (1965) bolometric albedo for Jupiter, 0.45, implies that Jupiter should have an effective temperature of 105 K. Brightness temperatures have now been measured at enough wavelengths (see Section 2.1.2) to make it seem most unlikely that the effective temperature can be as low as 105 K. The very broad band measurement by Aumann *et al.* (1969) covering 1.5–350 μ is most revealing, since more than 99% of the energy of a 105 K blackbody is emited in this wavelength range. It can be argued that the bolometric Bond albedo for Jupiter could be seriously in error. Being more than 5 AU from the Sun, Jupiter cannot be seen from Earth at phase angles greater than 12 deg, and the phase integral used to derive the bolometric albedo is an approximation. Even if Jupiter were a blackbody (with a bolometric albedo of zero), however, its effective temperature would only be 121 K, and Jupiter is clearly not a blackbody. Taylor (1965) estimates the total uncertainty in the bolometric Bond albedo to be 15% (or 0.45 ± 0.07). An albedo of 0.38 would raise the effective temperature to 109 K.

Jupiter rotates in less than 10 h. If the thermal relaxation time of the radiating 'surface' of Jupiter is long compared with 5 h, it must radiate effectively from the total surface of the planet. If it relaxes to a very low temperature in much less than 5 h, then it effectively radiates only from the lighted hemisphere, whose radiation balance temperature could be a factor of as much as $2^{1/4}$ greater than 105 K (or 124 K). These calculations have assumed a solar irradiance of 2 cal cm^{-2} min^{-1} at the Earth's mean distance from the Sun. However, the best existing curves of limb darkening for Jupiter indicate a temperature drop of about 5 K between disk center and a point near the limb (Murray *et al.*, 1964). Trafton (1967) found these curves to be so flat

* Private communication.

** See Appendix B for definition of photometric terminology.

that significant restrictions must be placed on possible models of the atmosphere. A large atmospheric thermal inertia is indicated. Theoretical calculations agree that the atmosphere should cool slowly. An effective temperature of even 125 K implies a contribution from an internal energy source of 7×10^3 erg cm^{-2} s^{-1}, an amount of energy equal to that absorbed from the Sun (assuming the bolometric albedo of 0.45 is correct). An important aspect of the planet Jupiter then is its emitted energy flux as a function of wavelength, phase, and local time of day. This can be determined accurately only from a spacecraft flying by or in orbit around Jupiter. If the emitted flux is indeed greater than the absorbed solar flux, this is a fundamental cosmogonic problem, and it has gross effects upon both models of the interior (see Section 2.2) and model atmospheres (see paragraphs immediately following).

Sources of energy external to the planet seem to be an unlikely explanation for the excess energy. For example, a particle falling from infinity to the 'surface' of Jupiter and releasing all of its kinetic energy at that point would supply 1.86×10^{13} erg g^{-1}. The apparent energy surplus then could be supplied by the impact of 3.85×10^{-10} g cm^{-2} s^{-1} of matter, or 2×10^{16} g day^{-1} over the entire planet (at 100% conversion efficiency). The total mass of material incident upon the Earth is currently estimated at $\sim 10^8$ g day^{-1} (Parkin and Tilles, 1968). Even with a surface area 120 times that of the Earth and being nearer the asteroid belt, a daily fall on Jupiter 10^8 greater than on Earth seems extremely unlikely. The incident energy from cosmic rays is probably greater than that from meteoric debris, though still at least 10^6 less than the observed energy excess.

2.1.4. *Atmospheric Structure (Models)*

A model attempts to account for some or all known observable data in the simplest possible way. Ignoring temporal variations, an atmosphere is in a sense 'defined' when its composition and variables of state are known as functions of altitude for various latitudes and local times of day. This 'vertical picture' of an atmosphere ignores most meteorology, but weather is normally a superimposed variation of 10% or less in the average conditions (with the obvious exception of phenomena involving a condensable constituent such as water).

Initially, then, atmospheric models typically assume a planeparallel geometry and ignore all horizontal forces, the dynamical components caused by rotation, and the advective components caused by horizontal thermal gradients. There is abundant visual evidence in the banded cloud structure of Jupiter (see Section 2.1.5) that such procedures are at best only approximations. Gierasch and Goody (1969) have indicated that both vertical and horizontal dynamical time constants are much shorter than the time for radiative decay of a thermal imbalance. This is emphasized with more detail by Gierasch *et al.* (1970). The purely vertical models may include convection, but by definition they ignore advection. There is no hope, however, of building a model of Jupiter at the present time which includes all of the dynamical forces. A complete, coupled model, adequate for long-range weather prediction, does not exist for Earth, where we have many orders-of-magnitude more factual data. Meanwhile,

a purely vertical, so-called radiative-convective model can give a useful first approximation to Jupiter's atmosphere and indicate the direction of future research.

The structure of a vertical model is defined by the balance between gravitational and thermal (pressure) forces. The thermal forces depend upon the sources of energy, the transport mechanisms, and the loss mechanisms. In the case of the terrestrial planets, the Sun is the sole source of energy, and if the atmospheres were sufficiently opaque, one might expect them to eventually reach an isothermal state at sufficient depth. If Jupiter indeed has an internal energy source, and the atmosphere is too opaque to transport the energy radiatively, then the lower Jovian atmosphere must be convective and have increasing temperature to an indefinitely great depth.

The behavior of the Jovian atmosphere at higher levels, where radiation can begin to penetrate to and from the outside, depends upon the opacity of the atmospheric gases. Trafton (1967) showed that the dominant source of opacity to thermal radiation (12–100 μ) is pressure-induced translational and rotational absorption of molecular hydrogen. Ammonia adds some opacity, particularly at 10 μ (Trafton, 1967 and 1971c). The Jovian atmospheric gases are relatively transparent in the visible regions of the spectrum, and the majority of sunlight (that is not reflected) is presumably absorbed by the clouds, although at least a few percent is absorbed by methane. Quantitative calculations of any sort are complicated by the fact that the abundances in the Jovian atmosphere are uncertain. The absorption coefficients for H_2 are a function of temperature, pressure, and the relative amount of helium present. Calculations are further complicated by another unknown, the opacity caused by scattering due to ammonia crystals. Most uncertain of all is the simplifying assumption of a purely vertical model, an assumption which ignores very obvious differences from zone to belt to polar region as well as all horizontal dynamics.

Within these constraints, there is a growing unanimity in acceptance of a two-cloud-layer model for the visible part of the Jovian atmosphere. The bottom layer of great opacity is thought to be essentially the classical pure reflecting layer, only at a temperature of $\sim$240 K. The upper layer in most versions is an optically thin region containing ammonia crystals in saturation equilibrium, extending from perhaps 150 K (the exact value depends upon the exact ammonia mixing ratio used) to a tropopause at $\sim$115 K. Between the two layers, there is insufficient ammonia for saturation and the area is free of particles. Models of this general type have been supported by Owen (1969), Hogan *et al.* (1969), Lewis (1969a, b) Danielson and Tomasko (1969), Divine (1971), Margolis (1971), Hunt (1972b), Axel (1972), and by Taylor and Hunt (1972), for example.

The two-layer model is in agreement with the survey from 2.8 to 14 μ by Gillett *et al.* (1969). They found a temperature of 230 K at 5 μ, and the 5 μ region is the most transparent infrared region in the Jovian atmosphere, there being no known absorption caused by H_2, and little by CH_4 or NH_3 at that wavelength. At 5 μ, one looks primarily at the reflecting layer (with some scattering and absorption by NH_3 crystals). The hot spots found in the NEB by Westphal (1969 and 1972) could well be holes in the clouds that constitute the reflecting layer, allowing penetration to deeper, hotter

regimes. The temperature of ~ 127 K observed from 9 to 12 μ occurs in the strong ν_2 absorption of ammonia, which should reach unit optical depth (if ammonia is saturated) at about that temperature level in the atmosphere. The higher temperature near 8 μ is suggested to come from methane in a temperature inversion region above the stratosphere created by absorption in the strong ν_3 band at 3.3 μ, and the $\nu_2 + \nu_4$ and $2\nu_4$ overtones which block the spectrum on up to 4 μ. Other explanations are also possible (e.g., Westphal, 1971).

Taylor and Hunt (1972) have been able to theoretically reproduce virtually every detail of Gillett *et al.*'s (1969) spectrum by means of a two-dimensional, two-layer model. Based upon Westphal's (1971) observations showing the Jovian belts to be hotter than the zones near 8.5 μ (where radiation cannot be originating from the main cloud deck), they assumed the zones to be dense ammonia cloud towers and the belts to be clear except for ammonia haze, having a calculated transmission of 55% at 5 μ. In this model, the reflection layer approximation, properly interpreted, is essentially valid near the center of the disk, but results for absolute abundance, temperature, and pressure will differ, depending upon whether a belt or a zone (or a mixture) is observed. The center-to-limb variation again requires a full inhomogeneous model treatment.

Axel (1972) has very recently published an interesting inhomogeneous two-layer model for the Jovian atmosphere. Unfortunately his use of the Dicke approximation rather than the full Galatry profile has introduced errors of some 30% in his equivalent widths for molecular hydrogen.* One result is too large an opacity for the upper cloud layer. With a proper Curtis-Godson base pressure determined by an inhomogeneous model using the correct optical depth, the reflecting layer model becomes quite applicable at the disk center.

Encrenaz and coworkers (Encrenaz *et al.*, 1971, and Encrenaz, 1972) have produced very high-resolution theoretical spectra for wavelengths of 6 to 14 μ and 40 to 1000 μ, using the basic thermal models of Hogan *et al.* (1969). These may prove useful as an aid to spacecraft experiment design and for comparison with future ground-based studies.

Little has been said about pressures because both spectral line widths and the absolute abundances of the gases which pressure-broaden spectral lines are still uncertain. Assuming a temperature of 220 K, Farmer (1969) derived a pressure at the reflecting layer of 4.6 ± 1.0 atm from his observations of the $3\nu_3$ methane band. This measurement was made with the spectrograph slit aligned equatorially in a belt (dark area), so the value may be somewhat larger than would be obtained in a zone or with a mixed (polar slit) exposure. Other workers (e.g., Owen, 1969; Divine, 1971) have generally found reflecting layer pressures of ~ 2 atm to fit their data reasonably well. Ammonia is a minor constituent and affects the lapse rate very little in spite of its condensation, so the temperature lapse rate remains essentially the dry adiabatic rate up through the convective region of the atmosphere to the top of the ammonia cirrus

* Private communications, J. Margolis and G. Hunt.

clouds which constitute the scattering layer. The pressure there, at the tropopause, may be ~ 0.2 atm. More accurate values for the base pressure and temperatures in all of these models will require both improved observations and a full inhomogeneous model treatment.

For study purposes, the *nominal* model atmosphere of Jupiter by Divine (1971) has proven useful to many workers in the field and is reproduced here as Table VI.

TABLE VI

Nominal model atmosphere of Jupiter[a]

P atm	T K	ϱ g cm^{-3}	Z[b] km	H_p km	H_ϱ km	w mg l^{-1}	Remarks
2.00×10^{-7}	145.0	3.86×10^{-11}	313.4	21.0	21.0		
3.00×10^{-7}	145.0	5.80×10^{-11}	304.9	21.0	21.0		
1.00×10^{-6}	145.0	1.93×10^{-10}	279.7	21.0	21.0		
3.00×10^{-6}	145.0	5.80×10^{-10}	256.6	21.0	21.0		
1.00×10^{-5}	145.0	1.93×10^{-9}	231.4	21.0	21.0		
3.00×10^{-5}	145.0	5.80×10^{-9}	208.3	21.0	21.0		
1.00×10^{-4}	145.0	1.93×10^{-8}	183.1	21.0	21.0		
3.00×10^{-4}	145.0	5.80×10^{-8}	160.0	21.0	21.0		
0.00100	145.0	1.93×10^{-7}	134.8	21.0	21.0		
0.00300	145.0	5.80×10^{-7}	111.7	21.0	21.0		
0.00650	145.0	1.26×10^{-6}	95.5	21.0	21.0		Top of inversion layer
0.0100	139.0	2.02×10^{-6}	86.7	20.1	18.3		
0.0300	124.8	6.73×10^{-6}	65.7	18.1	16.4		
0.0829	113.0	2.06×10^{-5}	48.3	16.3	16.3		Stratopause
0.100	113.0	2.48×10^{-5}	45.2	16.3	16.3		
0.225	113.0	5.59×10^{-5}	31.9	16.3	16.3		Tropopause
0.267	120.0	6.24×10^{-5}	29.1	17.4	26.8		
0.300	125.0	6.72×10^{-5}	27.0	18.0	27.9	0.00119	
0.350	132.0	7.44×10^{-5}	24.1	19.1	29.3	0.00583	
0.406	139.0	8.20×10^{-5}	21.2	20.1	30.8	0.0243	
0.469	146.0	9.00×10^{-5}	18.3	21.1	32.3	0.0888	NH_3 ice cloud base
1.00	189.1	1.48×10^{-4}	0.0	27.3	41.2		Zero of altitude[b]
1.27	205.0	1.74×10^{-4}	−6.9	29.7	44.4		
1.80	230.0	2.20×10^{-4}	−17.8	33.3	49.5	0.0743	
2.13	243.0	2.46×10^{-4}	−23.6	35.1	52.1	0.292	
2.41	253.0	2.68×10^{-4}	−28.0	36.6	54.2	0.758	
2.76	264.2	2.93×10^{-4}	−33.0	38.2	56.4	2.02	H_2O ice cloud base
3.00	271.3	3.10×10^{-4}	−36.2	39.2	57.8		
10.0	395.8	7.08×10^{-4}	−96.7	57.2	82.5		
30.0	550.0	1.53×10^{-3}	−168.3	79.6	112.6		
100.0	777.0	3.61×10^{-3}	−282.8	112.4	156.3		
300.0	1052.6	7.99×10^{-3}	−427.2	152.3	209.1		
1000.0	1452.9	1.93×10^{-2}	−643.7	210.1	285.4		

[a] From Divine (1971). The composition used is H_2 86.578%, He 13.214%, CH_4 0.062%, and NH_3 0.015%, H_2O 0.102%, Ne 0.013%, and other 0.016% by number. The symbol w is the mass of cloud per unit volume of gas. Other symbols have their usual meaning.

[b] The zero of altitude is arbitrarily shown at 1 atm pressure.

This model is now 2 years old and differs in small detail from previous data in this section, but there is sufficient uncertainty in all of the data that new models could easily be less accurate than this existing one. The Divine model assumes an isothermal exosphere at 145 K. Upper atmospheres are a problem for all the outer planets because there are no real observational data. Model upper atmospheres have been derived completely by theoretical extrapolation from the lower atmosphere.

The measurements of Gillett *et al.* (1969) and the thermal models of Hogan *et al.* (1969) imply the existence of a temperature inversion beginning somewhere above the (more or less) isothermal stratosphere, with temperatures increasing to perhaps 140–150 K. There is some uncertainty even about these atmospheric levels, however, because it is not certain that this structure is completely determined radiatively. Major uncertainty exists there and at still higher atmospheric levels, in part because the energy loss mechanisms are uncertain. Radiative loss in the 7.7 μ band of methane could dominate, or convective loss via eddy diffusion to lower levels in the atmosphere may prove most important, for example. The most recent consideration of these problems and the atmospheric models that result from a variety of assumptions have been given by Shimizu (1971), McGovern and Burk (1972), and by Prasad and Capone (1971). The recent occultation of β Scorpii by Jupiter indicated the possible existence of several ionospheric layers and exospheric temperatures ranging from 130 to 260 K or higher (Hubbard *et al.*, 1972). French workers obtained a mean exospheric temperature of 185 K (Combes *et al.*, 1971). These new results have not yet been incorporated into detailed models. It still seems likely that space probe measurements of ionospheric species and temperatures will be required for the derivation of a completely unambiguous model.

Theoretical studies by Lewis (1969a, b), based on an assumed solar composition and wet adiabatic equilibrium for the Jovian atmosphere, were in no small measure responsible for the wide acceptance of the two-cloud layer model. These works are still the most comprehensive consideration of the physical state of the Jovian atmosphere below the visible cloud surface. Beneath an upper thin layer of solid ammonia clouds (the scattering ammonia cirrus of previous paragraphs), Lewis found a thick layer of NH_4SH (ammonium hydrosulfide) particulate clouds (the reflecting layer) with a base at 230 K. Beneath the NH_4SH clouds, and to a small extent mixed into them, are solid H_2O (ice) clouds extending down to the melting point of ice. Beneath the ice clouds are clouds of aqueous ammonia solution, with a base at about 310 K. Beneath a clear region, Lewis then finds a deck of NH_4Cl clouds, with a base at about 480 K and 175 bar pressure and a layer of silicate clouds, with a base near 1600 K and 40000 bar pressure. This work is somewhat speculative, of course, being dependent upon a 'guessed' composition and uncertain conditions, but it does give an indication of what may eventually be found by Jovian entry probes.

2.1.5. *Visible Surface of Jupiter*

(a) *Rotation.* One of the interesting mysteries of Jovian meteorology is the fact that the clouds making up the visible surface rotate as two distinct systems. Points within

about 10 deg of the equator constitute System I, whose standard meridian rotates with a period of $9^h50^m30^s.003$. Points lying more than 10 deg from the equator in either hemisphere constitute System II, whose standard meridian rotates with a period of $9^h55^m40^s.632$ (Peek, 1958). Cloud motions relative to the standard meridians make a choice of period completely arbitrary, but some exact standard is needed for reference, and the numbers used have an historical significance.

It is difficult to define a 'true rotation period' unless a body has a solid surface for reference, and Jupiter may or may not have such a surface (see Section 2.2). The most likely true period would seem to be that in which the magnetosphere rotates. This rate can be measured at both decameter and decimeter wavelengths, and it is generally referred to as System III. The most probable value of the System III period based upon both decimeter and decameter studies is $9^h55^m29^s.75 \pm 0^s.04$ (Carr, 1971). If Jupiter should happen to be fluid throughout, the concept of 'average' or 'body' rotational period will be difficult to define and of small use.

In 1962 Spinrad (1962) reported an anomalous rotation of upper atmospheric ammonia on Jupiter. Shifted ammonia lines indicated an apparent lag in rotation of ammonia by 6 km s^{-1} relative to that layer of the atmosphere reflecting solar Fraunhofer lines. Later measurements of methane also seemed anomalous (Spinrad and Trafton, 1963). Since 1962, most spectrograms have not shown this effect. Work on this peculiar phenomenon has been summarized by Spinrad and Giver (1966). The prevalent tendency today is to dismiss the effect, attributing it to faulty observations.

(b) *Clouds.* For many years, it has been 'known' that the clouds which constitute the visible surface of Jupiter are ammonia cirrus, i.e., clouds of small particles of solid ammonia. As was indicated in the paragraphs on atmospheric structure, there is indeed a layer of ammonia cirrus clouds, but according to recent observations, they appear to be rather tenuous. At some wavelengths, one apparently sees below these clouds, through the clear atmosphere, to a second, more substantial cloud deck that is perhaps made up of particles of ammonium hydrosulfide.

There are very definite color effects observed in the cloud belts: grays, browns, pinks, yellows, and even blues and reds. The colors are pale, and Peek (1958, Chapter 5) has made it plain that, while some observed color effects may have been of optical or terrestrial atmospheric origin, all observers agree that there are real colors associated with Jupiter. There are several hypotheses as to the cause of the colors. Owen and Mason (1969) suggest that the dominant yellowish color might be caused by a dilute mixture of $(NH_4)_2S$ in the NH_4SH cloud deck. To this, Lewis and Prinn (1970) have added the suggestion of $(NH_4)_2S_x$, H_2S_x, or elemental sulfur. A detailed study of ultraviolet ($\lambda \leqslant 2700$ Å) radiation transfer and photolysis in the Jovian atmosphere by Prinn (1970) indicates that some radiation of wavelength greater than 1600 Å should penetrate through the atmosphere to the clouds and may result in photolysis of NH_3 and H_2S. He suggests that these begin a chain of reactions which may result in a freezing out of colored material such as that suggested. Sagan and Khare (1971) have reported on laboratory experiments in which various mixtures of CH_4, C_2H_6, NH_3, H_2S, and liquid H_2O were irradiated by mercury emission at 2537 or 2537 and

1849 Å. Reaction products included NH_4SH, CH_3CN, $(C_2H_5S)_2$, $(C_2H_5)_2S$, polymeric sulfur, and various amino acids. Another nonequilibrium process which may result in complex organic molecules is electrical discharge. Ponnamperuma and coworkers (Woeller and Ponnamperuma, 1969; Chadha *et al.*, 1971) have studied the products of electrical discharges in mixtures of CH_4 and NH_3. Hydrogen and nitrogen were liberated, and HCN and various nitriles were found among the volatile products. This was of considerable biological interest because nitriles hydrolize to amino acids. A reddish nonvolatile reactant was also formed which resulted in a number of amino and imino acids when acid hydrolyzed. If the Jovian atmosphere is convective to great depths, then the high temperatures will tend to destroy any complex organic molecules. Whether a steady-state production by photolysis and or discharge could, even so, maintain visible amounts of them depends on a number of completely unknown factors. Prominent ideas of a decade ago that the colors are caused by free radicals or solutions of sodium in ammonia have fallen into disfavor as the atmospheric structure of Jupiter has become better known.

The clouds of Jupiter are direct evidence of extremely complex dynamical behavior. Although they remain in alternating dark belts and light zones parallel to the equator of the planet, complex phenomena occur, particularly at the edges of the belts. A tremendous amount of data about the visible surface behavior of Jupiter has been collected and described by Peek (1958), whose book should also be consulted for the standard nomenclature for the visible surface. Information on the period of rotation within individual belts and zones has been gathered by Chapman (1969) and by Reese (1971a). For example, these data show that, since 1917, the north temperate current at the south edge of the north temperate belt has rotated more rapidly even than the equatorial belt. Over the years, there have been many attempts to correlate activity in the Jovian cloud belts or the Great Red Spot (see (c) below), as defined in various ways, with solar activity. A sampling of recent papers seems to say yes (Balasubrahmanyan and Venkatesan, 1970), no (Focas, 1971), and maybe (Banos, 1971; Prinz, 1971a; Prinz, 1971b).

Ingersoll and Cuzzi (1969) have attempted to explain the velocity differences between belts and zones on the basis of temperature differences between them, using the thermal-wind equation. This was quite successful, assuming the light zones are hotter than the dark belts. It is not what one would expect, if the temperatures are purely the consequence of absorbed sunlight, since the bright zones obviously have a higher albedo. Ingersoll and Cuzzi (1969) suggest that the bands may be convection cells driven by the internal energy source, with warm fluid rising in the zones and cold, sinking fluid in the belts. They suggest that differences in elevation could also provide the required temperature difference. Unfortunately the limited available data from Westphal's observations (1971) seem to indicate that the belts are warmer than the zones, although these temperatures may refer to different altitudes. Layton (1971) used the thermal wind equation in a study of vertical shear as measured by changes in the separation of spots at the same latitude and nearly the same longitude but apparently at different elevations. His work suggests that the dark north equatorial belt may be about 0.35 K

warmer than the equatorial zone. Barcilon and Gierasch (1970) suggest that the banded structure represents variable concentrations of a condensate, and the driving force for the convection cells is heat of condensation.

Stone and coworkers (Stone, 1967; Stone *et al.*, 1969; Stone, 1971) have studied a 'baroclinic-instability' model of the cloud structure. Here the atmospheric motions are driven by the difference in solar insolation from equator to poles on the rapidly rotating planet. The temperature gradient causes zonal thermal winds. In such a regime, various instabilities occur, their nature depending on the value of the 'Richardson number'. For one range of values ($0.25 < \mathrm{Ri} < 0.95$), symmetric instabilities would arise which should result in a formation of cloud bands not unlike those observed on Jupiter. There are some objections to this idea. For one thing, it seems clear that there is at least as much atmospheric heating on Jupiter from an internal energy source as from solar insolation; for another, there are quite stringent limitations on the value of the Richardson number. Nevertheless, the theory does have the appeal of offering a qualitative explanation of the observed band structure.

A particularly vexing problem has been the so-called equatorial jet, that part of the visible surface, constituting System I, which rotates more rapidly than the rest of the surface (except for the small north temperate current). Gierasch and Stone (1968) suggested that the growth of symmetric instabilities (as discussed above) transports angular momentum toward the equator. The nature of this and other dynamical problems concerning Jupiter have been summarized by Hide (1969, 1971a) who finds Gierasch and Stone's mechanism unconvincing. No clear answers yet exist in this virgin field of research. A close study via space probe may greatly enhance our understanding of the complex Jovian meteorology by means of detailed photography and radiometry of the cloud structure. Understanding the colors may prove more difficult, since they are very likely caused only by the condensed phase of trace molecules or by impurities in the condensed phase of NH_3 and, therefore, will be difficult to detect spectroscopically.

(c) *Great Red Spot.* The most permanent feature of the visible surface of Jupiter is the famous red spot. An elongated area of some 38 500 km in length by 13 800 km in width when at its largest in the 1880's (Reese, 1970), the Great Red Spot was probably seen 300 yr ago and is definitely noted in observations made more than 120 yr ago (Peek, 1958). The spot became most famous during the period 1879–1882, when its color was quite intense. Since that time, its visibility and color have waxed and waned, and although the color itself has disappeared entirely at times, the location of the spot, the so-called red-spot hollow, has always been obvious. The red spot was very prominent during 1962 and 1963, for example, and remained quite 'healthy' through 1965. It started to fade in 1966, and by February 1968 was extremely weak. Then, it suddenly began to strengthen and soon was back to its old prominence of 4 yr earlier (Reese, 1970, 1971b; Solberg, 1968a, b, 1969a; Reese and Solberg, 1965). This can be seen in the isodensitometry of Banos and Alissandrakis (1971). During 1969, its size averaged about 28 200 by 13 700 km (Reese, 1970).

The really remarkable feature of the spot is that it does not seem to be solidly

attached to any fixed surface but rather has wandered more or less at random through a total of 1200° of longitude during the past century (movement with respect to a mean motion of Jupiter which minimizes the red spot motion). There have been numerous short-period oscillations with respect to the steadier motion. Solberg (1969b) found a 3-month periodicity in these smaller excursions, and data for six consecutive years now give the oscillation an amplitude of 0°.8 and a period of 89.9 ± 0.2 days (Reese, 1970). The circulating current has had a rotational period of about 90 days with respect to System II during this time and may be driving the red spot in this oscillation. Meanwhile, the latitude of the center of the spot remained nearly fixed, as always. During 1968–9 it had a mean value of $-22°.25 \pm 0°.03$ and always remained between $-22°.0$ and $-22°.5$ (Reese, 1970). New data for 1969–70 have been given by Reese (1971b).

It is interesting that at 8 to 14 μ, the red spot appears 1.5 to 2.0 K cooler than its surroundings (Wildey, 1965). This is compatible with the observation that the red spot remains prominent in ultraviolet photographs, showing that it penetrates to very high atmospheric levels as a distinct feature (Owen, 1969). Infrared measurements are in agreement, indicating less absorption over the red spot (Binder, 1972).

In January 1966, a small dark spot moving along the north edge of the south temperate belt approached the red spot, started around its south side, and circled it almost 1–1/2 turns before it disappeared (Reese and Smith, 1968). Its period of circulation was 9 days. During the following year, four other dark spots, at least two coming from the south equatorial belt, showed similar behavior, though seen through only part of a turn around the red spot. These four spots had a circulation period of 12 days. Reese and Smith (1968), who reported these fascinating observations, suggest that perhaps different atmospheric levels were involved. Hess (1969) used these observations to show that geostrophy is reached on Jupiter (i.e., Coriolis forces are nearly balanced by pressure gradient forces), and that the Rossby number for the latitude of the red spot is $R_0 = 0.078$.

Older hypotheses of the nature of the red spot were variations on the theme of a solid island floating in a dense atmosphere (Peek, 1958). Increased knowledge of the physical conditions in the atmosphere of Jupiter, however, has made such theories seem impossible (Sagan, 1963). No known substance can both be solid and have a lower density than the Jovian atmosphere at the temperatures and pressures thought to exist there. If the floating object is supposed to have sufficient vertical extent to reach a depth where phase changes offer a level in which to float, then it would almost certainly be disrupted by the stresses at pressure levels of 0.1–10 Mbar (Hide and Ibbetson, 1966). Furthermore, an object floating in a density discontinuity would tend to be moved in latitude (toward the equator) by the Eötvös force (Sagan, 1963).

In 1961, Hide (1961, 1963) proposed that the red spot might be the upper end of a Taylor column, a stagnant column of fluid caused by a two-dimensional atmospheric flow unable to surmount a topographic feature. The gross motion in longitude is attributed to actual change in the period of rotation of the mantle of Jupiter caused by hydrodynamic motions in the core (Hide, 1961). Of course, if Jupiter has no solid

surface (see Section 2.2), then additional hypotheses must be invoked to save the Taylor column, such as the topographic feature being a magnetic loop or the upper end of an internal convection cell. Smoluchowski (1970b) has suggested that the topographic feature which causes the Taylor column could be nearly pure solid hydrogen floating in helium-rich liquid hydrogen. There would still be the problem of explaining the constraint in latitude. There have also been fluid-dynamic objections to the Taylor column hypothesis. The 'original' Taylor column was considered as an application of the Taylor-Proudman theorem for a homogeneous fluid. Such columns have been produced in the laboratory (Hide and Ibbetson, 1966). They are completely stagnant and have no vorticity or exchange with their surroundings. The question then is whether a similar structure can arise in a real baroclinic atmosphere and perhaps have some exchange with its surroundings. Hide (1971b) considers it likely. Stone and Baker (1968) consider it unlikely, as do Sagan (1971) and Kuiper (1972a, b). In part, this becomes a question of semantics, Should the resulting structure be called a 'Taylor column' even if it exists? Hide (1969, 1971b) himself continues to study the problem while viewing his hypothesis with caution.

Golitsyn (1970) suggests that the characteristic period for major changes in the Jovian circulation may be 3×10^5 yr or more, and, therefore, the red spot may simply be 'a large long-lived eddy'. Streett *et al.* (1971) have been studying the so-called 'Cartesian diver' hypothesis of the red spot in which a mass of hydrogen-rich solid floats in neutral buoyancy in a stratified fluid mixture of hydrogen and helium deep in the atmosphere and changes the surface appearance, perhaps through its effect on atmospheric convection or even the creation of a Taylor column. Kuiper (1972b) has been studying a model of 'organized cumulus convection' for the red spot, and he makes persuasive arguments in its behalf. In this theory, the visible red spot is a cirrus cover above an array of self-sustaining convection columns about one-sixth the size of the visible spot. Qualitative explanations of spot motions and interactions with the south tropical disturbance result rather naturally.

At the present time, then, the Great Red Spot of Jupiter is a fascinating, mysterious object, unique in its size and stability among atmospheric phenomena in the solar system. Until some hard, quantitative knowledge of Jovian atmospheric dynamics is obtained, it will remain one of the solar system's intriguing puzzles.

(d) *Photometric Properties.** Photometric observations of Jupiter are complicated in several ways. As observed from Earth, the phase angle of Jupiter never exceeds 12 deg. A phase coefficient of perhaps 0.005 mag/deg^{-1} seems to be an appropriate value for $\Delta m(\alpha)$. Attempts to measure $\Delta m(\alpha)$, even over the available 12 deg, are complicated by planetary rotation and by secular changes in the visible surface. Measured values of $V(1, 0)$, the absolute visual magnitude, have ranged from -9.03 to -9.48 at various oppositions since 1862; these changes are thought to be real, since similar measurements for Mars and Saturn by the same observers show only small variations (Harris, 1961). Harris (1961) suggests simply using the mean value

* Photometric systems and definitions are the subject of Appendix B.

of $V(1,0) = -9.25$. The corresponding mean opposition magnitude $V_0 = -2.55$.

Variation in color with phase is smaller than variation in brightness. No quantitative information on this seems to exist in the literature. The mean colors are quoted in Harris (1961) as:

Color	$U-B$	$B-V$	$V-R$	$R-I$
Value	0.48	0.83	0.50	−0.03

The brightness of Jupiter in each passband at mean opposition is then:

Passband	U	B	V	R	I
Magnitude	−1.24	−1.72	−2.55	−3.05	−3.02

When set equal at V, the color differences between Jupiter and the Sun are:

Passband	U	B	V	R	I
Difference ($J-\odot$)	+0.54	+0.20	0	−0.05	+0.27

A group associated with Harvard College Observatory carried out extensive photometry of Jupiter and Saturn from 1962 through 1965 in Southern France and South Africa (Irvine *et al.*, 1968a, b). They used 10 narrowband filters as well as UBV. Their detailed response curves are given by Young and Irvine (1967). They find Jupiter 0.15 magnitudes brighter at the 'present' time (1963–5) than the mean value suggested by Harris, which is a 92-yr average. This suggests that new observations should always be taken by anyone requiring the very highest photometric accuracy. The greater brightness in the 1963–5 period resulted in systematically larger geometric albedos, of course. The equatorial radius and oblateness in Table I imply a mean radius of 69400 km for Jupiter. This value, the visual magnitude of the Sun (−26.8), and solar colors from Appendix B (for (UBVRI) and Irvine *et al.* (1968b) (for the Harvard system, all colors are set to zero for the Sun) have been used to calculate the geometric albedos for the 15 passbands (Table VII). Magnitudes used for the UBV system are

TABLE VII

Jovian geometric albedos

Passband	Effective wavelength, Å	Geometric albedo
U	3530	0.269
B	4480	0.368
V	5540	0.443
R	6900	0.464
I	8200	0.345
v	3147	0.261
u	3590	0.305
s	3926	0.350
p	4155	0.404
m	4573	0.449
l	5012	0.483
k	6264	0.547
h	7297	0.415
g	8595	0.305
e	10635	0.295

the mean values from Harris (1961) quoted above, while the Harvard magnitudes used are an average of the South Africa (Irvine *et al.*, 1968a) and French (Irvine *et al.*, 1968b) data. When tabulated chronologically, these data show a change in Jovian color from 1963 to 1965 (Hopkins and Irvine, 1971). This simply has to be recognized and accepted.

Good reflected-light, integrated photometry of Jupiter at wavelengths beyond 1.1 μ does not exist. One reason for this is the extensive absorption by CH_4 and NH_3 beyond that wavelength, which leaves only a few windows through to the continuum. Spectra at longer wavelengths have been taken by Danielson (1966), Gillett *et al.* (1969), Cruikshank and Binder (1969), Johnson (1970), and Beer *et al.* (1972), but none of these authors give absolute integrated results (although Danielson's wide slit measurements come close).

With the advent of rockets and satellites, a number of ultraviolet measurements have been made of Jupiter. Calibration of ultraviolet data has been a difficult problem, and many of the early results are not mutually compatible. The latest photometry, which has benefited from the latest solar calibrations, is that of Wallace *et al.* (1972) from the second Orbiting Astronomical Observatory (OAO-2), covering $\lambda\lambda$2100–3600 at a resolution of 20 Å. The results show a radiance factor at 10 deg of 25% at 3000 Å, rising to 31% at 2500 Å, and dropping back to 25% between 2000 and 2100 Å. True geometric albedos would be perhaps 5% larger, while correction to the solar absolute magnitude and Jovian radius used in this document would decrease the final result by about 7%. OAO-2 was unable to detect a flux in its shorter wavelength channel (below 2000 Å), which is not surprising, since there is little solar continuum below about 1800 Å. The rocket measurements of Moos *et al.* (1969) show considerable flux down to 1500 Å, however, as well as features near 1300 Å and Ly-α at 1216 Å. Whether the differences result from relative instrument sensitivity or actual changes in Jupiter is not clear from the papers. The rocket photometry of Anderson *et al.* (1969) also goes to zero near 1800 Å. Kondo's photometry (1971) gives results numerically similar to those of OAO-2 above 2200 Å but uses different values for the solar flux, thus making numerical comparison difficult.

Since the phase angle of Jupiter never exceeds 12 deg, the phase integral q cannot be measured from Earth, of course. Harris (1961) used limb-darkening curves to suggest the following values for q:

Passband	$q(U)$	$q(B)$	$q(V)$
Value	1.55	1.60	1.65

There is no unique relationship between limb darkening and phase integral. These values could be in gross error, and both theory and observation need to be improved. The best solution would, of course, be to measure the phase integral from a spacecraft near Jupiter.

The visual Bond albedo $A(V)=p(V)\cdot q(V)=0.73$. Seventy-three percent of all light in a passband near 5540 Å is reflected back to space; only 27% is absorbed. Energy balance studies obviously require the value of the Bond albedo integrated over

all wavelengths, that is, the bolometric Bond albedo. Taylor (1965) measured a bolometric geometric albedo and has assumed a bolometric phase integral of 1.6 to derive a bolometric Bond albedo of 0.45, the value used in Section 2.1.3. He regards the uncertainty in his value to be about ± 0.07.

Limb darkening curves have been derived by a number of observers both in and out of specific molecular bands (e.g., Hess, 1953; Münch and Younkin, 1964; Teifel, 1966, 1969; Owen, 1969; Moroz and Cruikshank, 1969; Teifel, 1969; Avramchuk, 1970). Recent high quality, detailed photoelectric photometry has been carried out in 24 bands from 0.30 to 1.10 μ by Pilcher and McCord (1971), who compared the north and south tropical zones with the combined north equatorial belt and equatorial zone and found sizable differences. Binder (1972) has done even more detailed work using 8 bands from 1.4 to 1.63 μ, taking data at 41 points on the Jovian disk and at three phase angles. From these, he has derived an NH_3 absorption map of Jupiter, limb darkening coefficients, and some CH_4 distributional data.

A much neglected technique for atmospheric study is polarimetry. Hall and Riley (1969) find much stronger polarization at the poles of Jupiter than near the equator, for example, and Gehrels and coworkers (Gehrels, 1969; Gehrels *et al.*, 1969) even find considerable asymmetry between the two poles. At short wavelengths near the equator, the polarization is typical of molecular scattering. At longer wavelengths, there is some evidence for aerosols. Much larger optical depths appear to be reached near the poles, and this seems not completely consistent with the methane center-to-pole variation. With careful interpretation and improved models of the Jovian atmosphere, there is reason to believe that polarization measurements can offer fairly direct, local information on cloud heights and atmospheric aerosol content at the time of observation, and this is information difficult to obtain in any other way.

Rather unexpected was the recent report of circularly polarized visible (6800 Å) light from Jupiter (Kemp *et al.*, 1971a; Kemp and Wolstencroft, 1971; Kemp *et al.* 1971b). At first, polarization was positive in the south polar region, and twice as large and negative in the north polar region. Fractional values were all a few times 10^{-5}. As Jupiter approached opposition, the magnitude decreased to zero; after opposition it increased but with opposite sign, indicating atmospheric multiple scattering to be responsible for the effect.

2.2. Body Structure of Jupiter

Any theory of the interior of Jupiter must be dominated by one central fact, namely, that the mean density of the planet is only 1.31 g cm^{-3}. Among all solid substances, only hydrogen and helium have densities low enough to make up the bulk of such a planet. For 40 yr, models of Jupiter have been constructed using (1) various ratios of hydrogen and helium as a function of depth, (2) the best available theoretical equation of state for these elements, (3) the equations of hydrostatic equilibrium and conservation of mass and (4) boundary conditions set by the observed mass, oblateness, and gravitational quadrupole moment determined from the motions of the satellites. A good atmospheric model is another important boundary condition, especially since

it makes a relatively large contribution to the higher-order gravitational multipoles.

All interior models are critically dependent upon a good equation of state and good transport coefficients for the materials of the body in question. Experimental data on the densities of solid hydrogen and helium at 4.2 K exist to a pressure of 2×10^4 bar. For higher temperatures and pressures, model makers are dependent upon theory. For example, theory predicts that at a pressure of perhaps 2×10^6 bar, solid molecular hydrogen should undergo a change to a metallic phase. There could be other phase changes, although there is no evidence for them.

The calculations of Critchfield (1942) 30 yr ago indicated that the thermal conductivity of solid hydrogen at low temperatures is high even in the molecular phase. This seemed to indicate that most primordial heat should have been lost to Jupiter long ago and that the planet should be a solid one, at least out to a possibly fluid mantle and, of course, the atmosphere. De Marcus, Peebles, and others were able to develop completely consistent models based on the assumption of a relatively cold planet (De Marcus, 1958; Peebles, 1964).

Recently, a new observational result has caused a major perturbation in theories of the interior of Jupiter, namely, the discovery that Jupiter appears to be radiating about 2.7 times as much energy as it receives from the Sun (see Section 2.1.3). A very simple order-of-magnitude calculation illustrates the consequences of this discovery, which were first pointed out by Hubbard (1968). One can write for steady-state heat flow in a solid, not too transparent sphere

$$\frac{K(T_c - T_0)}{R} \simeq H,$$

where

K = thermal conductivity,
T_c = central temperature,
T_0 = surface temperature,
R = radius of the sphere, and
H = surface thermal flux.

Accepting the values from Section 2.1.3, $H \simeq 1.2 \times 10^4$ erg cm^{-2} s^{-1}. The radius of Jupiter $R \sim 7 \times 10^9$ cm. The thermal conductivity for solid hydrogen is $K \simeq 10^8$ erg cm^{-1} s^{-1} K^{-1} according to Hubbard's (1968) work. Then, $T_c - T_0 \simeq 8.4 \times 10^5$ K. Since $T_0 \ll T_c$, this calculation indicates a central temperature approaching 10^6 K. That, of course, implies that Jupiter cannot be solid after all, since hydrogen melts (it is thought) below 10^4 K. Once it melts (or at least once the hydrogen lattice breaks down sufficiently to begin flowing), convection takes over as the dominant mode of energy transport, and, in Hubbard's modeling, central temperatures of $\sim 10^4$ K result (Hubbard, 1969; 1970). The fact of central importance is that, unless there are gross errors in K and/or H, Jupiter must be hot and convective throughout much of its interior. The change in our ideas about Jupiter has come about because H is not essentially zero, as was usually assumed earlier, and because K, while large, appears likely to be an order of magnitude smaller than predicted by Critchfield (1942).

Smoluchowski (1971) has attempted semi-quantitative calculation of the effects of including 15% by volume of helium as an alloy on the melting point of metallic hydrogen in the Jovian interior. The melting temperature seems to be depressed some 1500 K, giving reasonable assurance that Jupiter will be liquid out to a radius of at least one-half. With only small amounts of helium, it is possible that Jupiter would not be melted anywhere in its interior, though presumably it must be convective in order to transport the required thermal flux to the surface.

Contemporary Jovian models clearly must consider the source of energy generated internally and the details of its transport to the surface. Bishop and De Marcus (1970) have used the conductivity expressions of both Critchfield and Hubbard to arrive at several important conclusions. They find that a fully conductive (solid) model – such as De Marcus (1958) model – cannot be radiating the observed energy, if its sole source is primordial heat, even if Critchfield's conductivity is used. They find that models with a conductive core and a convective envelope – such as Peeble's (1964) model – could radiate the observed energy only with very high initial temperatures and Critchfield's conductivity. Hubbard (1969) has found a completely convective model (his model 7) which fits the observational data quite well, but again initial temperatures required are quite high and there is considerable uncertainty about conditions near the surface. It is Bishop and De Marcus (1970) opinion that 'primordial heat, though not completely ruled out, is a fairly unlikely candidate for the source of the observed Jovian luminosity."

Smoluchowski (1967) has shown that a radial contraction of about 1 mm yr^{-1} would yield the observed excess flux from Jupiter. He suggests that this might occur through the expansion of the metallic hydrogen core at the expense of the molecular outer regions. Lacking any quantitative theory of the thermodynamics of hydrogen and helium at appropriate temperatures and pressures, Smoluchowski (1967) was able to show that such a change would not violate known principles, but he was not able to show that it would actually occur. Hubbard (1970) has developed a completely convective model, using an improved equation of state which includes the time variation of all parameters. He finds that gravitational contraction plus thermal cooling are just barely sufficient to account for the Jupiter we see today, since the Kelvin-Helmholtz time for such a model is only 4×10^9 yr. The present rate of contraction would be roughly 2/3 mm yr^{-1}. All secular changes required are far too small to be observationally detectable. Models with convective interiors do offer a reasonable explanation for Jupiter's large magnetic field, the usual dynamo mechanism.

Even the best Jovian models are probably only crude approximations to reality. No one yet knows the actual hydrogen-to-helium ratio, a critical parameter, and order-of-magnitude changes are still occurring in the theoretical values for the properties of these substances. Typical state variables for the center of Jupiter are temperatures of 5 to 15×10^3 K, pressures of 3 to 5×10^7 bar, and densities of 4 to 5 g cm^{-3}. The phase transition in hydrogen probably occurs between 2 and 5×10^6 bar but could be at a higher or lower pressure.

In the molecular layer, the problem becomes even more involved. In the 'deep

atmosphere', Smoluchowski (1970b) indicates that even though H_2 is supercritical and there can not be a true liquid surface, with enough helium there may be a steep density gradient which acts like a liquid surface. For pure H_2, using a model of Peebles (1964), Smoluchowski (1970b) suggests that, at a depth of about 4000 km, the fluid may become a solid at a pressure of about 10^5 bar and a temperature of 1700 K. Thus, Jupiter may have a 'solid' mantle, but Smoluchowski (1970a) indicates that he expects convection to occur within this solid, which probably has a viscosity of $\sim 10^{18}$ stokes. The convective velocities might be $\sim 10^{-5}$ cm s^{-1}, and this seems adequate in the mantle to handle the observed energy flux from Jupiter. Whether the molecular layer melts again at deeper levels or whether melting does not occur until the metallic phase is reached is unknown. In fact, it is not certain that there is any solid layer. Some reasonably acceptable models by Peebles (1964) apparently would exclude 'freezing' anywhere in the mantle.

Assuming solar composition, Jupiter should have several earth masses of heavy elements in its composition. These could be distributed homogeneously throughout the planet as a sort of impurity, as seems likely in a fully convective planet. Some models have placed a heavy element core at the center of Jupiter.

Hide (1967, and private communication) has suggested the possibility that conductivity in the deep, denser parts of the atmosphere could be sufficiently high to allow generation of the observed magnetic field of Jupiter and that sufficient energy is alternately stored and released in an associated toroidal field to account for the observed energy imbalance. In this hypothesis, there is no real energy imbalance, only a cyclic storage and release mechanism of long period which we happen to be observing during the release part of the cycle. Smoluchowski (1971) feels that the conductivity will be too low for this mechanism to work "unless there exist some unexpected impurities or unexpected molecular configurations."

Knowledge of the interior of Jupiter, then, is still quite uncertain. New theoretical work and new observations, many of them possible only with spacecraft, are required if models of Jupiter are to become more than hypotheses, an accurate hydrogen-to-helium ratio, for example, being a truly fundamental missing datum.

2.3. Radio frequency radiation

Radio emission from Jupiter has been observed over the wavelength range from ~ 1 mm longward to ~ 100 m. The average power spectrum of the radio emission is shown in Figure 1 (Carr *et al.*, 1964). At millimeter wavelengths, the spectrum is dominated by thermal emission which originates in the Jovian atmosphere. The observed spectrum at wavelengths shorter than 3 cm (10 GHz) lies close to the spectral curve calculated on the assumption that Juptiter's disk is an ideal blackbody radiator at 134K, the effective temperature for Jupiter (Aumann *et al.*, 1969). Departures from the blackbody curve are generally explained in terms of thermal emission from an atmosphere with an adiabatic lapse rate, and whose opacity is frequency-dependent. At decimetric wavelengths (0.1–1.0 m), the spectrum becomes almost flat, the average flux density being 6.7 ± 1.0 f.u. (1 f.u. $= 10^{-26}$ W m^{-2} Hz^{-1}) at a distance

of 4.04 AU. The distinguishing characteristics of the decimeter component are its nonthermal spectrum, its relatively large angular extent and distinctive shape of the emitting region, a high degree of linear polarization, a small degree of circular polarization, and a variation of intensity and polarization angle as the planet rotates. These can all be explained as being due to synchrotron emission by high-energy electrons trapped in an essentially dipolar magnetic field, leaving little doubt that this is the

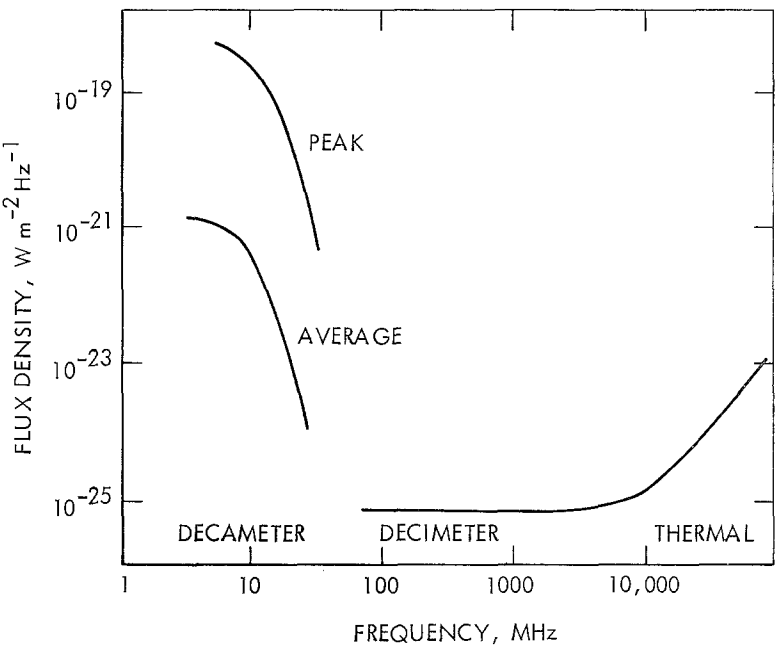

Fig. 1. Suggested appearance of Jupiter's ratio spectrum above 1 MHz (from Carr *et al.*, 1964).

correct explanation. At decametric wavelengths (7.5–100 m), Jupiter emits sporadic radiation of high intensity for short periods of time. There is some evidence that the planet is continuously emitting weak radiation at and below 10 MHz (Dulk and Clark, 1966). The average decametric points in Figure 1 represent flux density over active as well as inactive periods. The origin of this component is not well understood although it has been thoroughly observed. Current knowledge of Jovian radiation has been summarized recently by Warwick (1967) and Carr and Gulkis (1969). Dickel *et al.* (1970) have given a good summary of all the available brightness temperature observations of Jupiter's microwave spectrum.

2.3.1. *Decameter Radiation*

In the 16 yr since its discovery, the behavior of the decameter radiation has become quite clear, although our understanding of the mechanism of its generation is still quite vague. Decametric activity has been detected at ground-based observatories at frequencies between 3.5 (Zabriskie *et al.*, 1965) and 39.5 MHz (Warwick, 1964), with

a possible detection at 43 MHz (Krauss, 1958). The average spectrum of the decameter flux shows a rapid increase in flux density with decreasing frequency over the range from 40 to 5 MHz (7.5 to 60 m). This spectral slope is probably a property of the source itself, while the apparent cutoff near 5 MHz (60 m) is likely to be an observational effect caused by the terrestrial ionosphere. Recent observations (Weber and Stone, 1970) of Jupiter with Earth-orbiting radio telescopes tuned to frequencies well below the ionospheric critical frequency have failed to detect a continuous component of Jovian emission above the cosmic background, thus suggesting that the spectrum turns over somewhere between 0.5 and 3 MHz. It should be noted, however, that these observations cover a very limited time, making the detection of sporadic emission unlikely, and that the intensity of very low-frequency bursts may continue to increase below the ionospheric cutoff. The decameter flux often exceeds 10^{-20} W m^{-2} Hz^{-1} for short intervals of time. This is 3 to 4 orders of magnitude higher than indicated in the average spectrum shown in Figure 1.

On reception at the Earth, the decameter radiation usually consists of noise which is intensity-modulated to form randomly occurring bursts characterized by a hierarchy of time structure. An entire activity period containing many bursts is known as a Jovian noise storm. Noise storms ordinarily have durations ranging from several minutes to several hours. Quiescent periods between storms may last for hours, days, or weeks. Individual bursts, when observed at fixed frequencies, usually have durations of 0.5 to 5 s, but occasionally the bursts are much shorter or much longer. The bandwidths of individual bursts are usually between 0.05 and 2 MHz. Bursts with durations of 0.5 to 5 s are known as 'L' bursts, while those of shorter duration are called 'S' bursts. The L-burst waveform is believed to be due to diffraction effects in the interplanetary medium (Douglas and Smith, 1967). The S-burst waveform, on the other hand, is presumably of Jovian origin.

Measurements of all four polarization parameters have been made by Sherrill (1965) and Barrow and Morrow (1968). Sherrill concluded that the degree of polarization is usually at least 0.8 above 15 MHz and is practically 1.0 above 20 MHz. The polarization is always right-hand at 22.2-MHz and higher frequencies. The left-hand circular component becomes relatively more prominant as the frequency is reduced, but the right-hand component is still predominant down to 10 MHz. The average axial ratio of individual bursts is approximately |0.5|, but occasionally the bursts appear to be purely circular, with an axial ratio of unity. The true meaning of the polarization data are not known at this time. A likely interpretation is that the radiation is being emitted into some characteristic mode of polarization at the point of origin and is being substantially modified as it propagates out through the Jovian magnetosphere on its trip to the Earth. Thus, the polarization measured on Earth probably reflects both the initial conditions of the polarization at its point of origin and the superposed propagation effects.

A characterist feature of the Jovian bursts is the tendency for them to recur at nearly the same central meridian longitude (CML), measured in System II. Characteristic histograms of occurrence probability as a function of CML are shown in

Figure 2 for two different frequencies. In the vicinity of 18 MHz, the emission appears to originate from at least three longitude zones, generally referred to as sources A, B, and C (as indicated in Figure 2), or as the main source, the early source, and the late or third source. Similar histograms have been used to define a rotation period for Jupiter, for which the histograms or certain features of the histograms remain stationary in time. In 1962, the International Astronomical Union (1962) adopted the rotational period of $09^h55^m29^s.37$ as the 'best-fit' period to the data. This period has been named System III (1957.0). However, as the observations continued, it became

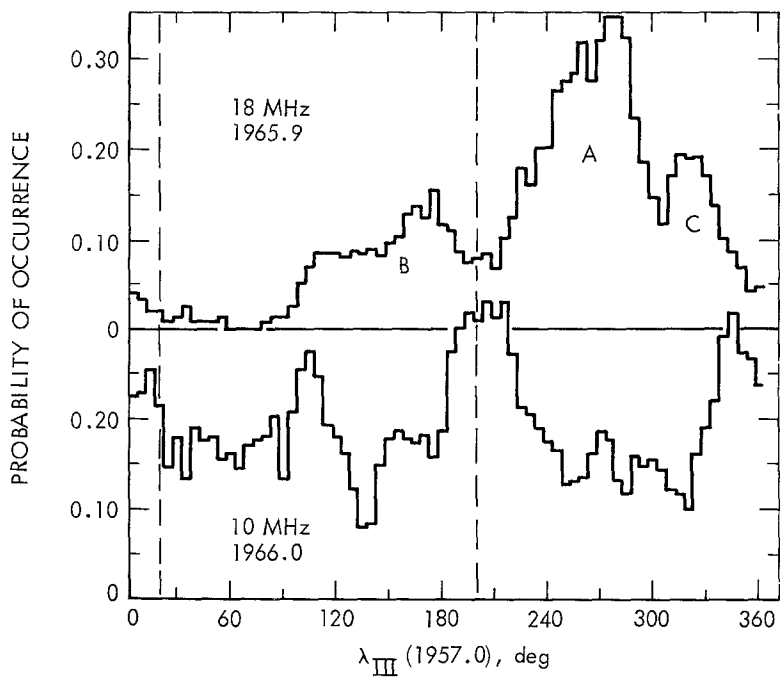

Fig. 2. Histograms of occurrence probability as a function of central meridian longitude (CML); CML values of magnetic poles are indicated by vertical dashed lines (from Carr and Gulkis, 1969).

evident that the histograms did not remain stationary in that longitude system. Recent work suggests that the rotational period either varies sinusoidally about a mean period near that of System III in a time of about 11.9 yr (Gulkis and Carr, 1966; Carr, 1971; Carr *et al.* 1970) or remains constant (Duncan, 1971). This apparent contradiction may be produced by the different methods of measuring the periods. The study of storm commencement times leads to a constant period, while the study based on using the centroid of the probability-of-occurrence histogram leads to the apparent time-variable period. Both methods give the same average period to within $0^s.04$.

Gulkis and Carr (1966) attribute the variable period to an asymmetrical beaming of the radiation, different parts of the beam being observed at different values of the

Jovicentric declination of the Earth D_E. The mean value of Jupiter's decametric rotation period is estimated (Carr, 1971) to be $09^h55^m29^s.75 \pm 0.04$. This period is $0^s.4$ longer than System III (1957.0).

Upper limits on the sizes of the sources of individual Jovian emission events have been determined with long-baseline interferometers. Dulk (1970), using baselines up to 487000λ, obtained an upper limit to the size of an incoherent source of $0.1''$ (400 km at Jupiter) at 34 MHz. Carr *et al.* (1970) have observed individual S bursts at 18 MHz with interferometers having baselines up to 450000λ. Their preliminary results indicate that if the S-burst sources are incoherent, at least some of them must be smaller than $0.1''$. Despite the high angular resolution which has been achieved, the positional uncertainties of the source of emission are still very large.

An unusual property of the decameter emission discovered by Bigg (1964) is the modulating effect of the satellite Io. Bigg found that the majority of the stronger source B emission events occur when the orbital position of Io is within a few degrees of 93 deg from superior geocentric conjunction, and that most of the source A events occur when Io is near 246 deg. This effect has been verified by several groups (see, e.g., Warwick, 1967; Carr and Gulkis, 1969); however, it is now apparent that while many of the source A events depend on Io's position, many do not. Conseil *et al.* (1971) have recently shown that a close relationship is exhibited between the solar wind velocity and the phase of Io during radio bursts from Jupiter. Most of the source B emission is Io-dependent. The Io effect is apparently much less pronounced at 10 MHz (Dulk and Clark, 1966; Register, 1968) than it is at higher frequencies. A careful search for modulation effects produced by the other Galilean satellites and/or Amalthea (Jupiter V) apparently gave negative results (Dulk, 1967). There is no widely accepted theory which explains how Io modulates the emission, although a number of ideas have been advanced (Field, 1966; Ellis, 1965; Warwick, 1967; Gledhill, 1967; Burns, 1967; Marshall and Libby, 1967; Goldreich and Lynden-Bell, 1969). The most complete model to date which considers the detailed interaction between the satellite Io and the Jovian magnetic field is that of Goldreich and Lynden-Bell (1969).

Our understanding of the entire mechanism of the creation of the decameter radiation is still highly speculative. There are probably two phenomena occurring: first, a generation of an anistropic distribution of particles or waves, and second, the generation of the decameter radiation by them, probably at the electron gyro frequency. Measurements of the true source positions relative to Jupiter's disk would help to eliminate a number of the many conflicting theories.

2.3.2. *Centimeter and Decimeter Radiation*

Jupiter emits a nearly constant flux density of about $6.7 \pm 1.0 \times 10^{-26}$ W m^{-2} Hz^{-2} (4.04 AU) at wavelengths from about 5 to 200 cm. Interferometric observations at wavelengths of 10 and 20 cm indicate that the radiation is coming from an area much larger than that of the planetary disk. Figure 3 shows Berge's (1966) suggested brightness contours of the 10-cm radiation. A rather interesting result of Berge's study is that the disk temperature for the thermal component at 2880 MHz appears to be

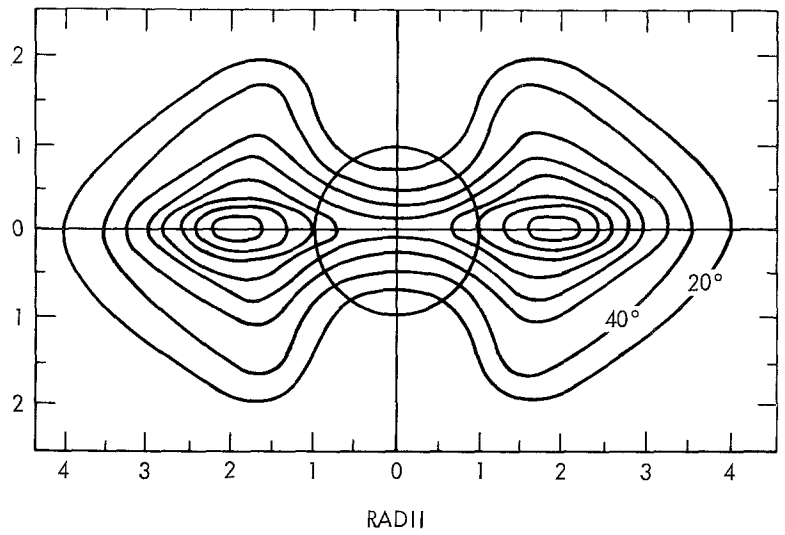

Fig. 3. Brightness temperature model of Berge (1966); contour interval is 20 K; CML (System III) is 20°.

$\sim$260 K, nearly twice the effective temperature of Jupiter. Branson (1968) obtained brightness temperature maps of the emitting regions at 1407 MHz at each of three values of CML spaced 120° apart. They illustrate strikingly the large extent of the emitting region, and the rocking of the emitting region as the planet rotates. A direct comparison of the Berge and Branson maps is dangerous because the polarizations used to obtain the maps are different. At wavelengths longer than 21 cm, the belt structure has not been measured accurately, and there is considerable disagreement in the available experimental data as to whether or not the overall extent of the emission increases with increasing wavelength (see, e.g., Gulkis, 1970).

Throughout most of the decimetric spectrum, the radiation is linearly polarized, and the degree of linear polarization reaches a maximum of $\sim$25% at 21 cm and decreases toward longer and shorter wavelengths (Dickel *et al.*, 1970). The direction of the electric vector rocks back and forth $\pm$10° relative to the rotational equator as the planet rotates. The radiation also shows a small degree of circular polarization (Berge, 1965; Seaquist, 1969; Komesaroff *et al.*, 1970). Observations of the circular polarization provide information about the polarity of the dipole and magnetic field strength within the Jovian magnetosphere. The circular polarization measurements of Komesaroff *et al.* (1970) have been used to derive a field strength in the radiation belts between 0.4 and 1.9 G. The results also confirm that Jupiter's magnetic dipole is antiparallel to that of the Earth, as was first pointed out by Warwick (1963) and corroborated by Berge (1965).

Measurements by Roberts and Ekers (1966) show that the mean centroid of the 11.3-cm emission is within 0.1 radius from the center of the disk of Jupiter in right ascension and 0.3 radius in declination. More recently, Berge (1970) used the inter-

ferometer at the Owens Valley Radio Observatory to determine the position of Jupiter's 21-cm emission in a rotating coordinate system fixed in the planet. His results show that the total displacement of the emission centroid is only 0.13 ± 0.07 polar semidiameters from the ephemeris position. The result rules out displacements of several tenths of a semidiameter. Berge states that the equatorial component of the displacement is in remarkable agreement with the periodic variation which appears in the right ascension measurements of Roberts and Ekers (1966).

The possible dependence of the decimetric flux density on solar activity has been discussed by many authors (see, e.g., Carr and Gulkis, 1969). Irregular fluctuations in the decimetric flux density have been measured; however, there are no really convincing data which prove that the effect is real. A recent attempt to investigate the possible dependence of the total flux density on solar activity was carried out by Gerard (1970) over the period December 1967 to August 1968. He found evidence for a positive correlation between the 11.13-cm Jovian total flux and solar activity as measured by the 10.7-cm solar flux. Klein *et al.* (1971) made measurements in 1971 at 12.7-cm wavelength which showed that Jupiter's flux density had varied by $\sim 20\%$ over a period of 8 yr; however they were unable to unambiguously correlate this change with solar activity.

A mean rotation period of Jupiter can be determined at decimeter wavelengths by comparing the longitude distribution either of polarization angle or total intensity with a similar distribution obtained several years later. The more precise decimetric results are given in Table VIII. Carr (1971) estimates that the weighted mean of these measurements is $09^h55^m29^s71 \pm 0^s07$, which is not significantly different from the period obtained at decametric wavelengths but is a significant departure from System III (1957.0). There is no indication that the period has changed over the interval for which the observations have been made. Decimetric determinations of the rotation period are as shown in Table VIII.

TABLE VIII

Decimetric determinations of Jupiter's rotation period

Reference	Rotation period	Date
Bash *et al.* (1964)	$09^h55^m29^s70 \pm 0^s04$	1964
Davies and Williams (1966)	$09^h55^m29^s50 \pm 0^s29$	1966
Komesaroff and McCulloch (1971)	$09^h55^m29^s83 \pm 0^s16$	1967
Whiteoak *et al.* (1969)	$09^h55^m29^s69 \pm 0^s05$	1969
Gulkis and Gary (1971)	$09^h55^m29^s72 \pm 0^s11$	1970

2.3.3. *Magnetosphere*

The evidence for a Jovian magnetosphere consists entirely of the observations at radio frequencies discussed earlier in this section. Jupiter's main magnetic field appears to be dipolar, with a dipole moment of $\sim 4 \times 10^{30}$ G cm^3, which corresponds to an equatorial field strength of ~ 10 G (e.g., Warwick, 1970). The magnetic dipole axis is inclined about 10 deg to the planetary axis of rotation, with an uncertainty of several

degrees. The zenographic north pole of the magnetic field was located near System III (1957.0) longitude 190° in 1963 and is advancing in longitude at a rate of ~3.5° per year. The direction of the magnetic field is determined directly from the decimeter circular polarization measurements. It is southward at the equator, implying that the magnetic moment and the angular momentum vector are parallel (i.e., opposite to the Earth). Whether the field is body-centered or somewhat displaced is strongly argued, but any displacement would seem to be at most a small fraction of the radius (Warwick, 1967; Roberts and Komesaroff, 1965; Berge, 1966, 1970; 1972). Referring to his measurements, Berge (1970) states, 'The result shows that the magnetic field is quite well centered and reasonably symmetric; it certainly rules out displacements of several tenths of a semidiameter'.

The extent of the Jovian magnetic field in the solar direction can be estimated by assuming a balance between magnetic field pressure and solar wind pressure. The average solar wind parameters at Earth and expected values at Jupiter (Brice and Ioannidis, 1970) are given tabulated as in Table IX.

TABLE IX

Average solar wind parameters at Earth and expected values at Jupiter

Parameters[a]	Earth	Jupiter
Density	7 proton cm^{-3}	0.26 proton cm^{-3}
B_{sw}	7 γ	1 γ
$B_{\perp}$	1.5 γ	0.05 γ
Angle to radial	45 deg	80 deg
Pressure	4×10^{-17} Nm^{-2}	7×10^{-19} N m^{-2}
Velocity	400 km s^{-1}	400 km s^{-1}
Travel time	104 h	540 h

[a] Values are given for the density, flow velocity (and resulting pressure), travel time from the Sun, the magnitude of the total solar wind magnetic field strength (B_{sw}) and a typical magnitude for the component normal to the ecliptic plane ($B_{\perp}$).

Using the solar wind parameters in Table IX, Brice and Ioannidis (1970) find the distance to the bow to be 26 R_J for a 1-G Jovian surface field and 53 R_J for a 10-G field. The corresponding value for the Earth is only 10 R_E.

Inside the magnetosphere, the magnetic field has control over the fast charged particles responsible for much of the Jovian microwave emission, and a background plasma with a broad spectrum of particle energies extending down into the thermal region. The relativstic electron energies, required to explain the decimetric radiation, range from about 3 to 30 MeV if the field strength within the belts is 1 G. The density of these relativistic electrons is estimated to be $\sim 10^{-3} cm^{-3}$. Proton flux data are virtually unknown. To date, there is little experimental data from which the thermal plasma density in Jupiter's magnetosphere can be directly deduced. Warwick and Dulk (1964) cite lack of a detectable Jovian Faraday effect in the decametic burst

radiation as evidence for excluding a plasma density $>10\,\mathrm{cm}^{-3}$ at distances ~ 1 radius from Jupiter.

If the information on the Jovian magnetosphere seems rather indefinite and incomplete, then it accurately reflects the present knowledge on the subject. Knowledge may well increase with more observations and with improved ground-based radio telescopes, but detailed solution must await a space probe mapping of the Jovian magnetic field and of the spatial and energy distribution of ionized particles within the magnetosphere.

2.4. Jupiter's Satellites

From the viewpoint of celestial mechanics, there are two types of satellites: regular and irregular (except for the Moon, which is perhaps intermediate). Regular satellites are characterized by direct motion in nearly circular orbits almost in the equatorial plane of the primary; irregular satellites by motion of almost any eccentricity and inclination. Jupiter has 12 known satellites: a group of five regular satellites (JV, JI, JII, JIII, and JIV) near the planet, and groups of three (JVI, JVII, and JX) and four (JXII, JXI, JVIII, and JIX) irregular satellites at greater distances. This arrangement is best shown in Table X, which lists the orbital elements of the Jovian satellites.

2.4.1. *Irregular Satellites*

The motion of the entire first group of irregular satellites at 11000000 km is direct, that of the second group at 23000000 km is retrograde. In the past, the possibility has been considered that this relationship indicated a common origin for each group, perhaps from one body (Kuiper, 1956). A new study by Bailey (1971) indicates that that the capture mechanism may be responsible for the groupings. He found satellite capture to be possible through the inner Lagrangian point when planet and satellite are both near perihelion or aphelion, the former usually resulting in direct orbits, the latter retrograde. Further, he found that perihelion captures should result in semi-major axes of about 11.48×10^6 km, while aphelion capture should give 21.7×10^6 km orbits. These are very close to the values for the actual axes of the Jovian outer satellites, as can be seen from Table X.

The extremely intricate motion of the irregular satellites is best illustrated by JVIII, a maverick among mavericks. During one period of a few years, its eccentricity varied from 0.291 to 0.660, and its inclination changed from 146 to 155 deg (Porter, 1960) Some of this irregularity is due to the fact that the Sun's attraction on JVIII can be more than 38% of that of Jupiter when the satellite is at apojove. A recent study of the motion of JVIII through JXII has been made by Herget (1968a). He has also given ephemerides for them for the years 1973 through 1982 (Herget, 1968b).

Nothing is known about the rotation periods of any of the irregular satellites. If they rotate slowly enough, they could give Pluto competition for the title of having the coldest spot in the solar system. Many have quoted Nicholson's remark that the outer satellites of Jupiter are so small and far from the planet that a 6-in. telescope

TABLE X

Orbital elements of Jovian satellites

Satellite	Semimajor axis, km	Eccentricity[a]	Inclination[a, b]	Sidereal period
JV[c]	181500	0.0028	0°27.3′	$11^h57^m22^s.70$
JI (Io)[c]	422000	0.0000	0°1.6′	$1^d18^h27^m33^s.51$
JII (Europa)[c]	671400	0.0003	0°28.1′	$3^d13^h13^m42^s.05$
JIII (Ganymede)[c]	1071000	0.0015	0°11.0′	$7^d3^h42^m33^s.35$
JIV (Callisto)[c]	1884000	0.0075	0°15.2′	$16^d16^h32^m11^s.21$
JVI[d]	11487000	0.158	27.6°	250.57 days
JVII[d]	11747000	0.207	24.8°	259.65 days
JX[d]	11861000	0.130	29.0°	263.55 days
JXII[d]	21250000	0.169	147°	631 days
JXI[d]	22540000	0.207	164°	692 days
JVIII[d]	23510000	0.378	145°	739 days
JIX[d]	23670000	0.275	153°	758 days

[a] The eccentricities and inclinations for the regular satellites are slightly variable. Those for the irregular satellites are extremely variable.
[b] To the equatorial plane of Jupiter.
[c] From Russell *et al.* (1945).
[d] From Porter (1960).

would be needed to see them from Jupiter itself. The visual magnitude of VI is 13.7, that of VII about 16, and of VIII through XII from 18.1 to 18.8 (Harris, 1961). Diameters, albedos, densities, masses, and shapes of the irregular satellites are completely unknown and seem likely to remain so until explored by space probes.

2.4.2. *Regular Satellites*

Jupiter's regular satellites consist of the four large Galilean satellites (they were discovered by Galileo in 1610) and the much smaller Jupiter V, sometimes called Amalthea, discovered by Barnard in 1892. Little is known about Amalthea. Its magnitude is about 13.0 (Russell *et al.*, 1945). Assuming that its geometric albedo lies in the range of 8–65%, it is 90–250 km in diameter (Dollfus, 1970). The principal physical data for the Galilean satellites are given in Table XI.

It is generally thought from observations of surface markings that the Galilean satellites keep one face toward Jupiter; that is, their periods of rotation on their axes and revolution about Jupiter are synchronous (Lyot, 1953; Johnson, 1971). The light curves of these bodies show a single maximum and minimum in each revolution about their primary, as might be expected for synchronous behavior (Harris, 1961). The markings bear considerable resemblance to lunar maria (Kuiper, 1952). The mean longitudes of the first three Galilean satellites have a fixed mathematical relationship $(\theta_1 - 3\theta_2 + 2\theta_3 = 180 \text{ deg})$ (Goldreich, 1965). For this reason, considerable caution must be exercised in correlating any physical phenomena with the position of an individual satellite.

There are considerable photometric data for the Galilean satellites. Mean magni-

TABLE XI

Jupiter's Galilean satellites: physical data

Parameter	JI (Io)	JII (Europa)	JIII (Ganymede)	JIV (Callisto)
Mass (Jupiter = 1)[a]	$3.81 \pm 0.30 \times 10^{-5}$	$2.48 \pm 0.05 \times 10^{-5}$	$8.17 \pm 0.10 \times 10^{-5}$	$5.09 \pm 0.40 \times 10^{-5}$
Mass (Moon = 1) (Calculated)[b]	0.985	0.641	2.112	1.316
Mean diameter, km	3658 ± 6[e]	3100 ± 150[f]	5550 ± 130[f]	5000 ± 150[f]
Mean radius (Moon = 1) (calculated)[c]	1.05	0.89	1.60	1.44
Mean density, g cm^{-3} (calculated)[d]	2.82	3.02	1.73	1.48
Mean surface gravity, cm s^{-2} (calculated)[d]	144	131	134	103
Escape velocity, km s^{-1} (calculated)[d]	2.30	2.01	2.73	2.27

[a] Kovalevsky (1970).
[b] Mass of Moon = 7.347×10^{22} kg (Haines, 1971).
[c] Mean diameter of moon = 1737.63 km (Haines, 1971).
[d] Mass of Jupiter = 1.899×10^{27} kg (Klepczynski *et al.*, 1971).
[e] Hubbard and Van Flandern (1972).
[f] Dollfus (1970).

TABLE XII

Galilean satellites, photometric data

Parameters	JI (Io)	JII (Europa)	JIII (Ganymede)	JIV (Callisto)
Mean absolute magnitude $V(1,0)$	−1.90	−1.53	−2.16	−1.20
Magnitude $\bar{U}_0$	7.27	6.56	5.87	6.91
Magnitude $\bar{B}_0$	5.97	6.04	5.37	6.36
Magnitude $\bar{V}_0$	4.80	5.17	4.54	5.50
Magnitude $\bar{R}_0$	4.14	4.60	3.95	4.89
Magnitude $\bar{I}_0$	3.82	4.29	3.64	4.57
Color $U-B$	1.30	0.52	0.50	0.55
Color $B-V$	1.17	0.87	0.83	0.86
Color $V-R$	0.66	0.57	0.59	0.61
Color $R-$I	0.32	0.31	0.31	0.32

tudes and colors in the UBVRI system are given by Harris (1961) as shown in Table XII. When set equal at V, the color differences between satellite (Sat.) and the Sun ⊙ are (Harris, 1961) as given in Table XIII.

Much more detailed photometry has been carried out by Johnson (1971) and by Johnson and McCord (1971), who used narrowband (~200 Å) interference filters centered 200 to 500 Å apart from 0.3 to 1.1 μ and somewhat wider filters (~500 Å passband) on 500-Å centers from 1.1 to 2.5 μ. Reference to the Sun was made via α Leo and o Vir in the first case and α Boo and α Lyr in the second. Their results emphasize those already apparent from the data above, namely, that Io differs radically from the other three Galilean satellites. Their results also add considerable detail. Io is distinctly orange in appearance, much redder than its companions. It exhibits spectral features between 0.5 and 0.6 μ and at 0.8 μ. None of the other Galilean satellites exhibit the 0.5–0.6 μ feature and only Callisto also shows the 0.8 μ feature. Io shows a much steeper decline in reflectivity between 0.3 and 0.5 μ than the other three. All four satellites show a downturn in reflectivity at about 0.95 μ, but that of Io is less steep than the other three. These features are quite obvious in the curves of an earlier article by Johnson and McCord (1970).

The changes of brightness and color of the Galilean satellites with orbital phase

TABLE XIII

Galilaen satellites, color compared to the Sun

Difference (Sat. − ⊙)	JI (Io)	JII (Europa)	JIII (Ganymede)	JIV (Callisto)
Passband U	1.70	0.62	0.56	0.64
Passband B	0.54	0.24	0.20	0.23
Passband V	0	0	0	0
Passband R	−0.21	−0.21	−0.14	−0.16
Passband I	−0.24	−0.14	−0.16	−0.19

are complex. Johnson (1971) is in good general agreement with Harris (1961). The orbital brightness variations are as given in Table XIV. Detailed curves are given in Johnson's (1971) paper. They are *not* simple sinusoids. Harris noted that the brightness variation for Callisto was for large solar phase angles only, while for phase angles less than 1°.5, it shows little brightness variation with orbital phase.

TABLE XIV

Galilaen satellites, orbital brightness variations

Satellite	Johnson (1971)		Harris (1961)	
	m_0[a], mag	Variation, mag	V_0, mag	Variation mag
Io	4.88	0.22	4.80	0.21
Europa	5.13	0.28	5.17	0.34
Ganymede	4.44	0.14	4.54	0.16
Callisto	5.41	0.14	5.50	0.16

[a] Mean opposition magnitude in a narrow-passband filter at 0.56 μ.

Harris (1961) found that Io shows large variations in color with orbital phase, $\Delta(U-B)=0.50$ and $\Delta(B-V)=0.18$, unique in this respect, although its change in visual magnitude ($\Delta V=0.21$) is no greater than that of the other bodies. Europa exhibits a total variation in visual magnitude larger than Io ($\Delta V=0.34$). Its $B-V$ color shows no variation, while its $U-B$ color does change by 0.19 from one side to the other. Ganymede, the largest and most massive of the Galilean satellites, a body possibly even larger than Mercury (although having only half of Mercury's mass), has given no spectroscopic evidence of an atmosphere. It varies in visual magnitude (ΔV) by 0.16 magn., shows no variation in $B-V$ color, and only about 0.04 magn. variation in $U-B$ (Harris, 1961). However, 0.3 $\mu-U$ shows a variation of 0.3 magn. for Ganymede (Johnson, 1971). Callisto exhibits little color change through the visible but suddenly shows a color change of about 0.3 magn. in 0.3 $\mu-U$ in the opposite sense to the other three satellites (Johnson, 1971). Callisto has a brighter trailing hemisphere at 0.3 μ, while the others have brighter leading hemispheres.

Johnson (1971) has derived a phase coefficient* for each Galilean satellite, as follows:

	Io	Europa	Ganymede	Callisto
Phase coefficient c_1 (mag deg^{-1})	0.0360	0.0262	0.0273	0.0830

The geometric albedos in Table XV are taken from several sources. Those for UBVRI are derived from the radii in Table XI and Harris magnitudes given above. The magnitude of the Sun, $V_\odot=-26.8$, is assumed, as well as the colors of the Sun in Appendix B. The narrowband albedos for JI, JII, and JIII are selected values from 48 passbands of Johnson and McCord (1971), but they have been 'corrected' to the

* See Appendix B for 'Photometric Systems and Definitions'.

radii of Table XI. The values for JIV are taken from Johnson (1970), again corrected to the radius of Table XI.

TABLE XV

Geometric albedos of the Galilean satellites

Wavelength, μ	JI (Io)	JII (Europa)	JIII (Ganymede)	JIV (Callisto)
Passband *U*	0.15	0.41	0.24	0.11
Passband *B*	0.44	0.58	0.34	0.17
Passband *V*	0.73	0.72	0.40	0.21
Passband *R*	0.89	0.81	0.46	0.24
Passband *I*	0.91	0.82	0.47	0.24
0.301	0.10	0.61	0.28	0.09
0.319	0.16	0.66	0.28	0.10
0.338	0.15	0.54	0.25	0.09
0.358	0.14	0.53	0.26	0.11
0.402	0.34	0.63	0.34	0.14
0.467	0.64	0.76	0.40	0.19
0.532	0.77	0.86	0.44	0.21
0.564	0.79	0.85	0.44	0.22
0.633	0.86	0.86	0.45	0.23
0.699	0.89	0.85	0.45	0.24
0.809	0.88	0.87	0.46	0.25
0.906	0.94	0.98	0.49	0.26
1.002	0.97	0.86	0.47	0.25
1.101	0.94	0.78	0.42	0.20
1.150	1.08	0.94	0.46	
1.199	0.95	0.82	0.46	
1.308	0.94	0.61	0.43	
1.454	1.02	0.26	0.46	
1.556	1.08	0.42	0.16	
1.658	1.03	0.33	0.24	
1.750	0.95	0.26	0.28	
1.997	1.01		0.24	
2.096	1.14		0.17	
2.195	1.15		0.19	
2.300	0.99		0.22	
2.394	1.15		0.28	
2.452	1.01		0.52	

Thus, Io has an extremely high geometric albedo in the red. (Note that geometric albedo is a quantity referenced to a Lambert plane surface and can therefore become become indefinitely large for a body with extreme backscattering properties; see Appendix B). Only that of Saturn's Dione appears greater among solar system satellites, and there is a good chance that the quoted radius for Dione is too small. Europa also has a high geometric albedo, while that of Ganymede is moderate and Callisto's is very low.

Moroz (1966) carried out photometry of the Galilean satellites from 0.8–2.5 μ, and Gillett *et al.* (1970) have added points at 3.5 and 5 μ. The latter authors have normalized all of this work to Harris' (1961) data to derive geometric albedos. The

radii used in the present document are 5–10% larger than the older values apparently used by Harris, and the geometric albedos derived in the previous paragraph hence are 10–15% smaller. Insufficient data are given to allow exact recalculation with the new radii, so the following numbers in Table XVI are read directly from the curves of Gillett *et al.* (1970).

TABLE XVI

Infrared geometric albedos of the Galilean satellites

Wavelength, μ	JI (Io)	JII (Europa)	JIII (Ganymede)	JIV (Callisto)
1.0	1.21	1.03	0.63	0.36
1.2	1.21	0.80	0.50	0.37
1.4	1.19	0.36	0.43	0.37
2.0	1.12	0.35	0.45	0.35
3.5	0.90	0.11	0.03	0.07
5.0	~0.90	0.36	0.08	0.21

These values do not include any correction to zero phase (phase was as great as 10°.2 during the observations).

Io is in many ways the most unusual of the Galilean satellites. Besides its dramatic effect on the decameter radiation (see Section 2.3) and its photometric peculiarities already discussed, there is an additional photometric oddity. Sometimes when Io reappears after solar eclipse by its primary, it is about 0.1 magn. brighter than normal, the effect decaying in about 15 min (Binder and Cruikshank, 1964). No such effect is ever observed upon ingress to eclipse. This discovery by Binder and Cruikshank on four nights in 1962 and 1963 was made in the *B* passband (0.45 μ). Confirming observations have been reported at 0.43 and 0.56 μ on 2 May 1969 by Johnson (1971), differing primarily in that the effect was much larger – 0.7 and 0.5 magn. in the two bands. Veverka (O'Leary and Veverka, 1971) found a similar but much smaller effect (0.1–0.2 magn. the same night at 0.503 μ. Negative results were obtained in careful searches by Franz and Millis (1971) at 0.43 and 0.56 μ on four dates in 1969 and 1970. Fallon and Murphy (1971) also found nothing during four reappearances in June 1970 while observing at four different wavelengths (0.41, 0.435, 0.47, and 0.65 μ). Initially, these observations were taken as possible evidence for an atmosphere on Io which, at least in part, condensed out onto the surface during eclipse (Binder and Cruikshank, 1964). Since the effect now appears to be sporadic (if it is real), a temporary atmosphere, perhaps associated with outgassing, has been suggested (Fallon and Murphy, 1971).

The recent occultation of β Scorpii by Io set an upper limit of about 2×10^{-7} atm as the atmospheric pressure (Bartholdi and Owen, 1972). This is almost identical to the amount of gaseous ammonia Lewis (1971) calculated would be required to cause the possible post-eclipse brightenings. Several astronomers have searched spectroscopically for an atmosphere on Io, but the results have always been negative. Thermal

conductivity studies of Ganymede during an eclipse suggest an upper limit of 1 mb on surface pressure of that satellite (Morrison, *et al.*, 1971).

Interior models for the Galilean satellites have been hypothesized by Lewis (1971). Since there is still considerable uncertainty (perhaps 30%) even in the densities of these objects (except Io, where the uncertainty is about 10%), and since their compositions have in no sense been measured, Lewis was forced to assume solar composition and to use chemical equilibrium calculations based upon various reasonable assumptions of the conditions in the primordial nebula. His most probable model for the Galilean satellites is a thin crust of relatively pure water ice over a deep liquid mantle of ammonia-rich water with a solid core of hydrous silicates and iron oxides.

The thermal inertia on Ganymede as determined by Morrison *et al.* (1971) is $(3 \pm 1) \times 10^4$ erg cm^{-2} s$^{-1/2}$K^{-1}. They feel that this is not incompatible with loose snow or rock powder but would be unlikely for ice. Hansen (1972) found that no homogeneous surface model could account for his eclipse data for Io, Europa, and Ganymede. He found good two-layer model fits for Io and Europa, with a rock or ice-like lower layer of high conductivity and a thin upper layer (2.6 to 1.8 mm) with thermal inertia between 1.19 and 1.80×10^3 erg cm^{-3} s$^{-1/2}$K^{-1}. An additional lateral inhomogeneity was required to fit Ganymede. Veverka's (1971) polarization studies indicate a bright, transparent surface (possibly frost) for all but Callisto, which is more like the Moon. The reddish color, especially of Io, indicates that there would have to be impurities in frost, however.

A number of measures of brightness temperature in the thermal infrared have been made in recent years for the Galilean satellites, and are presented in Table XVII. It is not clear what radii were used by most of these authors, making intercomparisons with other work hazardous and of indefinite value. Morrison *et al.* (1972) used the new occultation value for Io and increased the radii given in Table XI for the other

TABLE XVII

Brightness temperatures for the Galilean satellites (K)

Wavelength and Reference	JI (Io)	JII (Europa)	JIII (Ganymede)	JIV (Callisto)
7.5 – 13.5 μ (Low, 1965)	142 ± 5	122 ± 5	144 ± 5	159 ± 5
8 – 14 μ (Murray *et al.*, 1964)	< 135	< 141	~ 155	~ 168
8–8.8 μ (Gillet *et al.*, 1970)	151 ± 3	134 ± 3	145 ± 3	160 ± 3
10–12 μ (Gillett *et al.*, 1970)	141 ± 3	132 ± 3	143 ± 3	160 ± 3
10 and 20 μ[a] (Hansen, 1972)	144.4 ± 3	131.7 ± 3	148.5 ± 3	161.7 ± 3
18–25 μ (Morrison *et al.*, 1972)	127 ± 3	119 ± 3	134 ± 4	149 ± 5

[a] These are temperatures calculated for the subsolar point, not disk brightness temperatures.

satellites by 2%, assuming the error found for Io could be used to improve the other radii as well. Errors quoted are internal standard errors and make no allowance for systematic calibration errors or errors in radii. The temperature of a *nonrotating* blackbody at Jupiter's distance from the Sun would be 145K.Thus, many of these temperatures seem rather high, particularly the older ones, which (presumably) used smaller radii. The 8–14μ measurements do include the ν_2 fundamental vibration of NH_3. In a relatively pure surface of solid ammonia, one would expect high absorptivity and emissivity at these wavelengths. Mixed with H_2O, gross, unpredictable changes are likely. One might guess that Callisto is even larger than suggested here or has an atmosphere. The Galilean satellites are important members of the solar system about which little is known or is likely to become known without space probe scrutiny. Ultimately, they may prove the easiest objects in the outer solar system for detailed surface analysis.

3. Saturn

3.1. Atmosphere

Saturn appears similar to Jupiter in many ways, its ring system being the obvious exception. With a mean density of only 0.70 g cm^{-3}, the bulk of this planet must once again be dominated by hydrogen and helium, and, presumably, its atmosphere also, although no measurement of its mean molecular weight exists. Theoretically, the problems of atmospheric abundance are essentially the same as those discussed for Jupiter in Section 2.1 and they will not be discussed again here. Ground-based observation of Saturn is much more difficult, however. Saturn has only one-third the surface brightness of Jupiter, and all means of detection relying upon surface brightness require at least three times the exposure or integration time. The planet is nearly twice as far away from the Sun as Jupiter and twice as far from Earth, so the total flux received from Saturn at Earth is down by a factor of roughly 16 from that received from Jupiter. Also, geometric resolution of the surface of Saturn as seen from Earth is only half as great as for Jupiter. It is not surprising that knowledge of Saturn's atmosphere is much less extensive than of Jupiter's.

3.1.1. *Composition*

Molecular hydrogen was first identified spectroscopically on Saturn by Münch and Spinrad (1963) in 1962. They identified two lines of the 4–0 overtone in the quadrupole spectrum. Owen (1969) added the S(1) line of the 3–0 overtone, and he derived an abundance of 190 $\pm$40 km atm of H_2, assuming a reflecting layer model and an undiscussed treatment of the hydrogen line profile problem (see Section 2.1.1). Trafton (1972a) has just reported equivalent widths for the S(0) and Q(1) lines of the 3–0 overtone, as well as improved line strengths for the other three lines. These should soon lead to an improved abundance and a better value for the rotational temperature. There have been searches for pressure-induced dipole H_2 features on Saturn, but no detection has been reported.

The original identification of methane on Saturn (and Jupiter) was made by Wildt

in the early 1930's. A methane abundance of 350 m-atm was reported by Kuiper (1952) in 1952. He assumed an effective path length (air mass factor) of only two in deriving this value, because the Jovian planets are 'extended disks'. Presumably, something of the same problem as arose on Jupiter, caused by the temperature difference between laboratory and planet, exists on Saturn. A new value of 85 ± 35 m atm has been reported for the airmass abundance product by Trafton (1971a) from analysis of the $3\nu_3$ band at 1.1 μ. This would imply an abundance of perhaps 35 m atm, the exact amount being dependent upon the nature of Saturn's limb darkening. The meaning of this value is in further doubt because there is evidence that a reflecting layer model may be totally inappropriate for Saturn (see Section 3.1.3).

The abundance of NH_3, on Saturn is a matter of considerable debate. Dunham (1952) reported its presence in an amount "probably not more than 2 m at atmospheric pressure". Later ,Spinrad (1964) and Owen (1965) were unable to detect ammonia at all, and Owen suggested possible earlier confusion, with weak methane lines having been attributed to ammonia. In 1966, Giver and Spinrad (1966) again reported ammonia, the lines being about 0.15 ± 0.06 the strength of the corresponding band (6450 Å) in Jupiter. Small changes in temperature on Saturn would cause a considerable change in the amount of gaseous ammonia in the atmosphere 'above the clouds". Giver and Spinrad (1966) feel that there is "fairly impressive evidence for short-period changes (occurring in a few years) in the atmosphere of Saturn". The most recent 6450 Å spectra taken by Cruikshank (1971) in December 1970, show no ammonia, and an upper limit of 7 m atm was derived from this work. Cruikshank also reported that observations of the strong 1.5-μ ammonia band in 1969 by Kuiper *et al.* (1970) failed to detect ammonia and allowed an upper limit in abundenca of only 20 cm atm above optical depth unity to be set at that wavelength. On the other hand, Wrixon and Welch (1970) report 'a distinct minimum' in the millimeter spectrum of Saturn during 1969 at 23.7 GHz, the wavelength of the ammonia inversion band. Assuming that ammonia is saturated near Saturn's cloud tops, they derive an abundance of 0.36 cm atm of NH_3, above the clouds and 8 cm atm to optical depth unity at 23.7 GHz. A theoretical interpretation of the microwave spectrum of Saturn (see Section 3.3) by Gulkis *et al.* (1969) requires similar ammonia abundances. It seems very likely from the radio data that ammonia is a constituent of Saturn's atmosphere. Whether there is enough ammonia to be detected by optical wavelength spectroscopy in the weaker bands depends upon details of atmospheric structure which are unclear at the present time (see Section 3.1.3).

The principal means by which attempts have been carried out to find helium on Jupiter has been through studies of the pressure broadening of methane (see Section 2.1.1). On Saturn the $3\nu_3$ band of methane has now been observed, but the analysis has not yet resulted in a He abundance. There may well be helium on Saturn, but there is no evidence for or against that assumption at the present moment.

3.1.2. *Temperature and Energy Balance*

Attempts were made to measure the brightness temperature of Saturn in the radio-

metric window at the same time as the pioneering work on Jupiter was carried out. The values reported then are much higher than the modern values, and it is now generally assumed that Saturn was beyond the reach of the techniques available in the 1920's (although 'corridor discussions' have speculated about the possibility of variable temperatures). Modern temperature measurements on Saturn were first made, both in the infrared and microwave regions of the spectrum, at roughly the same time as those on Jupiter. The infrared brightness temperatures are given in Table XVIII and the microwave data will be found in Section 3.3.

TABLE XVIII

Saturn, infrared brightness temperatures

Wavelength μ	T_b, K[c]	Reference
5	~ 120	Low and Davidson (1969)
8–14	93 ± 3	Low (1964)
10[a]	99 ± 8	Murphy *et al.* (1972a)
10–14	99 ± 3	Allen and Murdock (1971)
17.5–25	95 ± 3	Low (1966b)
20[b]	93 ± 2	Murphy *et al.* (1972a)
1.5–350	97 ± 4	Aumann *et al.* (1969)

[a] Center of disk only, width of passband not specified.
[b] Center of disk only, width of passband probably 18–25 μ
[c] Not corrected to Saturn's mean distance. Saturn is 0.7 AU nearer the Sun in 1971 than in 1964.

In the full disk measurements it has generally been assumed that the flux from the rings is small. Allen and Murdock (1971) have measured a mean ring flux corresponding to a temperature of 82.7 K in 1969, so in fact there is a small contribution from the rings in a full disk measurement.

Using Giver and Spinrad's (1966) observations and Birnbaum and Poll's (1969) matrix elements, Owen (1969) derived a rotational temperature of 90K for Saturn. This work now needs to be repeated using Trafton's (1972a) new observations and the complete theoretical analysis. Trafton (1971a) derived a perliminary value of 132K for the rotational temperature of CH_4 in the 1.1 μ $3\nu_3$ band.

Photometry of Saturn is far more difficult than for Jupiter, especially because of the rings. No near-infrared photometry has been published beyond 1.06 μ. Many studies have simply used the bolometric Bond albedo of Jupiter, although such data as do exist tend to indicate that the value for Saturn is somewhat higher. Calculations in this document are based upon Walker's (1966) unpublished value of 0.61. This results in a calculated effective temperature of 71K. A rapidly rotating body of *zero* albedo at Saturn's distance from the Sun would have an effective temperature of 90K. The broad-band measurement of Aumann *et al.* (1969) is 97K. Thus it appears that Saturn, like Jupiter, is radiating more energy than it receives from the Sun – three and a half times as much, accepting the 0.61 bolometric albedo and the 97K temper-

ature. The maximum phase angle reached by Saturn as seen from Earth is 6 deg, so the bolometric albedo certainly needs to be measured from a spacecraft in order to obtain quantitative information on the energy balance, but the evidence at hand makes an internal energy source seem very likely.

3.1.3. *Atmospheric Structure (Models)*

With only a small fraction as many observational data as are available for Jupiter, it is not surprising that our knowledge of the structure of Saturn's atmosphere is extremely uncertain. Owen (1969) suggests "an effective pressure of ~ 1 bar in the line forming region" of Saturn based upon the apparent strengths of the S(1) line in the 3–0 and 4–0 molecular hydrogen quadrupole bands. An effective pressure of 1 bar implies a reflecting layer pressure of 2 bar, assuming the reflecting layer concept has any relevance. In fact, this model must be checked, as was done for Jupiter by Margolis (1971), and the proper Curtis-Godson base pressure must be determined by means of inhomogenous calculations even if the reflecting layer model does work (Hunt, 1972b).

The brightness temperatures at 10 and 20 μ are essentially identical to the effective temperature on Saturn, as would be expected from Trafton's (1967) calculations, showing that the thermal opacity is dominated by molecular hydrogen. Owen's (1969) rotation temperature for molecular hydrogen of 90 K is in reasonable agreement. At wavelengths shorter than 10 and longer than 100 μ, pure molecular hydrogen is relatively transparent, while inclusion of some helium makes the hydrogen relatively opaque out to several hundred microns (Trafton, 1967). In the millimeter region of the spectrum, Wrixon and Welch's (1970) observations indicate that the ammonia inversion band controls the opacity, and a deck of ammonia cirrus clouds should exist from perhaps 160 K up to a tropopause at a temperature near 80 K. Optical depth unity at 1.25 cm is reached at a temperature near 135 K and a pressure of about 2/3 atm (Wrixon and Welch, 1970). Low and Davidson's (1969) observation that the 5 μ temperature is only 120 K suggests either an unknown absorber or effective scattering or absorption by the ammonia cirrus clouds at this wavelength. Trafton's (1971a) methane rotational temperature of 132 K at 1.1 μ has similar implications. There is no evidence in any of the optical measurements for definite penetration of radiation from below a single ammonia cirrus cloud layer. Palluconi (1972) has produced a model atmosphere for Saturn, reproduced here as Table XIX. The Palluconi model has not yet been checked by use, but it is in general agreement with the few available observations, and it is interesting to note that mass of NH_3 cloud per unit volume of gas is about 2–1/2 times as great as on Jupiter. At greater depths other cloud layers are indicated, probably similar to those postulated for Jupiter. It is primarily because of the uncertainty about the scattering properties of Saturn's atmosphere that it is unclear whether or not ammonia can be observed in the optical bands, such as 6450 Å.

Limb darkening information is not as plentiful for Saturn as for Jupiter, but several facts seem evident. Equatorial scans in the 6190 Å methane band show virtually no

TABLE XIX

Values at selected pressures for nominal Saturn model atmosphere[a]

P atm	T K	ρ g cm^{-3}	z[b] km	β	dT/dz K km^{-1}	Hp km	$H\rho$ km	w mg l^{-1}	Comments
1.00×10^{-7}	119.0	2.32×10^{-11}	536.1	−0.0353	+0.101	41.5	40.1		
3.00×10^{-7}	114.5	7.25×10^{-11}	491.4	−0.0353	+0.101	39.9	38.6		
1.00×10^{-6}	109.7	2.52×10^{-10}	444.3	−0.0353	+0.101	38.3	37.0		
3.00×10^{-6}	105.5	7.86×10^{-10}	403.0	−0.0353	+0.101	36.8	35.6		
1.00×10^{-5}	101.1	2.73×10^{-9}	359.6	−0.0353	+0.101	35.3	34.1		
3.00×10^{-5}	97.3	8.53×10^{-9}	321.6	−0.0353	+0.101	34.0	32.8		
1.00×10^{-4}	93.3	2.97×10^{-8}	281.6	−0.0353	+0.101	32.5	31.4		
3.00×10^{-4}	89.7	9.25×10^{-8}	246.5	−0.0353	+0.101	31.3	30.2		
1.00×10^{-3}	86.0	3.21×10^{-7}	209.6	−0.0353	+0.101	30.0	29.0		
3.00×10^{-3}	82.7	1.00×10^{-6}	177.3	−0.0353	+0.101	28.9	27.9		
1.00×10^{-2}	79.3	3.49×10^{-6}	143.2	−0.0353	+0.101	27.7	26.7		
2.27×10^{-2}	77.0	8.17×10^{-6}	120.8	−0.0353		26.9	26.9		Upper boundary to stratosphere
3.00×10^{-2}	77.0	1.07×10^{-5}	113.4	0.0	0.0	26.9	26.9		
0.100	77.0	3.59×10^{-5}	81.1	0.0	0.0	26.9	26.9		
0.168	77.0	6.04×10^{-5}	67.1	0.0		26.9	26.9		Tropopause
0.300	95.0	8.37×10^{-5}	−49.8	0.359	−1.03	33.1	51.7		Correspondence level
0.727	130.0	1.55×10^{-4}	15.3	0.349	−0.999	45.4	69.7	0.00377	
1.00	145.2	1.91×10^{-4}	0.0	0.345	−0.988	50.7	77.3	0.0762	Zero of altitude[b]
1.12	151.0	2.05×10^{-4}	−5.9	0.343	−0.983	52.7	80.2	0.205	NH_3 cloud base
3.00	210.0	3.95×10^{-4}	−67.5	0.330	−0.946	73.4	109.5		
3.94	230.0	4.74×10^{-4}	−88.4	0.326	−0.935	80.3	119.1	0.0743	
5.10	250.0	5.64×10^{-4}	−109.9	0.323	−0.925	87.2	128.0	0.574	Solid H_2O
6.92	275.9	6.94×10^{-4}	−138.1	0.319	−0.913	96.3	141.3	4.82	Solution H_2O-NH_3 cloud base
10.0	309.9	8.93×10^{-4}	−175.5	0.314	−0.899	108.1	157.6		
30.0	434.1	1.91×10^{-3}	−317.0	0.300	−0.860	151.5	216.4		
100.0	617.8	4.48×10^{-3}	−536.0	0.287	−0.821	215.6	302.1		
300.0	841.3	9.99×10^{-3}	−813.7	0.276	−0.791	293.6	405.5		
1000.0	1166.2	2.37×10^{-2}	−1232.1	0.267	−0.764	406.9	554.9		

[a] From Palluconi (1972). The composition used is H_2 88.572%, He 11.213%, H_2O 0.105%, CH_4 0.063%, Ne 0.013%, NH_3 0.015%, and Others 0.019% by number; w is the mass of cloud per unit volume of gas. β is d log T/d log P. Other symbols have their usual meaning.

[b] The zero of altitude is arbitrarily selected at 1 atm pressure.

change in line strength from center-to-limb, while meridional scans from equator to pole first show an increase in line strength in the temperate belts and then a rapid decrease near the pole (Teifel, 1969). This is similar to the Jovian distribution, except that the polar decrease is more extreme for Saturn. In the stronger 7250 Å band of methane, however, Teifel (1969) finds that the line strength increases rather smoothly from equator to pole. The bright equatorial regions (low relative absorption) in methane light are a contrast to the dark equatorial band in broad passband visual light and a uniform appearing planet in the ultraviolet (Owen, 1969). These limb darkening data suggest a complex, three-dimensional atmosphere. They also suggest that there are difficulties with a pure reflecting layer model of the atmosphere.

The long-wavelength radio observations (see Section 3.3) yield the highest measured temperatures for Saturn. These measurements probably refer to levels deep in the atmosphere.

Any discussion of the ionsphere is rather speculative. McGovern (1968) suggests that the exospheric temperature must be quite low, perhaps 130–170 K, even near sunspot maximum.

3.1.4. *Visible Surface*

The clouds on Saturn appear to be in a state of differential rotation, the period increasing from 10^h2^m (± 4 min) at the equator to a period 6% greater at 27° latitude, 8% greater at 42° latitude, and 11% greater at 57° latitude, as determined from doppler spectroscopy by Moore (1939). Saturn has six named cloud belts in each hemisphere, a so-called dark equatorial band, and light zones between these, for a total of at least 25 distinct degrees of shading under optimum observing conditions (Reese, 1971c).

Various white spots appear on Saturn on rare occasions, persisting for a few days or weeks; these never achieve the prominence or lifetime of the sporadic spots on Jupiter (Alexander, 1962). A recent spot at latitude $-57^\circ.3$ set a record for both persistence and high south latitude. Its motion during a 490-day period from October 1969 to February 1971 appeared to be that of a damped, 169-day sinusoid about a mean rotation period of $10^h\ 36^m\ 27^s.9 \pm 0^s.2$ (Reese, 1971c). The spot measured 8000 km north and south by 6000 km east and west.

Dollfus (1963) gathered together data on the motions of eight earlier, well-observed spots and found that three high-latitude objects ($+57°$, $+36°$, and $-36°$) all had rotation periods around $10^h\ 38^m$, while four spots within 8° of the equator all had periods between $10^h\ 12^m$ and $10^h\ 15^m$. A spot at $-12^\circ.3$ had a period of $10^h\ 21^m$. Thus, spot motions are not in especially good agreement with the spectroscopic period of rotation. Moore recognized that sizeable errors were possible in his work, and a spot typically may be driven at a distinctly atypical rotation rate (or at least such is true on Jupiter), so perhaps the results are not surprising. Nine spots and one spectroscopic study are not really sufficient data to suggest anything firmly. Hide (1971a) feels that better observations will show a discrete equatorial jet as is present on Jupiter.

Color shadings of orange, blue, etc., have been reported on Saturn by experienced observers, but all colors are extremely subtle, except for the predominating variations

from white to pale yellow to brownish yellow (Alexander, 1962). As indicated in Section 3.1.3, there is evidence of ammonia cirrus clouds on Saturn, but all else is speculation.

Meaningful photometry of the disk of Saturn is extremely difficult because of the presence of the rings. Irvine and Lane (1971) have taken the 3 yr of Harvard photometry (Irvine *et al.*, 1968a, b), obtained with varying ring inclination relative to earth, and reduced it to edge-on (zero ring) data. Their data are quoted in Table XX even for

TABLE XX

Photometric data for Saturn

Magnitude at unit distance: $V(1, 0) = -8.80$
Mean opposition magnitude: $V_0 = 0.75$

Passband	Mean opposition magnitude	Geometric albedo p	Color difference, Saturn-Sun (set equal for V)
U	2.57	0.169	1.03
B	1.80	0.302	0.40
V	0.75	0.436	0.00
3590 Å	1.68	0.184	0.93
3926 Å	1.60	0.199	0.85
4155 Å	1.40	0.240	0.65
4573 Å	1.09	0.318	0.34
5012 Å	0.91	0.377	0.16
6264 Å	0.60	0.498	0.15
7297 Å	0.91	0.376	−0.16
8595 Å	1.16	0.297	−0.41
10635 Å	0.79	0.417	−0.04

Colors:				
$U-B$	$B-V$	V-7297	V-8595	V-10635
0.77	1.05	−0.16	−0.41	−0.04

UBV, although the latter is in agreement with Harris (1961) except for the U passband. The opposition magnitudes are a linear extrapolation to zero phase of data for $\alpha > 1°.5$ in order to avoid the nonlinear opposition effect*, which amounts to an additional 0.1–0.2 magn., depending upon wavelength (see Irvine and Lane, 1971, for the detailed tabulation).

The no-ring phase coefficients derived by Irvine and Lane (1971) are 0.013 ± 0.007 mag deg^{-1} for 3500–5000 Å and 0.035 ± 0.010 mag deg^{-1} for 6200–10600 Å. Geometric albedos in Table XX are also taken from Irvine and Lane, accepting their values for the solar flux but correcting the albedos to the radius and oblateness of Table I.

The OAO-2 has taken data on the disk and ring together from about 2200 Å into

* See Appendix B.

the visible (Wallace *et al.*, 1972). The combined brightness is about 30% higher at 2500 than at 3500 Å. It seems to decline at still shorter wavelengths. In the infrared, from 2 to 3.2 μ, Saturn has a higher reflectivity than Jupiter, but from 3.2 to 4.2 μ, its reflectivity is very low, just as is Jupiter's (Johnson, 1970).

3.2. Body Structure of Saturn

The problem of constructing a model interior for Saturn is basically very similar to that for Jupiter. Saturn is even less dense than Jupiter (0.70 g cm^{-3}). It is also less massive, and its gravitational acceleration is only about 40% of Jupiter's. This is the major reason for the difference in density, rather than any gross structural difference. Saturn has always given model makers more trouble than Jupiter, however, since the observed value of the quadrupole moment K requires very low-density outer layers. DeMarcus (1958) was not able to match the 'observed' K with a completely solid model. The values of the gravitational moments of Saturn are not as certain as might be desired, however, because of the unknown contribution of the rings to the motion of the inner satellites. Similarly, Peebles (1964) detailed models with very deep atmospheres and small solid cores resulted in too large a quadrupole moment. Peebles felt, however, that models with deep adiabatic atmospheres could definitely be constructed to fit the observed moments (Hubbard, 1968).

Accepting the current best values for the observed effective temperature of Saturn (97 K) and the calculated solar contribution (with $A=0.61$, 71 K) the apparent flux from the interior of Saturn is $H \simeq 3.6 \times 10^3$ erg cm^{-2} s^{-1}. This value is high enough to require some convective energy transport for Saturn. However, Hubbard's (1969) attempts to calculate a completely convective model for Saturn required more helium than for Jupiter and still could not match the required value of K. Smoluchowski (1971) feels that it is unlikely that Saturn has a liquid metallic interior and, as a result, that it has no large magnetic field such as Jupiter's.

The existing model interiors for Saturn are totally unsatisfactory. Accurate measurements of the hydrogen to helium ratio, the luminosity excess (over solar), the values of the gravitational multipoles (without ring contributions), the magnetic field strength (if any), and the structure of the atmosphere (as an upper boundary condition) are all needed if Saturn modeling is to become more than an intellectual exercise.

3.3. Radio-Frequency Radiation

Radio emission from Saturn has been observed over the wavelength range from $\sim$ 1 mm longward to $\sim$ 70 cm. The data in Table XXI give the published values of brightness temperature for Saturn. One clearly distinquishable feature of Saturn's spectrum is the wavelength dependence of the measured temperature. The temperature increases from a value near 130 K at millimeter wavelengths to a value close to 380 K at 50 cm. This behavior is qualitatively similar to the thermal radio spectrum of Jupiter. The measurement at 73 cm (McAdam, 1969) indicates that the brightness temperature is 1690 $\pm$430 K; however, this result appears to be inconsistent with the observed temperature at 50 cm. The exceedingly high brightness temperature may be

entirely due to background confusion effects. Until this measurement is repeated, little reliance can be placed on the result. Nevertheless, the long-wavelength radio measurements appear to be the only ones which probe deep into Saturn's atmosphere, and they should prove to be very important.

A number of suggestions have been put forward to explain the marked increase in temperature with wavelength. These include the possibilities that the excess radiation is due to (1) nonthermal emission from a trapped radiation belt, (2) thermal radiation from Saturn's rings, and (3) emission from Saturn's atmosphere. To date, there has been little experimental evidence which lends support to the first two of these mechanisms. At one time it was suggested, on the basis of an apparent high degree of linear polarization at 10 cm, that the excess radiation comes from a radiation belt similar to the belt surrounding Jupiter (Rose *et al.*, 1963). Later measurements, however, set an upper limit of a few percent on any possible linear polarization (Davies *et al.*, 1964; Kellermann, 1966).

A general discussion of these three possibilities has been given by Berge and Read (1968). These authors conclude that the enhanced microwave radiation from Saturn is entirely, or almost entirely, a phenomenon of Saturn's atmosphere. This conclusion is based strongly on their measurement of the angular extent of the emission source at 10 cm. Using the two-element interferometer at the Owens Valley Observatory, Berge and Read have shown that at least 90% of the 10-cm radiation comes from the visible disk and, within the accuracy of their measurements, that it is uniform across the disk. This result rules out both a trapped radiation belt and the rings of Saturn as the primary source of emission at 10 cm. Gulkis *et al.* (1969) and Gulkis and Poynter (1972) have shown that the gross features of Saturn's centimeter wavelength spectrum can be explained in terms of thermal emission by an atmosphere whose opacity is wavelength-dependent and in which ammonia is assumed to be the principal source of opacity at radio wavelengths. Wrixon and Welch (1970) also measured Saturn's spectrum in the vicinity of the 1.25 cm inversion band of ammonia and found marginal evidence for its presence in their observations. The long- and short-wavelength observations, taken together, argue circumstantially for ammonia being a constituent gas in the atmosphere of Saturn. The radiometric measurements of Saturn are given as shown on Table XXI.

3.4. Rings

The rings of Saturn were first seen by Galileo in 1610 as queer appendages on either side of the planet. The real nature of the appendages as part of a flat ring around the planet was discovered by Huygens in 1655. In the 1670's, Cassini found that the ring was double, a dark line separating it into two concentric rings. The dark line is called Cassini's division, the outer ring A, and the inner ring B. In 1850, Bond at Harvard and Davies in England independently discovered a very tenuous third ring, a 'crape ring' or Ring C, inside the first two. For many years there has been considerable controversy about the existence of a fourth, extremely tenuous ring outside the A ring. Some positive evidence of the reality of this 'D' ring was obtained by Feibelman

TABLE XXI

Disk temperatures of Saturn

Wavelength cm	Disk temperature K	Reference
0.12	140 ± 15	Low and Davidson (1965)
0.32	97^{+52}_{-42}	Tolbert (1966)
0.33	125 ± 13	Epstein *et al.* (1970)
0.34	130 ± 15	Epstein (1968)
0.43	103^{+70}_{-64}	Tolbert (1966)
0.80	132 ± 9	Salomonovich (1965)
0.82	132 ± 4	Kuzmin and Losovsky (1971a)
0.845	151.1 ± 7	Wrixon and Welch (1970)
0.86	116 ± 30	Tolbert (1966)
0.86	96 ± 20	Braun and Yen (1968)
0.96	126 ± 6	Hobbs and Knopp (1971)
0.984	138.1 ± 6	Wrixon and Welch (1970)
1.18	130.8 ± 5	Wrixon and Welch (1970)
1.27	127.2 ± 5.5	Wrixon and Welch (1970)
1.46	133.2 ± 7.5	Wrixon and Welch (1970)
1.53	146 ± 23	Welch and Thornton (1965)
1.53	141 ± 15	Welch *et al.* (1966)
1.90	140 ± 15	Kellermann (1970) [b]
3.12	137 ± 12	Berge (1968)
3.45	144 ± 30 [a]	Cook *et al.* (1960)
3.75	168 ± 11	Seling (1970)
6.0	179 ± 19	Kellermann (1966)
6.0	190 ± 45	Hughes (1966)
9.0	165 ± 25	Berge and Read (1968)
9.4	177 ± 30	Rose *et al.* (1963)
10.0	196 ± 44	Drake (1962)
10.7	172 ± 20	Berge and Read (1968)
11.3	196 ± 20	Kellermann (1966)
11.3	182 ± 20	Davies *et al.* (1964)
21.2	286 ± 37	Davies and Williams (1966)
21.3	303 ± 50	Kellermann (1966)
49.5	385 ± 65	Yerbury *et al.* (1970)
73.5	1690 ± 430	McAdam (1969)

[a] Corrected by Seling (1970) from 106 ± 21 K.

[b] Corrected by Kellermann (1970) from 200 ± 30 given in Kellermann Pauliny-Toth (1966).

during the most recent (1966) edge-on aspect (Feibelman, 1967). The question of its existence must still be considered open. Similarly there have been reports of material inside the crape ring (Bobrov, 1970, p. 382). Most convincing evidence of this has been presented by Guerin (1970). Copies of Guerin's superb Pic du Midi photographs of Saturn, sent to astronomers in the United States, certainly seem to confirm his claim that there is at least a small amount of ring material present virtually down to the atmosphere of the planet. This material is separated from the C ring by a dark

division; so Guerin calls it the D ring (logical, but offering an unfortunate possibility for confusion with material external to the A ring). It has been suggested that any material external to the A ring be called the D′ ring (Franklin *et al.*, 1971).

Arguments have also persisted about the existence of ring divisions other than Cassini's. Kuiper (1957a) has stated firmly that no other true 'divisions' exist, only minor ripples of 10–15% in intensity that vary somewhat with time (Kuiper, 1957a). Encke's 'division' is a permanent feature of Ring A but is only an area of reduced intensity (Dollfus, 1961). Even Cassini's division itself may not be a region devoid of matter. Bobrov (1970) suggests a small but finite value ($\sim 10^{-3}$) for the optical thickness of the Cassini division, and Sekiguchi (1968) in an independent study of the rings during the 1966 edge-on apparition also arrived at a perceptible value for the optical depth ($\sim 10^{-4}$). There does seem to be a real division between the C and D rings, which Franklin *et al.* (1971) have called the 'Guerin' division for obvious reasons.

Dollfus (1970b) has summarized the measurements of the radii of Saturn's rings made over the past 150 yr, and his best values are accepted below for the classical ring structure. The measurements of Franklin *et al.* (1971) are given for the new Guerin division (Table XXII). Whether the observed structure in the rings can be fully explained by resonance processes involving Mimas or other satellites is still being argued (Colombo *et al.*, 1968; Colombo and Franklin, 1969; Franklin *et al.*, 1971; Franklin and Colombo, 1970). For example, a particle at the center of the Cassini division would have a period of revolution very near to half that of Mimas (but just a bit more than half, 0.513, according to the values quoted in Table XXII).

Maxwell showed theoretically in 1857 that a solid ring rotating around a planet would not be stable, and Keeler showed spectroscopically in 1895 that the rings were

TABLE XXII

Saturn's rings, dimensions

Parameters	Kilometers	Saturn radii
Equatorial radius of Saturn	60000 ± 240	1.00
Outer edge of ring D	72600 ± 2000	1.21
Guerin division	Width ~ 4200 km	
Inner edge of ring C	76800 ± 2000	1.28
Inner edge of ring B	92000 ± 850	1.54
Outer edge of ring B	117800 ± 350	1.97
Cassini division	Width ~ 2600 km[a]	
Inner edge of ring A	120400 ± 400	2.01
Outer edge of ring A	136450 ± 350	2.28
Semimajor axis of orbit of Janus	168700 (Franklin *et al.*, 1971)	2.81

[a] The edges of the A and B rings are not sharp. Direct measurements of the width of the Cassini division often result in much larger values (i.e. ~ 3500 km, Dollfus, 1970b).

in differential rotation. Rather direct proof of the particulate nature of the rings is the fact that on at least six occasions stars have been seen right through the A ring, even though of magnitude 7.2 or fainter (Bovrov, 1963). On at least two occasions stars of eighth magnitude were seen part of the time during passage behind the brighter, more dense B ring (Bovrov, 1963).

The optical depth in the rings is quite variable as a function of radial distance from Saturn. Furthermore, since the occultations of various stars by the rings have not been observed photometrically, optical depths have been determined only by measurements of the visibility of Saturn's disk through the rings or by attempting to fit various photometric data with ring models. By the latter method, Franklin and Cook (1965) found an optical depth of 1.0 for the dense part of the B ring, while new modeling of Lumme (1970) gives 1.25. For the brightest part of the A ring, Franklin and Cook (1965) found optical density of ~ 0.4, and Lumme (1970) of 0.3. Cook and Franklin (1958) have interpreted old visual observations of an occultation of Iapetus observed by Barnard to indicate that optical depth in the C ring varies from zero at its inner edge to 0.18 at the outer edge.

All models of Saturn's rings are based upon matching photometric observations of the rings, giving the apparent surface brightness as a function of wavelength, phase angle, and angles of incidence and observation (see Appendix B on Photometric Systems and Terminology). Unfortunately, the maximum phase angle as seen from Earth never exceeds 6 deg nor does the angle of observation ever exceed 30 deg. Modern models have relied heavily upon interpretation of the open ring photometry of Franklin and Cook (1965) and the ring edge-on data of Focas and Dollfus (1969). Other data have been summarized in Bobrov (1970). Unfortunately, the results are not unique.

The only times the rings have been observed when Earth was exactly in their plane occurred in October and December of 1966 (Bobrov, 1970). Even then, the rings did not completely disappear in large telescopes as it had sometimes been predicted they would. Based upon these observations Focas and Dollfus (1969) found a ring thickness of 2.8 ± 1.5 km, while Kiladze reported a thickness of 0.9 ± 0.6 km in 1967*, amended to 1.42 ± 0.49 km in a paper given at the 1968 Kiev conference (Kiladze, 1968). While these measurements vary somewhat, principally because there is strong irradiation from the bright disk of Saturn, there is no longer any real probability that the ring is less than about 100 m thick. It is also extremely unlikely that it is more than 5–10 km thick.

The rings are far from completely defined by an optical depth and an approximate thickness. They exhibit a strong opposition effect (see Appendix B), and it was traditionally assumed that a model at least several particles thick was required, so that a reduction in the shadowing of one particle by another near zero plase could account for the increased brightness. Cook and Franklin (1970a) suggest that many individual large bodies exhibit an opposition effect (for example the Moon and Mars) and that

* From Franklin and Colombo (1970). Primary references not readily available.

a monolayer of large particles, perhaps a few hundred meters in size, is a very acceptable model of the rings and in fact has the advantage of no nodal collisions. Bobrov (1970) has calculated several suitable multilayer models, including some with dispersions of five orders of magnitude in particle size.

The problem of ring stability is a troublesome one. Several recent efforts have corrected and improved upon Maxwell's original work (Cook and Franklin, 1964, 1966; Yabushita, 1966) and find the rings to be quite stable, but all of these assume non-colliding particles, and all are concerned strictly with mechanical (non-radiative) effects. Collision of particles in nearly equal Keplerian orbits will be at low relative velocity and rather large coefficient of restitution, but there will inevitably be some collisional heating and loss of energy from the ring, as well as some particle disruption in more vigorous collisions. In a multilayer model, there must be collisions near the nodal points, and these will tend to reduce the rings to a monolayer. Bobrov (1970) suggests that there is a transformation of rotational energy into chaotic movement, because of the collisions, that assures a thickness of at least 120 m and that satellite perturbations may introduce an additional out of the plane component. There must be collisions, even in a monolayer, introduced by perturbations of the satellites. Watson *et al.* (1963) have shown that a 1-cm (radius) particle will be swept into Saturn from the outer edge of the A ring in just over one billion years by the Poynting-Robertson effect, while the C ring will have been swept clean of all 10-cm (radius) particles during the age of the solar system.

An upper limit on the mass of the rings has been set in the collisionless stability studies, being $\sim 10^{-2}$ of Saturn's mass for a reasonable ring model (Yabushita, 1966). No one seriously suggests the ring approaches this mass, however. Bobrov (1970) suggests a mass of 8×10^{23} g. This is 1.4×10^{-6} that of Saturn's mass. Franklin *et al.* (1971) argue for a mass of at least 6×10^{-6} of Saturn's mass. Even if the rings are only 100 m thick and have a volume density of only 10^{-4} and a particle density of 1 g cm^{-3}, they still have a mass of 3×10^{20} g. These numbers are far larger than those quoted fairly recently when a much thinner ring was in vogue.

The composition of the ring particles is of great importance in any attempt to understand the history of the Saturn system. Very low dispersion infrared scans made in the late 1940's suggested to Kuiper (1952) that they were frost or ice, or at least frost-covered particles. The vapor pressure of ice at the mean temperature of the rings is so low that evaporation is negligible even over eons (Watson *et al.*, 1963). Work by Owen (1965a) using higher dispersion seemed to him to confirm the ice identification. Later paraformaldehyde was suggested as a possible ring material (Mertz and Coleman, 1966), and there was a misidentification suggesting ammonia. The current best infrared spectra of the rings indicate the presence of water frost more strongly than ever (Pilcher *et al.*, 1970). The rings are not exclusively water, however. The reflection spectrum from 0.3–1.05 μ is incorrect for pure water, decreasing sharply in the blue and ultraviolet rather than remaining flat (Lebofsky *et al.*, 1970). The ring particles must be of mixed composition, either individually or collectively. A simple coating is probably not an adequate explanation, since calculations indicate that photo-

sputtering will erode several centimeters of ice in 5 eons (Harrison and Schoen, 1967). Spectrographic searches for a gaseous component to the rings have so far been unsuccessful when proper care was taken to exclude light scattered from Saturn (Franklin and Cook, 1969).

Photometry* of the rings indicates that they are somewhat more red than the Sun, $(B-V)_{\text{ring}}-(B-V)_{\odot}=0.28$ (Franklin and Cook, 1965). They show an opposition effect of about 0.29 magn. in the B passband and 0.24 magn. in the V passband, with a linear phase variation of 0.036 magn. deg^{-1} in each band. Franklin and Cook (1965) also give surface brightness at opposition for five different parts of the ring. Moving inward, with no special feature of the ring indicated by the numbers, they find the following data for the surface brightness of Saturn's rings (Table XXIII).

TABLE XXIII

Saturn's rings, photometric properties

Ring element	A_1	A_2	B_1	B_2	B_3
Optical depth	0.17	0.36	1.0	0.61	0.32
V magn (arc s)$^{-2}$	7.20	6.69	6.35	6.47	6.80
B magn (arc s)$^{-2}$	8.06	7.55	7.21	7.33	7.66

Values for the various types of albedo depend on the ring model chosen and on the value of the opposition effect. Lumme (1970) finds in both B and V passbands a geometric albedo of 0.82 and a Bond albedo of 0.90 for the ring particles, assuming a multilayer model and Franklin and Cook's phase variation. Other authors have found vastly different results. The average V magnitude of the disk of Saturn is 6.9 at opposition, so most of the ring has a higher surface brightness than the average part of the planetary disk. The individual particle albedo must be quite high, if the ring is a monolayer. Reflectivities at 22 wavelengths from 0.3 to 1.05 μ have been given for the B ring by Lebofsky *et al.* (1970).

Allen and Murdock (1971) measured a ring brightness temperature at 12.7 μ (10–14 μ) of 83 K. This is surprisingly high. If the Bond bolometric albedo of the individual ring particles is as high as the Bond visual albedo given in the preceding paragraph (0.90), their mean temperature should be only 50 K, assuming they rotate rapidly, or 60 K if they keep one face toward the Sun. The rings are not optically thick either, which would reduce the measured temperature a bit further. There will be a component of reradiation from Saturn to be added to the figures above. One is inclined to suspect a lower bolometric albedo than suggested by Lumme (1970). Kellermann (1970) notes that 2-cm observations at NRAO appear to show an effect of a changing ring aspect in the apparent flux from Saturn, but the results include a combination of effects, and the data are so far insufficient to disentangle them.

The rings of Saturn present a considerable challenge, their very structure and composition still being open to question as well as the more fundamental problems

* See Appendix B for definition of photometric terminology.

concerning their origin. Are they remnants of primordial material never able to form a satellite because it was inside Roche's limit, or could they somehow have been formed more recently? Lyttleton* has asked the very pregnant question, "How can the rings be exactly in the equatorial plane of a precessing planet?" In many ways the rings remain as puzzling as they are beautiful.

3.5. SATURN'S SATELLITES

Saturn has ten satellites, seven of them quite regular, two (Hyperion and Iapetus) rather borderline, and one (Phoebe) a distinctly irregular retrograde satellite. This can best be seen from Table XXIV, which is adapted from Porter (1960) except where noted.

TABLE XXIV

Satellites of Saturn: orbital data

Satellite	Semimajor axis, km	Eccentricity	Inclination[a]	Period, days
Janus[b]	168700	~0	~0	0.815
Mimas	185800	0.0201	1°31.0′	0.942422
Enceladus	238300	0.00444	0°01.4′	1.370218
Tethys	294900	0	1°05.6′	1.887802
Dione	377900	0.00221	0°01.4′	2.736916
Rhea	527600	0.00098	0°21′	4.517503
Titan	1222600	0.029	0°20′	15.945452
Hyperion	1484100	0.104	(17–56′)[c]	21.276665
Iapetus	3562900	0.02828	14.72°	79.33082
Phoebe	12960000	0.16326	150.05°	550.45

[a] To plane of ring.
[b] Adopted from Franklin *et al.* (1971).
[c] Varies from 17′ to 56′ according to Russell, *et al.* (1945).

Satellite X (Janus) was discovered during 1966 when Saturn's rings were 'edge-on'. Even with the light from the rings almost zero, Janus is a difficult object to see, having a magnitude of only 13–1/2 or 14 and located next to a very bright planet (Dollfus, 1967; *Sky and Telescope*, 1967; Texereau, 1967). Absolute confirmation that the object observed is, indeed, a satellite and not just a ring condensation will probably have to wait until the rings are again 'edge-on', although the best of the photographs are very convincing.

The satellites of Saturn are rather substantial bodies, Titan being somewhat larger and more massive than the Moon. The diameters in Table XXV are taken from Dollfus (1970), the masses from Kovalevsky (1970). Mean densities were calculated. New diameters have been calculated for Rhea and Iapetus by Murphy *et al.* (1972) using combined radiometric (20 μ) and visual photometric measurements. They as-

* Private communication.

TABLE XXV

Satellites of Saturn: physical data

Parameter	Mimas	Enceladus	Tethys	Dione	Rhea	Titan	Iapetus
Mass (Saturn = 1)[a]	$0.67 \pm 0.02 \times 10^{-7}$	$1.5 \pm 0.5 \times 10^{-7}$	$11.4 \pm 0.3 \times 10^{-7}$	$18.5 \pm 0.6 \times 10^{-7}$	$\sim 3 \times 10^{-6}$	$2.42 \pm 0.02 \times 10^{-4}$	$2.5 \pm 1.3 \times 10^{-6}$
Mass (Moon = 1)[b]	0.000052	0.001	0.0088	0.0143	~ 0.02	1.87	0.02
Mean diameter km[c]	[d]	550 ± 300	1200 ± 200	820 ± 400	1300 ± 300	4850 ± 300	1300 ± 400
Mean diameter (Moon = 1)[e]	[d]	0.16	0.35	0.24	0.37	1.40	0.37
Mean density g cm^{-3}	~ 0.7?[d]	~ 1.0	0.7	~ 3.6	~ 1.5	2.31	~ 1.2

[a] Mass of Saturn = 5.685×10^{26} kg (Klepczynski, 1971). Uncertainties quoted are probable errors (Kovalevsky, 1970).
[b] Mass of Moon = 7.347×10^{22} kg (Haines, 1971).
[c] Uncertainties quoted are said to be an estimate of the 'maximum error' (Dollfus, 1970a).
[d] If the albedo is the same as that of Enceladus, Mimas' diameter is $\sim 470 \pm 300$ km. A very low geometric albedo could make it three times that size.
[e] Diameter of Moon = 3475 km (Haines, 1971).

sumed unit emissivity and a bolometric albedo equal to the visual albedo and derived diameters of 1550 km and 1740 km respectively.

Older figures (Kuiper, 1952) made it appear that there was a general increase in density of the satellites with increasing distance from Saturn. Improved values for the radii, particularly of Tethys, have destroyed this trend. In fact, the most notable thing about the satellites now is the remarkably low apparent density of all but Dione and Titan. Certainly, all the radii need verification by means of spacecraft photography, since the possible errors vary from 17 to more than 50% ,except for Titan, and these errors are tripled in the density values.

Photometric data are difficult to obtain for Mimas because of its proximity to Saturn and the rings. Its mean visual magnitude is about $V_0 = 12.1$ (Russell *et al.*, 1945; Harris, 1961). Phoebe has been rather ignored, perhaps because of the greater effort required to find it. Kuiper (1961) has reported a blue photographic magnitude of 17.3, which is roughly equal to $B = 17.4$ and $V = 16.8$, assuming the same color as the Sun. This is more than two magnitudes fainter than given in some standard references and explains why Phoebe is often sought in vain in smaller telescopes.

Mean opposition magnitudes and colors for the other satellites in the UBVsystem have been given as follows by Harris (1961) except for UB and V for Titan which are taken from Blanco and Catalano (1971) (Table XXVI).

TABLE XXVI

Saturn's satellites, photometric data

Parameter	Enceladus	Tethys	Dione	Rhea	Titan	Hyperion	Iapetus
Magnitude $\bar{V}_0$	11.77	10.27	10.44	9.76	8.354	14.16	11.03
Magnitude $\bar{B}_0$	12.39	11.00	11.15	10.52	9.647	14.85	11.74
Magnitude $\bar{U}_0$	–	11.34	11.45	10.87	10.398	15.27	12.02
Color $U-B$	–	0.34	0.30	0.35	0.75	0.42	0.28
Color $B-V$	0.62	0.73	0.71	0.76	1.293	0.69	0.71
Color $V-R$	–	–	0.48	0.61	0.844	–	–
Color $R-I$	–	–	0.32	0.26	0.11	–	–

When set equal at V, the color differences between satellite and the Sun are as shown in Table XXVII.

McCord *et al.* (1971) used the same photometric system as for their Galilean satellite work (see Section 2.4) to study Tethys, Dione, Rhea, Titan, and Iapetus. Blanco and Catalano (1971) carried out detailed photometry of Rhea and Titan in the UBV system. These new data are an amplification of Harris' work, with some exceptions. McCord *et al.* (1971) find systematically brighter results in the blue and ultraviolet, except for Titan, while they find Dione, Rhea, and Titan to be fainter in the red than did Harris. The source of the disagreement is not obvious.

The magnitudes quoted are mean opposition magnitudes. Iapetus is most unusual in that it varies 2.12 visual magnitudes about that mean $\bar{V}_0$, a factor of more than six in brightness (Harris, 1961). The maximum occurs near western elongation from

TABLE XXVII

Saturn's satellites, color compared to the Sun

Difference (Sat. − ⊙)	Enceladus	Tethys	Dione	Rhea	Titan	Hyperion	Iapetus
Passband U	–	0.30	0.24	0.34	1.27	0.34	0.22
Passband B	−0.01	0.10	0.08	0.13	0.66	0.06	0.08
Passband V	0	0	0	0	0	0	0
Passband R	–	–	−0.03	−0.16	−0.39	–	–
Passband I	–	–	−0.06	−0.13	−0.21	–	–

Saturn, the minimum near eastern elongation. Yet, in spite of the large change in brightness, the colors $U-B$ and $B-V$ vary only 0.04 magn. (Harris, 1961). McCord *et al.* (1971) find a somewhat greater color change ($\sim$0.10 magn.) in the red near 7500 Å. Cook and Franklin (1970b) suggest that one side of Iapetus is 'ice'-covered while the other has had the ice largely eroded away by nonisotropic meteoroid bombardment. The small color change means that most of the sunlight must still be reflected from remnants of ice even on the dark side, the material under the ice having very low reflectivity. Murphy *et al.* (1972) derive a dark-side bolometric albedo of 0.04 and a temperature of 117 K, with a bright-side albedo of 0.28 and a temperature of 109 K. Large-scale 'preferential treatment' of one hemisphere is always a bit hard to accept, but whatever the cause, Iapetus is, photometrically, grossly asymmetric.

Rhea, Dione, and Tethys are similar, rather bluish objects according to McCord *et al.* (1971). All show a tendency, Rhea most strongly, for the leading side to be brighter than the trailing side. This would indicate synchronous rotation. Blanco and Catalano's (1971) more detailed data on Rhea show this asymmetry very clearly, the satellite being 0.23 magn. brighter in the V passband at 0 deg rotational phase than at 180 deg, with little or no variation in color. Blanco and Catalano's UBV results are in excellent agreement with Harris', but they did not observe in the R and I passbands.

Titan is a very reddish object, much more red than the Sun. None of the three teams that have carried out major photoelectric studies of Titan have found any variation of brightness with orbital phase. Blanco and Catalano (1971) have reported a clear variation with solar phase angle α, and give the following formula for the V passband:

$$V(\alpha) = 8^{m}.354 + 0^{m}.0092\alpha - 0^{m}.0005\alpha^{2}.$$

The fact that Titan is photometrically very different is not surprising, since it has an atmosphere. This is discussed in paragraphs which follow.

The geometric albedo is an important quantity, both absolutely and in its general trend with wavelength. Values to show the change with wavelength therefore are given in Table XXVIII even though the radii of most of the satellites are quite uncertain. These have been calculated from the radii in Table XXV and the magnitudes in the preceding paragraph. The magnitude of the Sun, $V_{\odot} = -26.8$, is assumed. It

TABLE XXVIII

Saturn's satellites, geometric albedo

Passband	Enceladus	Thethys	Dione	Rhea	Titan	Iapetus
U	–	0.46	0.89	0.61	0.07	0.21
B	0.73	0.56	1.04	0.74	0.12	0.24
V	0.73	0.61	1.12	0.83	0.22	0.26
R	–	–	1.15	0.96	0.31	–
I	–	–	1.18	0.94	0.27	–

must be remembered that the *U* values may be too low and the *R* and *I* values too high if the McCord *et al.* photometry is correct.

The albedos for the smaller bodies are generally quite high, except for Iapetus, and show small variation with wavelength, the type of behavior typical to a frost-covered object, for example. The behavior of Titan is completely different, normalized spectral reflectivity being practically identical to the center of the disk of Saturn itself (McCord *et al.*, 1971), while the absolute values are about half as great. Harris (1961) reports a rough measurement by Kuiper at a wavelength of 2 μ. The geometric albedo there is about 20% of what it is at 1 μ, roughly 0.05.

In 1944, Kuiper (1944) announced the definite detection of two methane bands on Titan, the 6190- and the 7260-Å bands. The work was done with a prism spectrograph having a dispersion of only 340 Å mm^{-1} at Hγ, but the absorptions were quite plain. Kuiper (1952) later empirically estimated the abundance at 200 m atm, without any correction for temperature effects. The actual abundance is very uncertain.

be $\sim$5 amagat. The abundance, with η (the atmospheric path length) equal to three, is then $\sim$200 km amagat. However, a reflecting layer model is particularly uncertain for Uranus. Rayleigh scattering alone implies need for a homogeneous scattering model when abundances approaching 500 km amagat are reached, and, in fact, there are probably methane hazes and ammonia clouds present as well (Prinn and Lewis, 1972), implying need for a full inhomogenous treatment of the atmosphere.

The 1968 occultation of a star by Neptune resulted in the measurement of a large-scale height, proving that the atmosphere of that planet, too, is extensive and largely hydrogen (Freeman and Lynga, 1970; Kovalevsky and Link, 1969).

Owen (1967a) found that weak lines in the spectra of Uranus and Neptune, unidentified for many years, result from extremely weak methane bands. According to him, the visibility of these lines indicates that Uranus must have 'on the order of 3.5 km atm of methane', while Neptune has perhaps 6 km atm. He cautions that nothing is yet known about the temperature sensitivity of the bands and that no correction was possible from laboratory temperature to the very low temperatures of Uranus and Neptune.

Ammonia has not been identified in optical spectra of Uranus or Neptune, which is not surprising considering the temperatures of these bodies. There is a hint, in the measurements of radio brightness temperature of both planets, that gaseous ammonia

12- and 20-μ results is another matter. The only common atmospheric gas that absorbs in the 18–25 μ region is H_2. Morrison *et al.* (1972) suggest that a few hundred kilometer amagats of H_2 may be present, resulting in a low temperature at 20 μ (and a surface pressure near 1 atm). Even a flat, nonrotating blackbody at the distance of Titan from the Sun can only have a temperature of 125 K. A fairly massive greenhouse effect is also needed to account for the high temperatures at 12 μ – additional evidence for a relatively massive atmosphere.

Titan has been known to have an atmosphere for more than a quarter century. Within the past 2 yr, evidence has been gathered that that atmosphere may be quite extensive, but composition and abundances are still most uncertain. A massive hydrogen atmosphere on so small a body initially sounds improbable, but some evidence points in that direction. Additional ground-based and probe studies are badly needed.

4. Uranus and Neptune

4.1. Atmospheres

4.1.1. *Composition*

Uranus and Neptune are smaller and colder than their companion giant planets. Their greater distance from Earth and the Sun has made them difficult objects to study photographically, spectrometrically, or radiometrically at any wavelength. Their spectra are dominated by tremendously strong methane absorption in the red and near-infrared. This absorption in the red is at least partially responsible for the greenish visual appearance of these bodies.

Hydrogen was first identified on Uranus and Neptune in 1952 through laboratory studies by Herzberg (1952), who identified a diffuse feature at 8270 Å as a line of the second harmonic (the 3–0 band) in the pressure-induced dipole spectrum of molecular hydrogen. In 1963, Spinrad (1963) reported observation of the S(0) transition in the 4–0 band of the dipole spectrum on both Uranus and Neptune. At that time, he also noted discovery of the S(0) line of the 4–0 band in the quadrupole spectrum of hydrogen on Uranus only. Later, Giver and Spinrad (1966) reported on both the S(0) and S(1) lines of the 4–0 quadrupole band on Uranus. No quadrupole lines have been reported on Neptune. The abundances of H_2 on Uranus and Neptune are very uncertain because of uncertainty about the conditions under which the spectral lines are formed, as well as the usual paucity of observations. The very existence of the high-overtone, pressure-induce features suggests higher abundances and pressures than on Jupiter or Saturn. A recent analysis of Giver and Spinrad's data by Belton *et al.* (1971) gives a vertical column abundance of 480 km atm, based upon a reflecting layer model. Other analyses have given both larger and smaller values (Poll, 1971), but none have used a proper Galatry profile for the quadrupole lines and taken proper account of saturation. Poll (1971) has attempted to derive an abundance from the pressure-induced dipole lines, using observations of Giver and Spinrad (1966). The result depends upon the density at the 'reflecting surface', which it is suggested may

be ~ 5 amagat. The abundance, with η (the atmospheric path length) equal to three, is then ~ 200 km amagat. However, a reflecting layer model is particularly uncertain for Uranus. Rayleigh scattering alone implies need for a homogeneous scattering model when abundances approaching 500 km amagat are reached, and, in fact, there are probably methane hazes and ammonia clouds present as well (Prinn and Lewis, 1972), implying need for a full inhomogenous treatment of the atmosphere.

The 1968 occultation of a star by Neptune resulted in the measurement of a large-scale height, proving that the atmosphere of that planet, too, is extensive and largely hydrogen (Freeman and Lynga, 1970; Kovalevsky and Link, 1969).

Owen (1967a) found that weak lines in the spectra of Uranus and Neptune, unidentified for many years, result from extremely weak methane bands. According to him, the visibility of these lines indicates that Uranus must have 'on the order of 3.5 km atm of methane', while Neptune has perhaps 6 km atm. He cautions that nothing is yet known about the temperature sensitivity of the bands and that no correction was possible from laboratory temperature to the very low temperatures of Uranus and Neptune.

Ammonia has not been identified in optical spectra of Uranus or Neptune, which is not surprising considering the temperatures of these bodies. There is a hint, in the measurements of radio brightness temperature of both planets, that gaseous ammonia may be present deep in the atmospheres (see Section 4.1.2).

McElroy (1969) has neatly summarized the problem of attempting to say anything about helium on Uranus or Neptune. His conclusion is that there is no good spectroscopic evidence one way or the other. Helium may or may not be present.

4.1.2. *Temperatures and Energy Balance*

In 1966, Low (1966) reported a brightness temperature for Uranus at 20 μ (17.5–25 μ) of 55 ± 3 K. Ney and Maas (1969) have reported values near 270 K at 3.6 μ (1-μ bandwidth) on Uranus. All other brightness temperatures have been measured at microwave frequencies.

Radio emission from Uranus has been observed over the wavelength range from 3 mm to 11 cm, while for Neptune, observations extend from 3 mm to 3 cm. The apparent disk brightness temperatures, based on the angular sizes obtained from the American Ephemeris and Nautical Almanac (AENA), are given in Tables XXX and XXXI. It should be noted that the measured disk temperatures for these planets may be systematically too high, owing to an underestimate of the angular sizes of the planets. The reported temperatures for Uranus should be decreased by $\sim 15\%$ if its radius is taken as 25400 km, as discussed in Section 4.2. For Neptune, the temperature should be decreased by $\sim 20\%$ if its radius is taken as 24750 km. These corrections alter the mean level of the temperature but do not change the shape of the spectrum, because all published values to date are based on the AENA values.

As was true for Saturn, the only analyzed molecular bands that has been observed on Uranus is the 4–0 quadrupole band of H_2. Belton *et al.* (1971) have used the data of Giver and Spinrad (1966) to derive a rotational temperature of 118 ± 40 K. No values

TABLE XXX

Disk temperatures of Uranus

Wavelength cm	Disk temperature K	References
0.33	105 ± 13	Epstein *et al.* (1970
0.35	111 ± 7	Pauliny-Toth and Kellermann (1970)
0.822	131 ± 15	Kuzmin and Losovsky (1971b)
0.95	125 ± 15	Pauliny-Toth and Kellermann (1970)
1.65	201 ± 16	Mayer and McCullough (1971)
1.95	181 ± 7	Pauliny-Toth and Kellermann (1970)
2.7	212 ± 16	Mayer and McCullough (1971)
3.1	169 ± 20[a]	Berge (1968)
3.75	170 ± 20[a]	Klein and Seling (1966)
6	210 ± 17	Mayer and McCullough (1971)
11.13	180 ± 40	Gerard (1969)
11.3	130 ± 40[a]	Kellermann (1966)

[a] Published temperatures have been increased by 7% to adjust the calibration flux scale to that given by Kellermann (1969).

TABLE XXXI

Disk temperatures of Neptune

Wavelength cm	Disk temperature K	References
0.35	88 ± 5	Pauliny-Toth and Kellerman (1970)
0.95	134 ± 18	Pauliny-Toth and Kellermann (1970)
1.65	194 ± 24	Mayer and McCullough (1971)
1.95	172 ± 22	Pauliny-Toth and Kellermann (1970)
2.7	225 ± 20	Mayer and McCullough (1971)
3.1	115 ± 36	Berge (1968)
6	227 ± 23	Mayer and McCullough (1971)
11.13	< 150	Gerard (1969)

exist for Neptune. An attempt at empirical temperature analysis of the 6800 Å band methane on Uranus led to 'strange' results (Owen, 1966). Even the H_2 temperature for Uranus has little real meaning until additional observations result in improved equivalent widths and some determination of the basic abundances and pressure to be associated with that temperature.

The large 98-deg inclination of Uranus must result in extremely severe seasonal changes, and the seasons on Uranus average 21 terrestrial years in length. During 1966, the axis of Uranus was practically in the plane normal to the solar radius vector, all parts of the planet seeing the sun during one rotational period of 10–11 h. In 1985, the north pole of Uranus will face the Sun continuously, and the effective temperature of the northern hemisphere should rise to about 1.2 times the 1966 planet-wide value, assuming there is no effective heat exchange between hemispheres and no fantastically

large latent heat sink. The dynamics of an extensive planetary atmosphere heated on only one side have been considered relative to Venus; similar studies have not been carried out for Uranus. In the middle 1980's (and at other seasonally similar times, which occur every 42 yr), Uranus will be such a rapidly rotating body, being heated over a hemisphere centered on one pole.

The 1966 effective temperature of Uranus should be about 57 K, assuming a bolometric albedo of 0.35 (see Section 4.1.4); however, it may rise to 68 K in the 1980's, as discussed above. Low's brightness temperature at 20 μ, 55 $\pm$3 K as given above, certainly is consistent with the predicted temperature. Thus, there is no evidence in this one measurement of any internal heat generation in Uranus. The effective temperature of Neptune should be 45 K, assuming the same bolometric albedo used for Uranus. No measurements of infrared brightness temperature have yet been reported for Neptune; such measurements present extraordinarily difficult instrumentation problems. Bolometric albedos are poorly determined for Uranus and Neptune since neither body ever exhibits significant phase as seen from Earth, and no good near-infrared spectrophotometry has been reported for Neptune.

The occultation of BD-17°4388 by Neptune, discussed in Section 4.1.3, implies that a high atmospheric temperature exists at high altitudes, but this is probably an ionospheric temperature and does not imply a temperature imbalance. The Ney and Maas (1969) 3.6-μ temperature is peculiar, since 3.6 μ is in the middle of strong CH_4 absorption and seems unlikely to penetrate from anything like a depth corresponding to 270 K on a cold planet.

As in the case of both Jupiter and Saturn, the radio brightness temperatures significantly exceed the expected equilibrium temperatures. It is of interest to note that the radio brightness temperatures of the four major planets are approximately the same at wavelengths near a centimeter, although their distance from the Sun ranges from 5.2 to 30 AU. It has been suggested that saturated ammonia vapor in the cooler upper atmospheres of all the major planets would cause them to have nearly the same brightness temperature at wavelengths near 1.25 cm, the characteristic strong inversion band of ammonia. For both Uranus and Neptune, there is a definite increase in brightness temperature with increasing wavelength from 3 mm to $\sim$2 cm. This can be explained in terms of thermal emission by an atmosphere whose opacity is wavelength-dependent (see Section 4.1.3). The longer-wavelength spectrum (>3 cm) of Uranus is considered highly uncertain.

4.1.3. *Atmospheric Structure*

The thermal opacities of the atmospheres of Uranus and Neptune are dominated by molecular hydrogen, as is the case for Jupiter and Saturn (Trafton, 1967). Fox and Ozier (1971) have suggested that additional thermal opacity is induced by methane, while Trafton (1972c) argues that the amount of gaseous methane available is insufficient to contribute significantly. All quantities are sufficiently uncertain at this time that it is necessary to remain conscious of all possibilities.

Visible atmospheric absorptions are small, except for the very strong methane

bands, which begin to absorb very strongly near 6190 Å and at many longer wavelengths. Both molecular and aerosol scattering may well play a significant role in the visible opacity, as already noted. The attempt of Belton *et al.* (1971) to reproduce the observed features of Uranus with a semi-infinite, pure molecular hydrogen atmosphere failed to match observed geometric albedos (Appleby and Irvine, 1971; Binder and McCarthy, 1972) or microwave brightness temperatures.

The observations of BD-17°4388 while it was being occulted by Neptune showed a number of spikes. They were well correlated in time for nearby telescopes and not at all correlated for great distances between receivers (telescopes), thus indicating structures 10–15 km thick with line-of-sight extent $\geqslant 1000$ km (Freeman and Lynga, 1970). These observations offer evidence of atmospheric structure, an atmospheric layering at high levels similar to that observed during the Jupiter occultation of β Scorpii. The extreme spikes or flashes could be caused by planetary scintillation (Kovalevsky and Link, 1969).

The measured scale height for Neptune is 28.9 ± 2.6 km according to Freeman and Lynga (1970), corresponding to a value of $T/\mu = 38$, where T is temperature in deg. K and μ is the mean molecular weight. An independent interpretation of the occultation by Kovalevsky and Link (1969) results in a scale height of 60 km and $T/\mu \sim 80$. The differences are caused entirely by differences in the techniques used to fit the observational data, those of Kovalevsky and Link being the more sophisticated. The high temperatures implied very probably refer to the ionosphere of the planet.

Trafton (1967) published radiative models for the atmospheres of Uranus and Neptune more than 5 yr ago. Little further progress has been made because of the lack of good observational data. It is suspected theoretically that the H/He ratio will be smaller on those bodies than on Jupiter and Saturn, but there is no observational evidence of any sort, one way or the other. Good abundances and rotational temperatures for H_2 and CH_4 are needed. Variation of absorption line strengths from center-to-limb would be valuable but difficult to obtain without a space probe. Variation of strength in a given location and absorption band from rotation line to rotation line may be possible to obtain from Earth. A repeat of the peculiar 3.6-μ flux measurement is needed, as are brightness temperatures in the 5-μ window and throughout the thermal emission spectrum. A number of these observational pieces must be obtained before there can be any hope of assembling the atmospheric puzzles of Uranus and Neptune.

4.1.4. *Visible Surfaces*

Under conditions of average viewing, Uranus appears in a telescope as a small, greenish disk, featureless except for some limb darkening. When the equatorial regions of the planet are visible and the viewing is excellent, two faint belts on either side of a bright zone are sometimes seen in larger telescopes (Alexander, 1965). Additional structure is occasionally reported. Most interesting is the fact that virtually all observers who have measured the position angle of the belts relative to the plane of the satellites, including E. E. Barnard (the doyen of visual observers) using the 91-cm

Lick refractor, have found the belts inclined by some 25° (Alexander, 1965). (The complete list of measurements contains values from 10 through 40°). As nearly as has been determined, the plane of motion of the satellites lies in the equatorial plane.

Neptune is almost always described as having a small, featureless green disk when seen in any telescope. Dollfus (1961) has described it as showing pronounced limb darkening and very weak spots of irregular shape but no band structure.

Whether the surface structures actually seen on Uranus and Neptune are ammonia clouds, methane clouds, or just density fluctuations in the predominating hydrogen can not be stated for certain until better temperature profiles and abundances become available for the two planets.

With no obvious surface features to help measure the periods of rotation, photometric techniques were attempted, with conflicting results (Harris, 1961; Alexander, 1965. Finally, the spectroscopic technique of measuring the rotational velocity from the doppler shift of spectral lines was applied. In 1930, Moore and Menzel (1930) published a rotation period for Uranus of 10.8 h (the period usually quoted today), noting that it could be in error by as much as 0.5 h. This should clearly be redetermined from Earth, using modern equipment. Similarly, Moore and Menzel (1928) published in 1928 the rotation period still quoted for Neptune, 15.8 $\pm$1.0 h.

Photometric data* in the UBV system, as given by Harris (1961), are as given in Table XXXII.

TABLE XXXII

Photometric data for Uranus, I

Magnitude at unit distance: $V(1.0) = -7.19$				
Mean opposition magnitude:		$V_0 = +5.52$		
Colors:				
$U-B$	$B-V$	$V-R$	$R-I$	
0.28	0.56	−0.15	−0.80	
Brightness at mean opposition:				
U	B	V	R	I
6.36	6.08	5.52	5.65	6.45
Color differences, Uranus-Sun (setting them equal for V):				
U	B	V	R	I
+0.07	−0.07	0	+0.60	+1.69

The following geometric albedos have been calculated using the new radius for Uranus (see Section 4.2) and Harris' data from above.

Passband	U	B	V	R	I
Geometric albedo	0.48	0.55	0.51	0.30	0.11

* Photometric nomenclature is discussed in Appendix B.

Both Uranus and Neptune have tremendous absorption in their atmospheres in the red and near-infrared caused by methane. This shows in the large color differences between the planet and the Sun in the *R* and *I* passbands.

Recently magnitudes and albedos for Uranus on the narrower passband, Harvard photometric system have been published by Appleby and Irvine (1971). Younkin (1970) has obtained very narrow passband (50 Å) measurements at 110 wavelengths between 0.33 and 1.11 μ. Binder and McCarthy (1972) have obtained data in ten medium width passbands from 0.60 to 2.27 μ. Intercomparison is somewhat complicated by the changing aspect of this oblate planet and by the inclusion of varying methane absorptions in passbands of varying width. In general, Uranus is highly reflective in the blue and green and heavily absorbing in the red and near-infrared.

In Table XXXIII only selected values have been taken from Younkin's work, mostly at wavelengths of high reflectivity between methane absorption features. A few values have been selected to fill gaps or to illustrate the extensive absorption. All data are corrected to the Uranian radius of Table I, but only Younkin's data are corrected, by him, for the changing planetary aspect. Harvard magnitudes are the average of Boyden and Le Houga results.

Younkin's values for geometric albedo are systematically a bit higher than Appleby and Irvine's. This may represent a difference in the calibration tying the measurements to the Sun.

Younkin and Munch (Younkin and Munch, 1967; Younkin, 1970) derived a bolometric geometric albedo for Uranus of 0.32. Correcting for the diameter in Table I, this becomes 0.28. Younkin (1970) suggests a phase integral of 1.25, thus deriving a bolometric Bond albedo for Uranus of 0.35. That value is adopted here for Neptune as well. Since the maximum phase angle achieved by Uranus is only 3°.1 as seen from Earth, and that for Neptune is only 1°.9, spacecraft measurements of the phase integral are clearly needed for accurate radiation balance studies.

The photometric data for Neptune given by Harris (1961) are as shown in Table XXXIV.

Again, the geometric albedos have been recalculated using the new radius and Harris' photometric data.

Passband	*U*	*B*	*V*	*R*	*I*
Geometric albedo	0.46	0.49	0.40	0.19	0.07

Narrowband photoelectric data for Neptune have not yet been published.

4.2. Body structures of Uranus and Neptune

Attempts to construct model interiors for Uranus and Neptune have followed the same approach as those described in Section 2.2 for Jupiter. Because of apparently greater mean densities in spite of lower mass, models have typically added large amounts of metallic ammonium NH_4 (Reynolds and Summers, 1965; Porter, 1961) or a mixture

TABLE XXXIII

Photometric data for Uranus, II

Effective wavelength Å	Bandwidth Å	Opposition magnitude	Geometric albedo	Source[a]
3147	290	5.60	0.479	A
3325	50	6.25	0.545	Y
3475	50	6.31	0.522	Y
3590	240	5.58	0.478	A
3775	50	6.02	0.563	Y
3926	90	5.48	0.526	A
4155	180	5.47	0.528	A
4325	50	5.92	0.606	Y
4573	170	5.41	0.558	A
4725	50	5.28	0.617	Y
5012	180	5.38	0.574	A
5377	50	5.81	0.408	Y
5632	50	5.47	0.568	Y
5923	50	5.67	0.489	Y
6264	320	6.32	0.247	A
6336	50	5.77	0.481	Y
6790	50	6.13	0.384	Y
7297	400	7.67	0.070	A
7530	50	6.58	0.295	Y
7950	50	8.46	0.057	Y
8298	50	6.99	0.240	Y
8595	180	8.53	0.033	A
8926	50	9.68	0.022	Y
9000	760	–	0.033	B
9391	50	7.23	0.240	Y
10120	50	10.06	0.021	Y
10500	840	–	0.035	B
10635	1540	8.12	0.046	A
10800	50	8.19	0.135	Y
12600	980	–	0.020	B
16200	940	–	0.015	B
17400	820	–	0.000	B
21700	620	–	0.006	B
22700	640	–	0.005	B

[a] A – Appleby and Irvine (1971), B – Binder and McCarthy (1972), Y – Younkin (1970).

of CH_4, NH_4, H_2O, and Ne in cosmic proportions called 'CHONNE' material by Ramsey (1967). The recent changes in the radii of Uranus and Neptune, discussed below, have made all published models completely worthless as models, although the work on high-pressure equations of state clearly remains of interest.

On April 7, 1968, Neptune occulted an eighth-magnitude star, BD-17°4388. From this occultation, Freeman and Lynga (1970) found a mean equatorial radius (at optical depth unity in an isothermal atmosphere of H_2 with 1% CH_4) of 24753 $\pm$59 km and flattening of 0.0259 $\pm$0.0051. Assumption of an adiabatic atmosphere would make the

TABLE XXXIV

Photometric data for Neptune

Magnitude at unit distance:		$V(1, 0) = -6.87$		
Mean opposition magnitude:		$V_0 = +7.84$		
Colors:				
$U-B$	$B-V$	$V-R$	$R-I$	
0.21	0.41	−0.33	−0.80	
Brightness at mean opposition:				
U	B	V	R	I
8.46	8.25	7.84	8.17	8.97
Color differences, Neptune-Sun (setting them equal for V):				
U	B	V	R	I
−0.15	−0.15	0	+0.78	+1.87

equatorial radius about 100 km less. Scattering would increase it again. The figure quoted has been used in Table I as a reasonable reference value. The flattening measured here was 1/38.6. The dynamical flattening given by Brouwer and Clemence (1961), corrected for the new radius, is 1/50, indicating that the planet may be somwhat more flattened visually than dynamically.

Before the occultation, the most commonly quoted value for the Neptune radius was 22300 km, the result of a 1949 study by Kuiper (1949). Camichel (1953) achieved very similar results – 22700 km. If these careful measurements contained effects causing a 10% systematic error, it seems possible that the results for Uranus were similarly affected. The equatorial radius of Uranus usually quoted in recent years was the result of independent measures by Camichel (1953), using his disk meter and by Kuiper (1952), using a double-image micrometer; the average result was 23650 km. The scatter in Camichel's measurements is given as about 3% (quoted probable error 0.3%); the scatter is not given for Kuiper's work. Kuiper calls his result a 'mean radius', but since Uranus was essentially 'pole-on' during this period of measurement, the figure is more probably also the equatorial radius. Recently, Dollfus (1970) has reported the result of a large number of new measurements of Uranus which result in an equatorial radius of 25400 km and an oblateness of 1/33. These values, about 7–1/2% greater than the previous results, have been used in Table I and elsewhere in this document, but the size of the change strongly signals caution in placing too much confidence in any particular value until a Uranus occultation occurs or a spacecraft measurement is made. The dynamical oblateness of Uranus as recently determined from the motion of the pericenter of Ariel is only about half as great as this optical oblateness (Dunham, 1971).

The result of these new radii has been to reduce the densities of Uranus and Neptune to 1.31 and 1.66 g cm^{-3}, respectively, much nearer to the value for Jupiter. All existing interior models of Uranus and Neptune were obviously rendered meaningless by these huge changes in mean density. Similarly, the rotation periods discussed in

Section 4.1.4, 10.8 ±0.5 h for Uranus and 15.8 ±1.0 h for Neptune, are far from adequate for purposes of interior models.

Among the more important measurements that can be made by a deep space probe are those of the polar and equatorial radii of Uranus and Neptune, accurate to at least 1%. Similar accuracies for the dynamical flattening are needed but probably are not obtainable without orbiters or a very close flyby. Improved rotation periods can be measured from Earth, although perhaps not to the accuracy desired. With this information and improved abundances, particularly of hydrogen and helium, the formulation of useful quantitative models of the interiors of Uranus and Neptune should become feasible.

4.3. Satellites of Uranus and Neptune

The five satellites of Uranus form an extremely regular system, as can be seen from the orbital data given in Table XXXV. Physical parameters are given in Table XXXVI.

Orbital data for the satellites of Neptune are given in Table XXXVII. The two satellites of Neptune are as unusual as those of Uranus are regular. The large and

TABLE XXXV

Satellites of Uranus: orbital data[a]

Satellite	Semimajor axis, km	Eccentricity	Inclination	Period, days
Miranda	129800	$\leqslant 0.01$	0[b]	1.41349
Ariel	190900	0.0028	0[b]	2.52038
Umbriel	266000	0.0035	0[b]	4.14418
Titania	436000	0.0024	0[b]	8.70587
Oberon	583400	0.0007	0[b]	13.46325

[a] Adapted from Kuiper (1956).
[b] The inclinations to the equator are less than 1′, the attained accuracy of measurement. Dunham (1971) reports that small mutual inclinations do definitely exist.

TABEL XXXVI

Satellites of Uranus: physical data[a]

Parameter	Miranda	Ariel	Umbriel	Titania	Oberon
Mass[b] (Earth = 1)	$1\text{-}1/2 \times 10^{-5}$	22×10^{-5}	9×10^{-5}	73×10^{-5}	42×10^{-5}
Magnitude V_0	16.5	14.4	15.3	14.01	14.20
Color $U-B$	–	–	–	0.25	0.24
Color $B-V$	–	–	–	0.62	0.65
Color $V-R$	–	–	–	0.52	0.49
Color $R-I$	–	–	–	0.41	0.33

[a] Data from Harris (1961), except for masses.
[b] From Kuiper (1956); values extremely uncertain.

TABLE XXXVII

Satellites of Neptune: orbital data[a]

Satellite	Semimajor axis, km	Eccentricity	Inclination[b] deg	Period, days
Triton	355550	0	159.945	5.876844
Nereid	5567000	0.74934	27.71	359.881

[a] Adapted from Porter (1960).
[b] To equator of Neptune.

massive Triton is in retrograde motion in a small orbit of undetectable eccentricity, while tiny Nereid is in direct motion in a large, highly eccentric orbit.

Steavenson (1950) has reported the apparent brightness of Titania and Oberon to be definitely variable and that of Ariel very probably so. This variability occurs when the plane of the satellite orbits is virtually normal to the line of sight, indicating that the axes of the satellites must be at a large angle to the normal to the orbits (Steavenson, 1948, 1950). Other wise, rotation could have little effect upon the apparent brightness. Variations are also observed when the Earth is essentially in the plane of the orbits (Steavenson, 1948). The distribution of angular momentum in the Uranian system is truly unusual.

A theoretical study of the motion of Triton by McCord (1966) indicates that, within the lifetime of the solar system, tidal friction could have reduced the orbit of Triton to its present form from a highly eccentric (or even parabolic) orbit and that Triton will probably be destroyed in $10\text{–}100 \times 10^6$ yr by orbital decay into Neptune's atmosphere. Interaction with Nereid during the decay may be responsible for Nereid's large eccentricity, although more recent capture of Nereid after Triton passed through Nereid's present region of motion is quite possible also. McCord's calculations of tidal friction in the Neptune-Triton system show the possibility of a capture origin for Triton but in no sense rule out Lyttleton's (1936) suggestion that Triton may have interacted strongly with Pluto at some time in the past and that Pluto may even have originally been a satellite of Neptune. In fact, although measurements are somewhat uncertain for both bodies, Triton and Pluto are very similar in radius, color, and albedo.

Little is known about the physical properties of Nereid, which has an apparent photographic magnitude of only 19.5 (equivalent to $V_0 \simeq 18.7$, assuming a $B-V$ of 0.8) (Harris, 1961). Information about Triton, which is somewhat better known is as given in Table XXXVIII. Geometric albedos have also been given by Harris (1961), but these are extremely uncertain because the radius of Triton is so imprecisely known.

Triton is massive enough and cold enough to be fully capable of holding an atmosphere, but none has been found. A recent search by Spinrad (1969) set an upper limit of 8 m atm of methane. On Triton, most methane would be frozen out on the surface (Lewis, 1971).

TABLE XXXVIII

Triton, physical parameters

Property	Value	Reference
Mass (Earth = 1)	$2.27 \pm 0.40 \times 10^{-2}$	Kovalevsky (1970)
Mass (Moon = 1)	1.85 ± 0.33	–
Radius, km	1885 ± 650	Dollfus (1970)
Mean density, g cm^{-3}	~ 4.8	(Calculated)
Magnitude V_0	13.55	Harris (1961)
Color $U-B$	0.40	Harris (1961)
Color $B-V$	0.77	Harris (1961)
Color $V-R$	0.58	Harris (1961)
Color $R-I$	0.44	Harris (1961)

5. Pluto

5.1. General background and physical data

Pluto was discovered on February 18, 1930, after 25 yr of deliberate, intense search (Tombaugh, 1961). Its orbit is the most eccentric and the most highly inclined of any planet. Near perihelion, which it next reaches in 1989, it is nearer the Sun than Neptune can ever come, and midway between its nodes, it lies a billion and a quarter kilometers above the ecliptic plane. Because of that inclination, there is no chance at the present time of a catastrophic encounter with Neptune. In 1965, Cohen and Hubbard (1965) presented results of a special perturbation study covering a period of 120000 yr which uncovered an apparently stable libration in the Pluto-Neptune couple with a period of 19670 yr. The study indicated, in fact, that Neptune and Pluto never approach nearer than 18 AU to each other, and that the closest approach always occurs when Pluto is near aphelion. A number of more recent studies have only reinforced this conclusion. Williams and Benson (1971) have carried out a 4.5×10^6 yr integration which confirms the 20000-yr oscillation over the longer period and which has uncovered other resonances, one important one with a period of 3955000 yr. The summed effect of all these terms is to increase the minimum Pluto-Neptune distance and the apparent stability of the outer solar system.

Lyttleton (1936) originated the idea that Pluto might be an escaped satellite of Neptune. Kuiper (1957) and Rabe (1957a, b) later championed the escape hypothesis as a likely outcome of Kuiper's protoplanet theory of the origin of the solar system. The two escape mechanisms proposed are completely different, however. Pluto is certainly physically more like a satellite of a giant planet than one of the planets themselves. On the other hand, the resonance studies noted in the previous paragraph seem to indicate extreme stability for Pluto's orbit. Williams and Benson (1971) suggest that it seems unlikely that the 20000-yr libration began more recently than the time at which the planetary masses stabilized at their present values. The current stability and an earlier escape from Neptune are not necessarily incompatible, but any semblance of a firm answer to this intriguing question about Pluto's origin must await detailed study of the nature of Pluto and detailed comparison with giant-planet satellites, especially Triton.

Pluto appears as a point source in all but the largest telescopes, and even in the largest telescopes it can be resolved only under the finest conditions of observation. Kuiper (1950) made a direct measurement of the diameter of Pluto in 1950: 0.23″, or about 5860 km. Such a result may be subject to uncertainties approaching 50%. A far more accurate technique for measuring such small angles is photometric observation of a stellar occultation, but such an occultation is a rare chance occurrence. A 'very near miss' recently fixed the extreme upper limit of Pluto's diameter at 6800 km (Halliday *et al.*, 1966).

The mass of Pluto has been difficult to determine, since it requires measuring the perturbations on a large body, Neptune, by a smaller one, Pluto. Further complicating the effort to determine the mass of Pluto is the fact that the planet has completed only a fraction of one revolution since its discovery. Including all known prediscovery observations back to 1846, Pluto has made only half a revolution in its orbit, whereas Neptune has completed less than one revolution since its discovery. The best mass figure for Pluto available today is 0.11 that of Earth (Seidelmann *et al.*, 1971). This mass, together with a diameter of 6400 km, implies a density of 4.9 g cm^{-3}, which seems high for so small a body. In fact, the history of attempts to determine the mass of Pluto is one of continuous uncertainty, with the 'best' value being 0.91 that of Earth until as recently as 1968. Halliday (1969) suggested that a small change in the mass of either Saturn or Uranus could easily cause a large change in the mass determined for Pluto. The safest conclusion may be that of Ash *et al.* (1971) that "Pluto's mass cannot be determined reliably from existing data".

Quite obviously, new measurements of radius and mass are needed. The former is dependent upon chance occurrence of a favorable occultation, construction of a suitable interferometer (a monstrous task for so faint an object), or direct measurement by a spacecraft. A better mass determination from Earth will require waiting many decades for Pluto and Neptune to traverse more of their orbits. Only a spacecraft flyby will allow an accurate mass determination any time in the near future.

The period of rotation of Pluto was determined by phasing of photometric data and was found to be $6^{d}9^{h}16^{m}54^{s} \pm 26^{s}$ (Hardie, 1965; Walker and Hardie, 1955).

5.2. Atmosphere

The low mass and low temperature of Pluto suggest that it may not have an atmosphere. Many potential atmospheric molecules such as CO_2, H_2O, and NH_3 would largely lie frozen on the surface. Others such as H_2 and He may well have escaped. A best guess might be an atmosphere of small amounts of methane and/or molecular nitrogen on the dayside and little or no atmosphere on the nightside. The heavier inert gases such as neon and argon could form a permanent atmosphere, if present, but they could never be detected from Earth unless they happen to 'pressure-broaden' a spectroscopically detectable gas such as methane.

Kuiper (1944) could detect no evidence of an atmosphere spectroscopically in the visible red at dispersions of 720 and 340 Å mm^{-1}. Much higher dispersion than this is certainly available with modern equipment. A good image tube on a large telescope

might permit 25 Å mm^{-1} study of the red methane band region. The best hope for detecting an atmosphere would be by means of a spacecraft occultation experiment.

5.3. PHOTOMETRIC PROPERTIES

The absolute visual magnitude of Pluto $V(1,0)=-1.01$, which corresponds to a mean opposition magnitude $V_0=14.90$ (Harris, 1961). Because of the large eccentricity of its orbit, Pluto is more than a magnitude brighter near perihelion than it is at its mean distance. There is also a peak-to-peak fluctuation of about 0.11 magn. with a period of 6.39 days caused by the rotation of the planet (Walker and Hardie, 1955). The complete list of magnitudes at mean opposition and colors is given in Table XXXIX (Harris, 1961).

TABLE XXXIX

Photometric data for Pluto

Passband	U	B	V	R	I
Magnitude	15.97	15.70	14.90	14.27	13.99
Color	$U-B$	$B-V$	$V-R$	$R-I$	
Value	0.27	0.80	0.63	0.28	

When set equal at V, the color differences between Pluto and the Sun are:

Passband	U	B	V	R	I
Difference ($P-\odot$)	0.30	0.17	0	−0.18	−0.17

Thus, Pluto is somewhat more red than the Sun. Fix *et al.* (1970) recently measured the relative brightness of Pluto spectrophotometrically in 21 equally spaced passbands between 3400 and 5900 Å. Their passbands had a full width of 128 Å at half-maximum flux. Their work seems to show a general increase in brightness below 3800 Å.

The radius of Pluto is so indefinite that attempts to quote a geometric albedo are almost meaningless. Harris (1961) picked a radius of 0.45 that of Earth, which gives $p_v=0.13$. He then chose a phase integral equal to that for Mars ($q_v=1.04$) to derive a visual Bond albedo $A_v=0.14$. The albedo of Pluto seems to change only slowly with wavelength, so this value was inserted in Table I as a guess at the bolometric Bond albedo. It is obvious that an accurate radius and a phase integral for at least one wavelength must be measured before such numbers can have much real meaning. It does seem likely that the bolometric Bond albedo for Pluto is enough smaller than Neptune's to give Pluto the higher effective temperature. However, Pluto's slow rotation will assure considerable difference in actual dayside and nightside temperatures, the former reaching perhaps 50 K.

5.4. Body structure of Pluto

With even the density grossly uncertain, there are no interior models of Pluto nor are there likely to be until many measurements are made from a spacecraft. A magnetic field is unlikely, since Pluto is small and rotates slowly.

Acknowledgements

We wish to thank our colleagues R. Beer, C. B. Farmer, G. Hunt, M. Klein, J. Margolis and F. Taylor for numerous helpful comments and suggestions covering many points in this manuscript. We thank N. Divine and F. Palluconi for permission to include their models of Jupiter and Saturn, respectively. J. Margolis and F. Taylor read the entire document and commented critically on its contents. This was a most arduous task, and we are deeply indebted to them. We thank D. Rea for his vital support, which has made this entire undertaking possible.

Appendix A. Abundance Definitions and Relations

A number of somewhat specialized units are in common use by atmospheric physicists to describe abundances. A brief glossary of some of these terms is given below, followed by the numerical relationships between some of them.

Amagat	The amagat is a dimensionless unit of density normalized to STP conditions (1 atm + 0 °C). One amagat implies a number density equal to Loschmidt's number.
Meter atmosphere (m atm)	A meter atm of gas is that abundance which would occupy a path length of 1 m at 1 atm pressure. The temperature is often assumed (as here) to be 0 °C, but this is not a part of the latest spectroscopic definition wherein the temperature must be specified. Units of cm atm, km atm, etc., have obvious analogous definitions.
Meter amagat (m amagat)	A meter amagat of gas is that abundance which would occupy a path length of 1 m at a density of 1 amagat.
Grams per square centimeter	On occasion, an abundance will be given in units of the mass of a given molecule above some unit area, $g\,cm^{-2}$ being the most commonly used.
Partial pressure units	For the terrestrial planets, abundances of a gas are often given as the partial pressure in atmospheres, millibar, Torr, etc. This is only rarely done in Jovian planet studies.

Other measures of abundance or relative abundance include volume percent (or volume mixing ratio), mass percent, and number density, all of which have obvious meaning.

$M(\text{g cm}^{-2}) = 4.4601 \times 10^{-3}\ \mu l(\text{m amagat})$
$M(\text{kg m}^{-2}) = 4.4601 \times 10^{-2}\ \mu l(\text{m amagat})$
$P(\text{newton m}^{-2}) = 4.4601 \times 10^{-2}\ \mu g l(\text{m amagat})$
$P(\text{mb}) = 4.4601 \times 10^{-4}\ \mu g l(\text{m amagat})$

M = mass per unit area
μ = molecular mass (physical scale)
l = path length
P = pressure
g = local acceleration of gravity (m s^{-2})

Under conditions in which the perfect gas law is a reasonable description of the state of the atmospheric gases, the following rather obvious relationships hold:

volume ratio = ratio of path lengths

mass ratio = (volume ratio) $\left(\frac{\mu}{\bar{\mu}}\right)$

$n = \varrho_{\text{ama}}\, n_0$ [definition of amagat]

$\eta = \frac{N_A}{\mu} M$

$\bar{\mu}$ = mean molecular mass of all atmospheric gases
n = number density
ϱ_{ama} = density in amagats
n_0 = Loschmidt's number (2.687×10^{19} molecule cm^{-3})
η = molecules per unit area
N_A = Avogadro's number (physical scale) (6.025×10^{23} molecules mole^{-1})

Appendix B. Photometric Systems and Definitions

The photometric properties of any extended celestial body may be divided conveniently into integrated photometric properties, i.e., studies of the entire body as a unit, and detailed photometric properties, i.e., studies of the body point by point. In practice, any remote sensing technique integrates over a considerable area, but there has been very useful detailed photometry of the Moon and Mars. Only Jupiter among the giant planets exhibits much interesting surface detail visible from Earth, and that detail changes constantly, both because of the rapid rotation and actual secular change. Until very recently, detailed photometry of the outer planets has been limited largely to limb darkening curves at different wavelengths, and most detailed photometry was photographic.

Care must be taken to differentiate between photometric and radiometric data. Photometric data refer to the response of some particular detector system. The data are convolved with the spectral response of the filters, optical coatings, detectors, etc. In the very strictest sense, 'photometric data' are those received by the human eye, and 'physical photometric units' assume an international spectral luminous efficiency

curve for the eye. In astronomy, the word photometric is used in the broader sense.

The most common photometric system in use today is the UBV (ultraviolet, blue, visual) system, sometimes with red (R) and near-infrared (I) and even longer (JKLMN) wavelength measurements added. The exact system is defined by a set of magnitudes for a group of standard reference stars to which observations with any local system must be transformed. Each passband is approximately fixed in any given photometer by a standard detector-filter combination. Colors are given by magnitude differences between passbands in order of increasing wavelength; e.g., $U-B$, $B-V$, $V-K$. Zeros of the system have been chosen so that all colors are 0.00 for an unreddened star of spectral type A0 V, and so that passband V agrees in zero point with an older 'classic' photometric system.

The UBVRI data in this document are mostly those of Harris (1961), since only Harris has given such data for all of the planets and most of the satellites. Harris' passbands R and I are those of Hardie and are at different effective wavelengths than the standards of Johnson (1966), so care should be taken in comparisons with data from other sources. The 'effective wavelengths' (the mean wavelength integrated over the passbands) of these five passbands are as follows (Harris, 1961):

Passband	U	B	V	R	I
Effective λ, μ	0.353	0.448	0.554	0.690	0.820

The colors of the Sun in this system are (Harris, 1961):

Color	$U-B$	$B-V$	$V-R$	$R-I$
Value	0.14	0.63	0.45	0.29

Additional similar passbands at longer wavelengths have been used for Jupiter and Saturn in a thesis by Walker (1966), but this work is under a no-quote restriction.

The UBV system was designed for stellar work. It has broad passbands, making it easy to work with faint objects, and so long as the objects under study have energy distributions similar in form (such as a blackbody curve), no problems arise. Even in stellar work, a slight variation in the ultraviolet passband from photometer to photometer can cause discrepancies (because of departures from a blackbody at the Balmer discontinuity), as can interstellar reddening. Differences in observatory altitudes can make data reductions difficult because of varying atmospheric opacity in the U-passband. Thus, planets with large molecular absorption bands and planet or satellite surfaces which are far from pure white make poor objects for UBV photometry. An additional problem is that the V magnitude of the Sun is uncertain by as much as 0.1 magn., making planetary comparisons to it of limited accuracy.

The ubvy system of Strömgren is a system of intermediate width-passbands coming into increased general astronomical use, but there are no giant-planet data in this

system. Much planetary photometry of high quality is now being done either with a very large number of narrow passbands defined by interference filters or by a spectrometer using a wide slit in the image plane. Each worker or group of workers then has his own photometric system, and only with great care in calibration can the data be compared to other photometric systems or converted to radiometric data. In planetary photometry, a measurement of the Sun in the same system would usually be of more value than an absolute calibration for those parts of the spectra that are strictly reflected sunlight. Because of the great differences between Sun and planet or satellite in both flux and angular size, such direct comparison is not practical and most calibration is done via other stars or occasionally the Moon (if, in fact, it is done at all). Where necessary, individual systems are described briefly in the main body of this document.

In the UBV or any other astronomical photometric system, values are usually given in magnitudes, a logarithmic scale of ancient origin. One magnitude difference is exactly the fifth root of $100 (\sqrt[5]{100})$ ratio in flux, that is, approximately 2.512. Five magnitudes is exactly a factor of 100, of course, and 10 magn. a factor of 10000. The simple formula relating magnitudes m_a and m_b and fluxes f_a and f_b is

$$\log (f_a/f_b) = -0.4 (m_a - m_b).$$

The magnitude scale is an inverse one, that is, the brighter the object the smaller its numerical magnitude. An object brighter than magnitude 1 may be magnitude 0 or have a negative magnitude. In colors, this means, for example, that the object with the larger value of $B-V$ is the more red of the two.

The integrated photometric properties of an object include total brightness, average color, the variation of brightness and color with phase, the Bond (or spherical or Russell-Bond) albedo, the geometric albedo, the phase function, and the phase integral. All of these may vary somewhat as the object rotates, and a planet such as Jupiter may also show secular changes. Ignoring rotational or secular changes, the visual magnitude of a planet is given by the expression

$$V = V(1, 0) + 5 \log rd + \Delta M(\alpha),$$

where

$V(1, 0)$ = magnitude at unit distance from Earth and Sun, whether this configuration is physically possible or not. It is a form of absolute magnitude for solar system objects;
r = distance from Earth, in AU;
d = distance from Sun, in AU;
$\Delta M(\alpha)$ = correction for phase angle α.

Another useful quantity is the mean oppostion magnitude V_0 given by

$$V_0 = V(1, 0) + 5 \log a (a - 1),$$

where

a = mean distance of the object from the Sun, in AU.

Identical relations also can be written for any other passband, of course.

The phase function of a body $\phi(\alpha)$ describes the flux reflected as a function of phase angle, normalized to zero (full) phase, i.e.,

$$\phi(\alpha) = F(\alpha)/F(0).$$

Astronomers tend to give the quantity $F(\alpha)$ as a polynomial in α and in units of magnitude, i.e.,

$$\Delta M(\alpha) = c_1\alpha + c_2\alpha^2 + c_3\alpha^3 \ldots .$$

Since it is impossible to see the giant planets at large phase angle from Earth, usually only a linear term, called the phase coefficient, is given. There can be a problem if the body exhibits an 'opposition effect', a brightening at very small phase angles beyond a linear interpolation to zero phase of data suitable for $|\alpha| > 5$ deg. This can be included by adding negative powers of α but is usually just given as the amount of brightening in magnitudes beyond the linear extrapolation to zero or as a graph.

Detailed photometric properties include brightness and color of localized areas as a function of phase, the normal albedo, the photometric function, the radiance factor, and the radiance coefficient. Limb darkening is the variation of brightness from the center of an object to the limb and is thus a relationship between points rather than part of the description of a point.

The large body of photometric terms, mentioned in the three preceding paragraphs, is in general use, with precisely defined meaning in planetary astrophysics. The following list includes definitions of all such terms used in this document and a few additional terms which may be encountered in some of the references:

Albedo	Essentially a synonym for reflectivity, but it always has qualifying adjectives or phrases which indicate the precise sort of reflectivity. (See geometric albedo, Bond albedo, and normal albedo).
Bolometric	An adjective implying radiometric (rather than photometric) data integrated over all wavelengths. A bolometric magnitude is thus a measure of total power, and a bolometric albedo is a mean albedo over all wavelengths, unaffected by atmospheric or photometric system absorptions and response.
Bond (sometimes Russell-Bond or spherical) albedo	The ratio of the power (flux) reflected in all directions by a body to the power incident upon it in a collimated beam. It is the fraction of incident solar flux that is not absorbed.
Detailed photometry	Point-by-point photometry of an extended source. Only selected points or features may be measured in a given study, however.
Geometric albedo	The ratio of mean luminance of a body at full phase (phase angle zero) to the luminance of an 'intrinsically white' plane surface normal to the source of illumination (Sun). An intrin-

sically white surface scatters all of the power incident upon it (absorbing none) and does so according to Lambert's cosine law.

Integrated photometry — Photometric study of an entire body as a unit, as opposed to detailed photometry.

Lambert surface — A surface which has the same radiance when viewed from any angle.

Lambert's cosine law — A surface radiating (or reflecting or transmitting) an amount of flux per unit area and unit solid angle proportional to the cosine of the angle between the surface normal and the direction of observation is said to follow Lambert's cosine law. Such a surface is a Lambert surface.

Luminance — The photometric equivalent of radiance, the power per unit solid angle and unit projected area leaving a surface within the passband of a photometric system. In the narrowest sense, this refers only to the passband of the human eye, but in astronomy the broader sense is often used, applying the terminology to any defined photometric system.

Luminance equator — The intersection of the phase plane with the surface under study.

Luminance latitude — The angle between the phase plane and the normal to the surface at the point of observation (see Figure B-1).

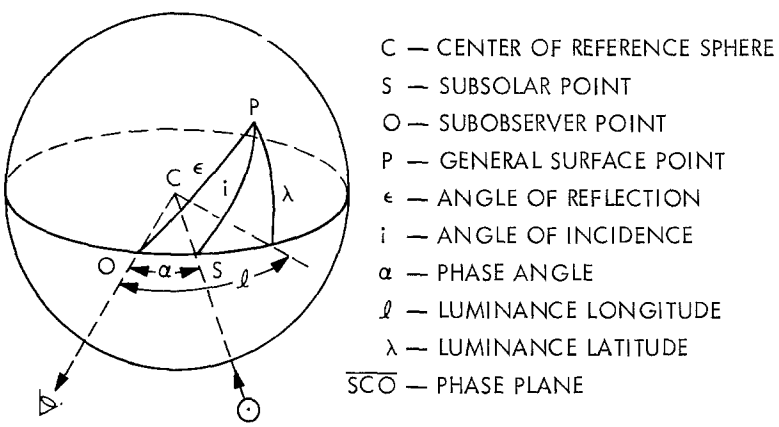

Fig. B-1. Photometric coordinates.

Luminance longitude — The angle of observation (reflection angle) projected into the phase plane (see Figure B-1).

Magnitude — A logarithmic unit of electromagnetic flux, ancient in origin, used in astronomy. In modern usage, one magnitude is equivalent to a ratio of 2.512 in flux. (See earlier paragraphs in Appendix B.)

Normal albedo	The ratio of luminance of a point at zero phase to the luminance of an intrinsically white plane Lambert surface normal to the illumination. This is the photometric equivalent in detailed photometry to geometric albedo in integrated photometry. (See geometric albedo.)
Opposition effect	An enhanced brightness occurring for phase angles $\lvert\alpha\rvert \lesssim 5$ deg. (See earlier paragraphs in Appendix B.)
Phase angle	Astronomically, the object (body)-centered angle between the source of illumination (the Sun) and the observer (detector). (see Figure B-1).
Phase coefficient	The linear term (c_1) in an expression for the phase function, usually given in magnitudes per degree.
Phase function	The ratio of power (flux) scattered at phase angle α to that scattered at zero phase. The phase function is often given as a polynomial approximation, in tabular form, or as a polar graph.
Phase integral	The ratio of power (flux) scattered in all directions to that scattered at zero phase, per unit solid angle. The phase integral multiplied by the geometric albedo equals the Bond albedo.
Phase plane	The Sun-object-observer plane, the plane containing the phase angle (see Figure B-1).
Photometric data	Flux data convolved with the response of a particular detector system. In the strictest sense, photometric data are those received by a 'standard' human eye, but astronomically the term is applied to any calibrated combination of filters, detectors, etc.
Photometric function	The ratio of the radiance factor to the normal albedo for a point on a sphere. The photometric function is a function of three parameters, i.e., the phase angle, angle of incidence, and angle of observation, or, alternately, the phase angle, luminance longitude, and luminance latitude.
Radiance	Radiometric term for power per unit solid angle and unit projected area leaving a surface.
Radiance (luminance) coefficient	The ratio of radiance (luminance) observed to that of a white plane Lambert surface at the same inclination to the source of illumination.
Radiance (luminance) factor	The ratio of radiance (luminance) observed to that of a white plane Lambert surface normal to the source of illumination.
Radiometric data	Flux data given in absolute units, deconvolved of any photometric system response curve. These units can be either astronomical (magnitude) or physical (watt) and may still refer to a particular region of the spectrum rather than be integrated over all wavelengths (bolometric data).

Radiometric window	The wavelength interval from 8 to 14 μ, a region that is relatively transparent in the Earth's atmosphere and widely used for Earth-based radiometry.
Spectral irradiance	Radiometric term for power incident per unit area and wavelength upon a surface.
Spectral radiant exitance	Radiometric term for power per unit area and wavelength coming from a surface.
Solar constant	The irradiance (power per unit area) from the Sun at a distance of one astronomical unit.

Appendix C. Pronunciation of Outer Planet Satellite Names

As ground-based and space probe research on the outer parts of the solar system has come to the fore, there has been increasing use and increasing mispronunciation of the names of the satellites of the solar system. The following guide is taken from the unabridged *Random House Dictionary of the English Language*. These pronunciations seem to be in reasonable agreement with other, less complete, classic sources. The list follows *Random House* practice, using the 'schwa', written ə. The schwa has the sound of *a* in above, of *e* in system, of *i* in easily, of *o* in gallop, and of *u* in circus. Other markings include *â* as in air and *th* as in thin or path, as well as the usual long vowels, marked '*ā*' for example, and the short vowels which are unmarked.

Jovian Satellites

Amalthea	am′ əl thē′ə
Io	ī′ ō
Europa	yo͝o rō′ pə
Ganymede	gan′ ə mēd′
Callisto	kə lis′ tō

Saturnian Satellites

Janus	jā′ nəs
Mimas	mī′ mas
Enceladus	en sel′ ə dəs
Tethys	tē′ this
Dione	dī o′ nē
Rhea	rē′ə
Titan	tīt′ ən
Hyperion	hī pēr′ ē ən
Iapetus	ī ap′ i təs
Phoebe	fē′ bē

Uranian Satellites

Miranda	mi ran′ də

Ariel	âr′ ē əl
Umbriel	um′ brē el′
Titania	ti tā′ nē ə
Oberon	ō′ bə ron′

Neptunian Satellites

Triton	trīt′ ən
Nereis	nēr′ ē id

References

Alexander, A. F. OD: 1962, *The Planet Saturn*, Faber and Faber, London.
Alexander, A. F. OD.: 1965, *The Planet Uranus*, American Elsevier, New York.
Allen, D. A. and Murdock, T. L.: 1971, *Icarus* **14**, 1.
Anderson, R. C., Pipes, J. G., Broadfoot, A. L., and Wallace, L.: 1969, *J. Atmospheric Sci.* **26**, 874.
Appleby, J. F. and Irvine, W. M,: 1971, *Astron. J.* **76**, 617.
Ash, M. E., Shapiro, I. I., and Smith, W. B.: 1971, *Science* **174**, 551.
Aumann, H. H., Gillespie, C. M., Jr. and Low, F. J.: 1969, *Astrophys. J.* **157**, L69.
Avramchuk, V. V.: 1970, *Soviet Astron.–AJ* **14**, 462.
Axel, L.: 1972, *Astrophys. J.* **173**, 451.
Baars, J. W. M., Mezger, P. G., and Wendker, H.: 1965, *Z. Astrophys.* **61**, 134.
Bailey, J. M.: 1971, *J. Geophys. Res.* **76**, 7827.
Balasubrahmanyan, V. K. and Venkatesan, D.: 1970, *Astrophys. Letters* **6**, 123.
Banos, C. J.: 1971, *Icarus* **15**, 58.
Banos, C. J. and Alissandrakis, C. E.: 1971, *Astron. Astrophys.* **15**, 424.
Barcilon, A. and Gierasch, P.: 1970, *J. Atmospheric Sci.* **27**, 550.
Barrow, C. H. and Morrow, D. P.: 1968, *Astrophys. J.* **152**, 593.
Bartholdi, P. and Owen, F.: 1972, *Astron. J.* **77**, 60.
Bash, F. N., Drake, F. D., Gundermann, E., and Heiles, C. E.: 1964, *Astrophys. J.* **139**, 975.
Baum, W. A. and Code, A. D.: 1953, *Astron. J.* **58**, 108.
Beckman, J. E.: 1967, *Astrophys. J.* **149**, 453.
Beer, R. and Taylor, F. W.: 1972, 'The Abundance of CH_3D and the Deuterium-Hydrogen Ratio in Jupiter', Third Annual Meeting, AAS Div. for Planetary Science, Kona, Hawaii, March 20–24.
Beer, R., Farmer, C. B., Norton, R. H., Martonchik, J. V., and Barnes, T. G.: 1972, *Science* **175**, 1360.
Belton, M. J. S., McElroy, M. B., and Price, M. J.: 1971, *Astrophys. J.* **164**, 191.
Berge, G. L.: 1965, *Astrophys. J.* **142**, 1688.
Berge, G. L.: 1966, *Astrophys. J.* **146**, 767.
Berge, G. L.: 1968, *Astrophys. Letters* **2**, 127.
Berge, G. L.: 1970, 'The Position of Jupiter's Radio Emission Centroid at 21 cm Wavelength', paper presented to XIV General Assembly of IAU, Brighton, England.
Berge, G. L.: 1972, in A. J. Beck (ed.), 'Some Recent Observations and Interpretations of the Jupiter Decimeter Emission', *Proc. of the Jupiter Radiation Belt Workshop*, Tech. Mem. 33–543, Jet Propulsion Laboratory, Pasadena, Calif., U.S.A., p. 223.
Berge, G. L. and Read, R. B.: 1968, *Astrophys. J.* **152**, 755.
Bergstralh, J. T.: 1971, *Bull. Amer. Astron. Soc.* **3**, 282.
Bibinova, V. P., Kuzmin, A. D., Salomonovich, A. E., and Shavlovskii, I. V.: 1963, *Soviet Astron.–AJ* **6**, 840.
Bigg, E. K.: 1964, *Nature* **203**, 1008.
Binder, A. B.: 1972, *Astron. J.* **77**, 93.
Binder, A. B. and Cruikshank, D. P.: 1964, *Icarus* **3**, 299.
Binder, A. B. and McCarthy, D. W., Jr.: 1972, *Astrophys. J.* **171**, L1.
Birnbaum, A. and Poll, J. D.: 1969, *J. Atmospheric Sci.* **26**, 943.
Bishop, E. V. and De Marcus, W. C.: 1970, *Icarus* **12**, 317.
Blanco, C. and Catalano, S.: 1971, *Astron. Astrophys.* **14**, 43.

Bobrov, M. S.: 1963, *Soviet Astron.–AJ*, **6**, 525.
Bobrov, M. S.: 1970, in A. Dollfuss (ed.), *Surface and Interiors of Planets and Satellites*, Academic Press, New York, Chapter 7.
Branson, N. J. B. A.: 1968, *Monthly Notices Roy. Astron. Soc.* **139**, 155.
Braun, L. D. and Yen, J. L.: 1968, *Astron. J.* **73**, S168.
Brice, N. M. and Ioannidis, G. A.: 1970, *Icarus* **13**, 173.
Brouwer, D. and Clemence, G. M.: 1961, in G. P. Kuiper and B. M. Middlehurst (eds.), *The Solar System* Vol. III: *Planets and Satellites*, University of Chicago Press, Chicago, Ill., p. 31.
Burns, J. A.: 1967, *Science* **159**, 971.
Camichel, H.: 1953, *Ann. Astrophys.* **16**, 41.
Carr, T. D.: 1971, *Astrophys. Letters* **7**, 157.
Carr, T. D. and Gulkis, S.: 1969, *Ann Rev. Astron. Astrophys.* **7**, 577.
Carr, T. D., Brown, G. W., Smith, A. G., Higgins, C. S., Bollhagen, H., May, J. and Levy, J.: 1964, *Astrophys. J.* **140**, 778.
Carr, T. D., Smith, A. G., Donivan, F. F., and Register, H. I.: 1970, *Radio Sci.* **5**, 495.
Chadha, M. S., Flores, J. J., Lawless, J. G., and Ponnamperuma, C.: 1971, *Icarus* **15**, 39.
Chapman, C. R.: 1969, *J. Atmospheric Sci.* **26**, 986.
Code, A. D.: 1960, in M. J. L. Greenstein (ed.), *Stellar Atmospheres*, Univ. of Chicago Press, Chicago, Ill., p. 50.
Cohen, C. J. and Hubbard, E. C.: 1965, *Astron. J.* **70**, 10.
Colombo, G. and Franklin, F.: 1969, *Mem. Soc. Astron. Italiana* **40**, 205.
Colombo, G., Franklin, F. A., and Mumford, C. M.: 1968, *Astron J.* **73**, 111.
Combes, B., Lecacheux, J., and Vapillon, L.: 1971, *Astron. Astrophys.* **15**, 235.
Conseil, L., Leblanc, Y., Antonini, and Quemoda, D.: 1971, *Astrophys. Letters* **8**, 133.
Cook, A. F. and Franklin, F. A.: 1958, *Smithsonian Contr. Astrophys.* **2**, 377.
Cook, A. F. and Franklin, F. A.: 1964, *Astron. J.* **69**, 173.
Cook, A. F. and Franklin F. A.: 1966, *Astron. J.* **71**, 10.
Cook, A. F. and Franklin, F. A.: 1970a, *Astron. J.* **75**, 195.
Cook, A. F. and Franklin, F. A.: 1970b, *Icarus* **13**, 282.
Cook, J. J., Cross, L. G., Bair, M. E., and Arnold, C. B.: 1960, *Nature* **188**, 393.
Critchfield, C. L.: 1942, *Astrophys. J.* **96**, 1.
Cruikshank, D. P.: 1971, *Bull. Am. Astron. Soc.* **3**, 282.
Cruikshank, D. P. and Binder, A. B.: 1969, *Astrophys. Space Sci.* **3**, 347.
Danielson, R. E.: 1966, *Astrophys. J.* **143**, 949.
Danielson, R. E. and Tomasko, M. G.: 1969, *J. Atmospheric Sci.* **26**, 889.
Davies, R. D. and Williams, D.: 1966, *Planetary Space Sci.* **14**, 15.
Davies, R. D., Beard, M., and Cooper, B. F. C.: 1964, *Phys. Rev. Letters* **13**, 325.
De Marcus, W. C.: 1958, *Astron. J.* **63**, 2.
Dickel, J. R.: 1967, *Astrophys. J.* **148**, 535.
Dickel, J. R., Degioanni, J. J., and Goodman, G. C.: 1970, *Radio Sci.* **5**, 517.
Divine, N.: 1971, 'The Planet Jupiter (1970)', NASA Space Vehicle Design Criteria (Environment), NASA SP-8069, Dec.
Dollfus, A.: 1961, in G. P. Kuiper and B. M. Middlehurst (eds.), *The Solar System*, Vol. III: *Planets and Satellites*, Univ. of Chicago Press, Chicago, Ill., p. 534.
Dollfus, A.: 1963, *Icarus* **2**, 109.
Dollfus, A.: 1967, IAU Circular No. 1995, Feb. 1.
Dollfus, A.: 1970a, in A. Dollfuss (ed.). *Surfaces and Interiors of Planets and Satellites*, Academic Press, New York, p. 50.
Dollfus, A.: 1970b, *Icarus* **12**, 101.
Douglas, J. N. and Smith, H. C.: 1967, *Astrophys. J.* **148**, 885.
Drake, F. D.: 1962, *Nature* **195**, 893.
Dulk, G. A.: 1967, *Astrophys. J.* **148**, 239.
Dulk, G. A.: 1970, *Astrophys. J.* **159**, 671.
Dulk, G. A. and Clark, T. A.: 1966, *Astrophys.* J. **145**, 945.
Dulk, G. A., Eddy, J. A., and Emerson, J. P.: 1970, *Astrophys. J.* **159**, 1123.
Duncan, R. A.: 1971, *Planetary Space Sci.* **19**, 391.
Dunham, D.: 1971, *Bull. Amer. Astron. Soc.* **3**, 415.

Dunham, T., Jr.: 1952, in G. P. Kuiper (ed.), *The Atmospheres of the Earth and Planets*, Univ. of Chicago Press, Chicago, Ill., p. 288.
Efanov, V. A., Moiseev, I. G., Kislyakov, A. G., and Naumov, A. I.: 1971, *Icarus* **14**, 198.
Ellis, G. R. A.: 1965, *Radio Sci.* **69D**, 1513.
Encrenaz, Th.: 1972, *Astron. Astrophys*, **16**, 237.
Encrenaz, Th., Gautier, D., Vapillon, L., and Verdet, J. P.: 1971, *Astron. Astrophys.* **11**, 431.
Epstein, E. E.: 1968, *Astrophys. J.* **151**, L149.
Epstein, E. E., Dworetsky, M. M., Montgomery, J. W., Fogarty, W. G., and Schorn, R. A.: 1970, *Icarus* **13**, 276.
Fallon, F. W. and Murphy, R. E.: 1971, *Icarus* **15**, 492.
Farmer, C. B.: 1969, *J. Atmosperic Sci.* **26**, 860.
Feibelman, W. A.: 1967, *Nature* **214**, 793.
Field, G. B.: 1966, in A. Brown, G. J. Stanley, D. O. Muhleman, and G. Münch (eds.), 'Remarks on Jupiter', *Proc. of the Caltech-JPL Lunar and Planetary Conference*, Jet Propulsion Laboratory, Pasadena, Calif., U.S.A., p. 141.
Field, G. B., Somerville, W. B., and Dressler, K.: 1966, *Ann. Rev. Astron. Astrophys.* **4**, 207.
Fink, U. and Belton, M. J. S.: 1969, *J. Atmospheric Sci.* **26**, 952.
Fix, J. D., Neff, J. S., and Kelsey, L. A.: 1970, *Astron. J.* **75**, 895.
Focas, J. H.: 1971, *Icarus* **15**, 56.
Focas, J. H. and Dollfus, A.: 1969, *Astron. Astrophys.* **2**, 251.
Fox, K. and Ozier, I.: 1971, *Astrophys. J.* **166**, L95.
Fox, K., Mantz, A. W., Owen, T., and Rao, K. N.: 1972, 'A Tentative Identification of $C^{13}H_4$ and an Estimate of C^{12}/C^{13} in the Atmosphere of Jupiter', Third Annual Meeting, AAS Div. for Planetary Sciences, Kona, Hawaii, Mar. 20–24, 1972.
Franklin, F. A. and Colombo, G.: 1970, *Icarus* **12**, 338.
Franklin, F. A. and Cook, A. F.: 1965, *Astron. J.* **70**, 704.
Franklin, F. A. and Cook, II, A. F.: 1969, *Icarus* **10**, 417.
Franklin, F. A., Colombo, G., and Cook, A. F.: 1971, *Icarus* **15**, 80.
Franz, O. G. and Millis, R. L.: 1971, *Icarus* **14**, 13.
Freeman, K. C. and Lynga, G.: 1970, *Astrophys. J.* **160**, 767.
Gehrels, T.: 1969, *Icarus* **10**, 410.
Gehrels, T., Herman, B. M., and Owen, T.: 1969, *Astron. J.* **74**, 190.
Gerard, E.: 1969, *Astron. Astrophys.* **2**, 246.
Gerard, E.: 1970, *Radio Sci.* **5**, 513.
Gierasch, P. J. and Goody, R. M.: 1969, *J. Atmospheric Sci.* **26**, 979.
Gierasch, P. J. and Stone, P. H.: 1968, *J. Atmospheric Sci.* **25**, 1169.
Gierasch, P., Goody, R., and Stone, P.: 1970, *Geophys. Fluid Dynamics* **1**, 1.
Gillett, F. C., Low, F. J., and Stein, W. A.: 1969, *Astrophys. J.* **157**, 925.
Gillett, F. C., Merrill, K. M., and Stein, W. A.: 1970, *Astrophys. Letters* **6**, 247.
Giordmaine, J. A., Alsop, L. E., Townes, C. H., and Mayer, C. H.: 1959, *Astron. J.* **64**, 332.
Giver, L. P. and Spinrad, H.: 1966, *Icarus* **5**, 586.
Gledhill, J. A.: 1967, *Nature* **214**, 155.
Goldreich, P.: 1965, *Monthly Notices Roy. Astron. Soc.* **130**, 159.
Goldreich, P. and Lynden-Bell, D.: 1969, *Astrophys. J.* **156**, 59.
Golitsyn, G. S.: 1970, *Icarus* **13**, 1.
Goody, R.: 1969, *J. Atmospheric Sci.* **26**, 997.
Guerin, P.: 1970, *Sky Telesc.* **40**, 88.
Gulkis, S.: 1970, *Radio Sci.* **5**, 505.
Gulkis, S. and Carr, T. D.: 1966, *Science* **154**, 257.
Gulkis, S. and Gary, B.: 1971, *Astron. J.* **76**, 12.
Gulkis, S. and Poynter, R.: 1972, 'Thermal Radio Emission From Jupiter and Saturn', paper presented at Lunar Science Institute Conference on High Pressure Physics and Planetary Interiors, Houston, Texas, March 1–3, 1972. (Proceedings to be published in *Physics of the Earth and Planetary Interiors.*)
Gulkis, S., McDonough, T. R., and Craft, H.: 1969, *Icarus* **10**, 421.
Haines, E. L. (ed.): 1971, 'Selenodesy and Lunar Dynamics', *Lunar Scientific Model*, Section 1, Document 900-278, Jet Propulsion Lab., Pasadena, Calif., U.S.A.

Hall, J. S. and Riley, L. A.: 1969, *J. Atmospheric Sci.* **26**, 920.
Halliday, I.: 1969, *Pub. Astron. Soc. Pacific* **81**, 285.
Halliday, I., Hardie, R. H., Franz, O. G., and Priser, J. B.: 1966, *Publ. Astron. Soc. Pacific* **78**, 113.
Hansen, O. L.: 1972, 'Infrared Observations of the Galilean Satellites', Third Annual Meeting, AAS Div. for Planetary Sciences, Kona, Hawaii, March 20–24, 1972.
Hardie, R.: 1965, *Astron. J.* **70**, 140.
Harris, D. L.: 1961, in G. P. Kuiper and B. M. Middlehurst (eds.), *The Solar System*, Vol. III: *Planets and Satellites*, Univ. of Chicago Press, Chicago, Ill., p. 272.
Harrison, H. and Schoen, R. I.: 1967, *Science* **157**, 1175.
Herget, P.: 1968a, *Astron. J.* **73**, 737.
Herget, P.: 1968b, 'Ephemerides of Comet Schwassmann-Wachmann I and the Outer Satellites of Jupiter With Text', Publ. of the Cincinnati Observatory No. 23, Cincinnati.
Herzberg, G.: 1952, in G. P. Kuiper (ed.), *The Atmospheres of the Earth and Planets*, rev. ed., Univ. Chicago Press, Chicago, p. 406.
Hess, S. L.: 1953, *Astrophys. J.* **118**, 151.
Hess, S. L.: 1969, *Icarus* **11**, 218.
Hide, R.: 1961, *Nature* **190**, 895.
Hide, R.: 1963, *Mem. Soc. Roy. Sci. Liège, Series 5*, **7**, 481.
Hide, R.: 1967, in W. R. Hindmarsh, F. J. Lowes, P. H. Roberts, and S. K. Rumcorn (eds.), *Magnetism and the Cosmos*, American Elsevier, New York, p. 378.
Hide, R.: 1969, *J. Atmospheric Sci.* **26**, 841.
Hide, R.: 1971a, *Meteorol. Mag.* **100**, 268.
Hide, R.: 1971b, *J. Fluid Mech.* **49**, 745.
Hide, R. and Ibbetson, A.: 1966, *Icarus* **5**, 279.
Hobbs, R. W. and Knapp, S. L.: 1971, *Icarus* **14**, 204.
Hogan, J. S., Rasool, S. I., and Encrenaz, Th.: 1969, *J. Atmospheric Sci.* **26**, 898.
Hopkins, N. B. and Irvine, W. M.: 1971, in C. Sagan, T. C. Owen, and H. J. Smith (eds.), 'Planetary Atmospheres', *IAU Symp.* **40**, 349.
Hubbard, W. B.: 1968, *Astrophys. J.* **152**, 745.
Hubbard, W. B.: 1969, *Astrophys. J.* **155**, 333.
Hubbard, W. B.: 1970, *Astrophys. J.* **162**, 687.
Hubbard, W. B. and Van Flandern, T. C.: 1972, *Astron. J.* **77**, 65.
Hubbard, W. B., Nather, R. E., Evans, D. S., Tull, R. G., Wells, D. C., van Citters, G. W., Warner, B., and Vanden Bout, P.: 1972, *Astron. J.* **77**, 41.
Hughes, M. P.: 1966, *Planetary Space Sci.* **14**, 1017.
Hunt, G. E.: 1972a, *J. Q. Spectr. Radiative Transfer* **12**, 387.
Hunt, G. E.: 1972b, 'Spectroscopic Evidence for the Structure of the Visible Jovian Clouds From Observations of Methane and Hydrogen Quadrupole Lines', Third Annual Meeting, AAS Div. for Planetary Sciences, Kona, Hawaii, March 20–24.
Hunten, D. M.: 1969, *J. Atmospheric Sci.* **26**, 826.
Ingersoll, A. P.: 1969, *J. Atmospheric Sci.* **26**, 744.
Ingersoll, A. P. and Cuzzi, J. N.: 1969, *J. Atmospheric Sci.* **26**, 981.
International Astronomical Union: 1962, *IAU Information Bull.* No. 8.
Irvine, W. M. and Lane, A. P.: 1971, *Icarus* **15**, 18.
Irvine, W. M., Simon, T., Menzel, D. H., Charon, J., Leconte, G., Griboval, P., and Young, A. T.:. 1968a, *Astron. J.* **73**, 251.
Irvine, W. M., Simon, T., Menzel, D. H., Pikoos, C., and Young, A. T.: 1968b, *Astron. J.* **73**, 807.
James, T. C.: 1969, *J. Opt. Soc. Am.* **59**, 1602.
Jenkins, E. B.: 1969, *Icarus* **10**, 379.
Johnson, H. L.: 1966, *Ann. Rev. Astron. Astrophys.* **4**, 193.
Johnson, H. L.: 1970, *Astrophys. J.* **159**, L1.
Johnson, T. V.: 1971, *Icarus* **14**, 94.
Johnson, T. V. and McCord, T. B.: 1970, *Icarus* **13**, 37.
Johnson, T. V. and McCord, T. B.: 1971, *Astrophys. J.* **169**, 589.
Kalaghan, P. M. and Wulfsberg, K. N.: 1967, 'Radiometric Observations of the Planets Jupiter, Venus, and Mars at a Wavelength of 8.6 Millimeters', AFCRL-67-0409. Air Force Cambridge Research Laboratory, Bedford, Mass., July.

Kellermann, K. I.: 1966, *Icarus* **5**, 478.
Kellermann, K. I.: 1970, *Radio Sci.* **5**, 487.
Kellermann, K. I. and Pauliny-Toth, I. I. K.: 1966, *Astrophys. J.* **145**, 954.
Kellermann, K. I., Pauliny-Toth, I. I. K., and Williams, P. J. S.: 1969, *Astrophys. J.* **157**, 1.
Kemp, J. C., Swedlund, J. B., Murphy, R. E., and Wolstencroft, R. D.: 1971a, *Nature* **231**, 169.
Kemp, J. C. and Wolstencroft, R. D.: 1971, *Nature* **231**, 170.
Kemp, J. C., Wolstencroft, R. D., and Swedlund, J. B.: 1971, *Nature* **232**, 165.
Kiess, C. C., Corliss, C. H., and Kiess, H. K.: 1960, *Astrophys. J.* **132**, 221.
Kiladze, R. I.: 1968, 'Observations of the Saturn Rings in the Period of the Earth's Passage Through Their Plane in 1966', *Abstracts, Kiev Int. Symp. Lunar Planet Phys. Kiev, October 15–22, 1968.*
Kislyakov, A. G. and Lebskii, Yu. V.: 1968, *Soviet Astron. AJ* **11**, 561.
Klein, M. J. and Gulkis, S.: 1971, *Bull. Amer. Astron. Soc.* **3**, 276.
Klein, M. J. and Seling, T. V.: 1966, *Astrophys. J.* **146**, 599.
Klein, M. J., Gulkis, S., and Stelzreid, C.: 1971, *Bull. Amer. Astron. Soc.* **3**, 475.
Klepczynski, W. J., Seidelmann, P. K., and Duncombe, R. L.: 1971, *Celest. Mech.* **4**, 253.
Komesaroff, M. M. and McCulloch, P. M.: 1971, *Astrophys. Letters* **1**, 39.
Komesaroff, M. J., Morris, D., and Roberts, J. A.: 1970, *Astrophys. Letters* **7**, 31.
Kondo, Y.: 1971, *Icarus* **14**, 269.
Kovalevsky, J.: 1970, in A. Dollfus (ed.), *Surfaces and Interiors of Planets and Satellites*, Academic Press, New York, p. 1.
Kovalevsky, J.: 1971, *Celest. Mech.* **4**, 213.
Kovalevsky, J. and Link, F.: 1969, *Astron. Astrophys.* **2**, 398.
Krauss, J. D.: 1958, *Proc. IRE* **46**, 266.
Kuiper, G. P.: 1944, *Astrophys. J.* **100**, 378.
Kuiper, G. P.: 1949, *Astrophys. J.* **110**, 93.
Kuiper, G. P.: 1950, *Publ. Astron. Soc. Pacific* **62**, 133.
Kuiper, G. P. (ed.): 1952, *The Atmospheres of the Earth and Planets*, rev. ed., Univ. of Chicago Press, Chicago, Ill., p. 306.
Kuiper, G. P.: 1956, in A. Beer (ed.), *Vistas in Astronomy*, Vol. II, Pergamon, New York, p. 1631.
Kuiper, G. P.: 1957a, *Trans. IAU* **IX**, 1955, Cambridge Univ. Press, London, p. 256.
Kuiper, G. P.: 1957b, *Astrophys. J.* **125**, 287.
Kuiper, G. P.: 1961, in G. P. Kuiper and B. M. Middlehurst (eds.), *The Solar System*, Vol. III: *Planets and Satellites*, Univ. of Chicago, Chicago, Ill., p. 575.
Kuiper, G. P.: 1972a, *Sky Telesc.* **43**, 4.
Kuiper, G. P.: 1972b, *Sky Telesc.* **43**, 75.
Kuiper, G. P., Cruikshank, D. P., and Fink, U.: 1970, *Bull. Amer. Astron. Soc.* **2**, 235.
Kuzmin, A. D. and Losovsky, B. Ya.: 1971a, *Solar System Res.* (trans. of *Astron. Vestnik*) **5**, 78.
Kuzmin, A. D. and Losovsky, B. Ya.: 1971b, *Icarus* **14**, 196.
Law, S. E. and Staelin, D. H.: 1968, *Astrophys. J.* **154**, 1077.
Layton, R. G.: 1971, *Icarus* **15**, 480.
Lebofsky, L. A., Johnson, T. V., and McCord, T. B.: 1970, *Icarus* **13**, 226.
Lewis, J. S.: 1969a, *Icarus* **10**, 365.
Lewis, J. S.: 1969b, *Icarus* **10**, 393.
Lewis, J. S.: 1971, *Icarus* **15**, 174.
Lewis, J. S. and Prinn, R. G.: 1970, *Science* **169**, 472.
Lieske, J. H., Melbourne, W. G., O'Handley, D. A., Holdridge, D. B., Johnson, D. E., and Sinclair, W. S.: 1971, *Celest. Mech.* **4**, 233.
Low, F. J.: 1964, *Astron. J.* **69**, 550.
Low, F. J.: 1965, *Lowell Observ. Bull.* **6**, 184.
Low, F. J.: 1966a, *Astrophys. J.* **146**, 326.
Low, F. J.: 1966b, *Astron. J.* **71**, 391.
Low, F. J. and Davidson, A. W.: 1965, *Astrophys. J.* **142**, 1278.
Low, F. J. and Davidson, A. W.: 1969, *Bull. Amer. Astron. Soc.* **1**, 200.
Lumme, K.: 1970, *Astrophys. Space Sci.* **8**, 90.
Lyot, B.: 1953, *Astronomie* **67**, 3.
Lyttleton, R. A.: 1936, *Monthly Notices Roy. Astron. Soc.* **97**, 108.
Margolis, J. S.: 1971, *Astrophys. J.* **167**, 553.

Margolis, J. S. and Fox, K.: 1968, *J. Chem. Phys.* **49**, 2451.
Margolis, J. S. and Fox, K.: 1969a, *J. Atmospheric Sci.* **26**, 862.
Margolis, J. S. and Fox, K.: 1969b, *Astrophys. J.* **157**, 935.
Margolis, J. S. and Hunt, G. E.: 1972, 'On the Level of H_2 Quadrupole Absorption in the Jovian Atmosphere', *Icarus* (in press).
Marshall, L., and Libby, W. F.: 1967, *Nature* **214**, 126.
Mason, H. P.: 1970, *Astrophys. Space Sci.* **7**, 424.
Mayer, C. H. and McCullough, T. P.: 1971, *Icarus* **14**, 187.
Mayer, C. H., McCullough, T. P., and Sloanaker, R. M.: 1958, *Astrophys. J.* **127**, 11.
McAdam, W. B.: 1969, *Proc. Astron. Soc. Australia* **1**, 199.
McBride, J. D. P. and Nicholls, R. W.: 1972a, *J. Phys. B: Atom. Molec. Phys.* **5**, 408.
McBride, J. D. P., and Nicholls, R. W.: 1972b, *Can. J. Phys.* **50**, 93.
McCord, T. B.: 1966, *Astron. J.* **71**, 585.
McCord, T. B., Johnson, T. V., and Elias, J. H.: 1971, *Astrophys. J.* **165**, 413.
McElroy, M. B.: 1969, *J. Atmospheric Sci.* **26**, 798.
McGovern, W. E.: 1968, *J. Geophys. Res.* **73**, 6361.
McGovern, W. E. and Burk, S. D.: 1972, *J. Atmospheric Sci.* **29**, 179.
McNesby, J. R.: 1969, *J. Atmospheric Sci.* **26**, 594.
Melbourne, W. G., Mulholland, J. G., Sjogren, W. L., and Sturms, F. M., Jr.: 1968, 'Constants and Related Information for Astrodynamic Calculations', TR 32-1306. Jet Propulsion Laboratory, Pasadena, Calif.
Mertz, L., and Coleman, I.: 1966, *Astron. J.* **71**, 747.
Moore, J. H.: 1939, *Publ. Astron. Soc. Pacific* **51**, 274.
Moore, J. H. and Menzel, D. H.: 1928, *Publ. Astron. Soc. Pacific* **40**, 234.
Moore, J. H. and Menzel, D. H.: 1930, *Publ. Astron. Soc. Pacific* **42**, 330.
Moos, H. W. and Rottman, G. J.: 1972, 'The Far Ultraviolet Emission Spectrum of Jupiter', Third Annual Meeting, AAS Div. for Planetary Sciences, Kona, Hawaii, March. 20–24.
Moos, H. W., Fastie, W. G., and Bottema, M.: 1969, *Astrophys. J.* **155**, 887.
Moroz, V. I.: 1966, *Soviet Astron.–AJ* **9**, 999.
Moroz, V. I. and Cruikshank, D. P.: 1969, *J. Atmospheric Sci.* **26**, 865.
Morrison, D., Cruikshank, D. P., and Murphy, R. E.: 1972, *Astrophys. J.* **173**, L143.
Morrison, D., Cruikshank, D. P., Murphy, R. E., Martin, T. Z., Beery, J. G., and Shipley, J. P.: 1971, *Astrophys. J.* **167**, L107.
Münch, G. and Spinrad, H.: 1963, *Mem. Soc. Roy. Sci. Liège Series 5*, **7**, 541.
Münch, G. and Younkin, R. L.: 1964, *Astron. J.* **69**, 553.
Murphy, R. E., Cruikshank, D. P., and Morrison, D.: 1972a, 'Limb Darkening of Saturn and Thermal Properties of the Rings From 10 and 20 Micron Radiometry', Third Annual Meeting, AAS Div. for Planetary Sciences, Kona, Hawaii, March 20–24.
Murphy, R. E., Cruikshank, D. P., and Morrison, D.: 1972b, 'Albedos, Radii, and Temperatures of Iapetus and Rhea', Third Annual Meeting, AAS Div. for Planetary Sciences, Kona, Hawaii, March 20–24.
Murray, B. C., Wildey, R. L., and Westphal, J. A.: 1964, *Astrophys. J.* **139**, 986.
Nautical Almanac Office: 1961, 'Explanatory Supplement to the Ephemeris', Her Majesty's Stationary Office, London.
Newburn, R. L., Jr., McDonald, W. S., Gasteiger, R. L., and Eisenman, A. R.: 1970, *Astronaut. Aeronaut.* **8**, 39.
Ney, E. P. and Maas, R.: 1969, *Bull. Amer. Astron. Soc.* **1**, 202.
Oke, J. B.: 1965, *Ann. Rev. Astron. Astrophys.* **3**, 23.
O'Leary, B. and Veverka, J.: 1971, *Icarus* **14**, 265.
Öpik, E. J.: 1962, *Icarus* **1**, 200.
Owen, T.: 1965a, *Science* **149**, 974.
Owen, T.: 1965b, *Astrophys. J.* **142**, 782.
Owen, T.: 1965c, *Astrophys. J.* **141**, 444.
Owen, T.: 1966, *Astrophys. J.* **146**, 611.
Owen, T.: 1967a, *Icarus* **6**, 108.
Owen, T.: 1967b, *Icarus* **6**, 138.
Owen, T.: 1969, *Icarus* **10**, 355.

Owen, T. and Mason, H. P.: 1969, *J. Atmospheric Sci.* **26**, 870.
Palluconi, F. D.: 1972, 'The Planet Saturn (1970)', NASA Space Vehicle Design Criteria (Environment), NASA SP-8091.
Parkin, D. W. and Tilles, D.: 1968, *Science* **159**, 936.
Pauliny-Toth, I. I. K. and Kellermann, K. I.: 1970, *Astrophys. Letters* **6**, 185.
Peebles, P. J. E.: 1964, *Astrophys. J.* **140**, 328.
Peek, B. M.: 1958, *The Planet Jupiter*, Faber and Faber, London.
Pilcher, C. B., Chapman, C. R., Lebofsky, L. A., and Kieffer, H. H.: 1970, *Science* **167**, 1372.
Pilcher, C. B. and McCord, T. B.: 1971, *Astrophys. J.* **165**, 195.
Poll, J. D.: 1971, in C. Sagan, T. C. Owen and H. J. Smith (eds.), 'Planetary Atmospheres', *IAU Symp.* **40**, 384.
Porter, J. G.: 1960, *Brit. Astron. Assoc. J.* **70**, 33.
Porter, W. S.: 1961, *Astron. J.* **66**, 243.
Prasad, S. S. and Capone, L. A.: 1971, *Icarus* **15**, 45.
Prinn, R. G.: 1970, *Icarus* **13**, 424.
Prinn, R. G. and Lewis, J. S.: 1972, 'The Atmosphere of Uranus', Third Annual Meeting, AAS Div. of Planetary Sciences, Kona, Hawaii, March 20–24.
Prinz, R.: 1971a, *Icarus* **15**, 68.
Prinz, R.: 1971b, *Icarus* **15**, 74.
Rabe, E.: 1957a, *Astrophys. J.* **125**, 290.
Rabe, E.: 1957b, *Astrophys. J.* **126**, 240.
Ramsey, W. H.: 1967, *Planetary Space Sci.* **15**, 1609.
Reese, E. J.: 1970, *Icarus* **12**, 249.
Reese, E. J.: 1971a, 'Summary of Jovian Latitude and Rotation-Period Observations From 1898 to 1970', Dept. of Astronomy Rpt. TN-71-36, N. Mex. State Univ., Las Cruces.
Reese, E. J.: 1971b, *Icarus* **14**, 343.
Reese, E. J.: 1971c, *Icarus* **15**, 466.
Reese, E. J. and Smith, B. A.: 1968, *Icarus* **9**, 474.
Reese, E. J. and Solberg, H. G., Jr.: 1965, 'Recent Measures of the Latitude and Longitude of Jupiter's Red Spot', TN-557-65-7. New Mexico State Univ.
Register, H. I.: 1968, 'Decameter-Wavelength Radio Observations of the Planet Jupiter, 1957–1968', Ph.D. Thesis, Univ. of Florida, Gainsville.
Reynolds, R. T. and Summers, A. L.: 1965, *J. Geophys. Res.* **70**, 199.
Roberts, J. A.: 1965, *Radio Sci.* **69D**, 1543.
Roberts, J. A. and Ekers, R. D.: 1966, *Icarus* **5**, 149.
Roberts, J. A. and Komesaroff, M. M.: 1965, *Icarus* **4**, 127.
Rose, W. K., Bologna, J. M., and Sloanaker, R. M.: 1963, *Phys. Rev. Letters* **10**, 123.
Russell, H. M., Dugan, R. S., and Stewart, J. Q.: 1945, *Astronomy*, Vol. 1, rev. ed., Ginn and Co., Boston, Mass.
Sagan, C.: 1963, *Mem. Soc. Roy. Sci, Liège Series 5*, **7**, 506.
Sagan, C.: 1971, *Comments Astrophys. Space Phys.* **3**, 65.
Sagan, C. and Khare, B. N.: 1971, *Astrophys. J.* **168**, 563.
Salomonovich, A. E.: 1965, *J. Res. NBS* **69D**, 1576.
Seaquist, E. R.: 1969, *Nature* **224**, 1011.
Seidelmann, P. K., Klepczynski, W. J., Duncombe, R. L., and Jackson, E. S.: 1971, *Astron. J.* **76**, 488.
Sekiguchi, N.: 1968, *Publ. Astron. Soc. Japan* **20**, 193.
Seling, T. V.: 1970, *Astron. J.* **75**, 67.
Sherrill, W. M.: 1965, *Astrophys. J.* **142**, 1171.
Shimizu, M.: 1971, *Icarus* **14**, 273.
Sinton, W. M.: 1964, 'Physical Researches on the Brighter Planets, Final Report', AFCRL-64-926. Air Force Cambridge Research Laboratory, Bedford, Mass.
Sky and Telescope: 1967, 'A Tenth Satellite of Saturn?' **33**, 71.
Smoluchowski, R.: 1967, *Nature* **215**, 691.
Smoluchowski, R.: 1970a, *Phys. Rev. Letters* **25**, 693.
Smoluchowski, R.: 1970b, *Science* **168**, 1340.
Smoluchowski, R.: 1971, *Astrophys. J.* **166**, 435.

Solberg, H. G., Jr.: 1968a, *Icarus* **8**, 82.
Solberg, H. G., Jr.: 1968b, *Icarus* **9**, 212.
Solberg, H. G., Jr.: 1969a, *Icarus* **10**, 412.
Solberg, H. G., Jr.: 1969b, *Planetary Space Sci.* **17**, 1573.
Spinrad, H.: 1962, *Astrophys. J.* **136**, 311.
Spinrad, H.: 1963, *Astrophys. J.* **138**, 1242.
Spinrad, H.: 1964, *Appl. Opt.* **3**, 181.
Spinrad, H.: 1969, *Publ. Astron. Soc. Pacific* **81**, 895.
Spinrad, H. and Giver, L. P.: 1966, *Publ. Astron. Soc. Pacific* **78**, 175.
Spinrad, H. and Trafton, L. M.: 1963, *Icarus* **2**, 19.
Squires, P.: 1957, *Astrophys. J.* **126**, 185.
Steavenson, W. H.: 1948, *Mon. Nat. Roy. Astron. Soc.* **108**, 183.
Steavenson, W. H.: 1950, *British Astron. Assoc. J.* **74**, 54.
Stone, P. H.: 1967, *J. Atmospheric Sci.* **24**, 642.
Stone, P. H.: 1971, *Geophys. Fluid Dynamics* **2**, 147.
Stone, P. H. and Baker, D. H., Jr.: 1968, *Q. J. Royal Meteorol. Soc.* **94**, 576.
Stone, P. H., Hess, S., Hadlock, R., and Ray, P.: 1969, *J. Atmospheric Sci.* **26**, 991.
Streett, W. B., Ringermacher, H. I., and Veronis, G.: 1971, *Icarus* **14**, 319.
Strobel, D. F.: 1969, *J. Atmospheric Sci.* **26**, 906.
Taylor, D. J.: 1965, *Icarus* **4**, 362.
Taylor, F. W. and Hunt, G. E.: 1972, 'The Infrared Spectrum of Jupiter and Radiative Properties of the Clouds', Third Annual Meeting, AAS Div. for Planetary Sciences, Kona, Hawaii, March 20–24.
Teifel, V. G.: 1966, *Soviet Astron. - AJ* **10**, 121.
Teifel, V. G.: 1969, *J. Atmospheric Sci.* **26**, 854.
Texereau, J.: 1967, *Sky Telesc.* **33**, 226.
Tolbert, C. W.: 1966, *Astrophys. J.* **71**, 30.
Tombaugh, C. W.: 1961, in G. P. Kuiper and B. M. Middlehurst (eds.), *The Solar System*, Vol. III: *Planets and Satellites*, Univ. of Chicago Press, Chicago, Ill., p. 12.
Trafton, L. M.: 1967, *Astrophys. J.* **147**, 765.
Trafton, L. M.: 1971a, *Bull. Amer. Astron. Soc.* **3**, 282.
Trafton, L.: 1971b, *Bull. Amer. Astron. Soc.* **3**, 282.
Trafton, L.: 1971c, *Icarus* **15**, 27.
Trafton, L.: 1972a, 'Quadrupole H_2 Absorption in the Spectra of Jupiter and Saturn', Third Annual Meeting, AAS Div. for Planetary Sciences, Kona, Hawaii, March 20–24.
Trafton, L.: 1972b, 'Newly Discovered Absorptions in Titan's Infrared Spectrum', Third Annual Meeting, AAS Div. for Planetary Sciences, Kona, Hawaii, March 20–24.
Trafton, L.: 1972c, *Astrophys. J.* **172**, L117.
Veverka, J.: 1971, *Icarus* **14**, 355.
Veverka, J.: 1972, 'Titan: Polarimetric Evidence for an Optically Thick Atmosphere', Third Annual Meeting, AAS Div. for Planetary Sciences, Kona, Hawaii, March 20–24.
Walker, M. F. and Hardie, R.: 1955, *Publ. Astron. Soc. Pacific* **67**, 224.
Walker, R. G.: 1966, 'Infrared Photometry of Stars and Planets', Ph.D. Thesis, Harvard University, Cambridge, Mass.
Wallace, L., Caldwell, J. J., and Savage, B. D.: 1972, *Astrophys. J.* **172**, 755.
Warwick, J. W.: 1963, *Astrophys. J.* **137**, 1317.
Warwick, J. W.: 1964, *Ann. Rev. Astron. Astrophys.* **2**, 1.
Warwick, J. W.: 1967, *Space Sci. Rev.* **6**, 841.
Warwick, J. W.: 1970, 'Particles and Fields Near Jupiter', NASA Report No. CR-1685.
Warwick, J. W. and Dulk, G. A.: 1964, *Science* **145**, 380.
Watson, K., Murray, B. C., and Brown, H.: 1963, *Icarus* **1**, 317.
Weber, R. R. and Stone, R. G.: 1970, *Nature* **227**, 591.
Welch, W. J. and Thorton, D. D.: 1965, *Astron. J.* **70**, 149.
Welch, W. J., Thornton, D. D., and Lohman, R.: 1966, *Astrophys. J.* **146**, 799.
Westphal, J. A.: 1969, *Astrophys. J.* **157**, L63.
Westphal, J. A.: 1971, 'Observations of Jupiter's Cloud Structure Near 8.5 μ,' C. Sagan, T. C. Owen, and H. J. Smith (eds.), 'Planetary Atmospheres', *IAU Symp.* **40**, 359.

Westphal, J. A.: 1972, 'Observations of Isolated Five Micron Sources on Jupiter', Third Annual Meeting, AAS Div. for Planetary Sciences, Kona, Hawaii, March 20–24.
Whiteoak, J. B., Gardner, F. F., and Morris, D.: 1969, *Astrophys. Letters* **3**, 81.
Wildey, R. L.: 1965, *Science* **147**, 1035.
Wildey, R. L., Murray, B. C., and Westphal, J. A.: 1965, *J. Geophys. Res.* **70**, 3711.
Williams, J. G. and Benson, G. S.: 1971, *Astron. J.* **76**, 167.
Woeller, F. and Ponnamperuma, C.: 1969, *Icarus* **10**, 386.
Wrixon, G. T. and Welch, W. J.: 1970, *Icarus* **13**, 163.
Wrixon, G. T., Welch, W. J., and Thornton, D. D.: 1971, *Astrophys. J.* **169**, 171.
Yabushita, S.: 1966, *Monthly Notices Roy. Astron. Soc.* **133**, 247.
Yerbury, M. J., Condon, J. J., and Jauncey, D. L.: 1971, *Icarus* **15**, 459.
Young, A. T. and Irvine, W. M.: 1967, *Astron. J.* **72**, 945.
Younkin, R. L.: 1970, 'Spectrophotometry of the Moon, Mars, and Uranus', Ph.D. Thesis, Univ. of California at Los Angeles.
Younkin, R. L. and Munch, G.: 1967, *Astron. J.* **72**, 328.
Zabriskie, F. R., Solomon, W. A., and Hagan, J. P.: 1965, *Astron. J.* **70**, 151.